Institut für Erd- und Umweltwissenschaften
Angewandte Geoökologie

# Interaction of spatial variability characterized by soil electrical conductivity and plant water status related to generative growth of fruit trees

**Dissertation**
**zur Erlangung des akademischen Grades**
**"doctor rerum naturalium"**
**(Dr. rer. nat.)**
**in der Wissenschaftsdisziplin "Geoökologie"**

**eingereicht an der**
**Mathematisch-Naturwissenschaftlichen Fakultät**
**der Universität Potsdam**

**von**

**Jana Käthner**

***Potsdam, den 05.10.2016***

First reviewer: apl. Prof. Dr. habil. Oswald Blumenstein

Second reviewer: Prof. Dr. habil. Manuela Zude-Sasse

Third reviewer: Prof. Dr. Kerry Walsh

Submitted: 05.10.2016

Defense: 03.04.2017

Published online at the
Institutional Repository of the University of Potsdam:
URN urn:nbn:de:kobv:517-opus4-397666
http://nbn-resolving.de/urn:nbn:de:kobv:517-opus4-397666

Contents

## Preface

The present dissertation is organized as a "cumulative thesis" consisting of three manuscripts that are published and are in preparation for publication in ISI-listed peer-reviewed journals. In all manuscripts, the International System of units was used for all physical units. The empirical work for this thesis in the area of Precision Fruticulture was performed at the Leibniz Institute for Agricultural Engineering and Bioeconomy (ATB). All necessary qualifications for the dissertation were acquired at the University of Potsdam.

Yield losses and reduction in the quality of products in the plantation are the result of a water shortage. The irrigation amount and interval are often determined in the soil water content with tensiometers or later analysis of weather data, but in this process the most precious commodity of water is lost, since the actual demand of the plant is not included. For these reasons, it is necessary to develop water-saving methods for yield optimization.

This study investigated how the spatial soil information correlates with plant water status, generative plant growth and final fruit quality. With this, it should be possible to determine the optimal water conditions for the plant. The main studies took place in an experimental plum orchard in Potsdam, Brandenburg and in grapefruit in a research facility in Adana, Turkey. The findings were evaluated in a plum and grapefruit production system.

By funding the work of two transnational projects "3D-*Mosaic* (FP7, ICT-AGRI, 2810ERA095) Advanced Monitoring of Tree Crops for Optimized Management – How to Crop with Variability in Soil and Plant Properties" and "Usability of Environmentally Sound and Reliable Techniques in Precision Agriculture – USER -PA (FP7, ICT-AGRI, 2812ERA038)", the hypotheses (see Chapter 1.3) could be examined and tested in several orchards.

A short overview of the manuscripts, including the contributions of the authors, is given in the section entitled "Thesis at a glance". Following this, a short summary of the thesis is presented. Chapter 1 presents a general introduction presenting the scientific rationale and objectives of this thesis. Chapters 2-4 contain the manuscripts, which can be divided into two parts: methodological approaches (Chapter 2-3) and research papers (Chapter 2 and 4). The methodological manuscripts introduce novel approaches that facilitate and optimize the concept of precision fruticulture. The research manuscript focuses on applying methods, but due to the new approach even in chapter 4 the methodology needed adaptation for the orchard located in semi-humid climate. The whole discussion can be found in Chapter 5. Chapter 6 gives a synthesis of the most important findings presented in the manuscripts and highlights the accomplished scientific advances.

**Thesis at a glance**

MANUSCRIPT 1

Interaction of 3D soil electrical conductivity and generative growth in *Prunus domestica* L.

(European Journal of Horticultural Science. 2015, 80, 5: 231-239)

Authors — Jana Käthner and Manuela Zude-Sasse

Rationale — The concept of precision agriculture has been introduced in horticulture only recently. A deeper look into the interaction of generative growth (e.g. number of flowers per tree) of fruit trees and spatially measured soil properties is missing.

Methods — An experimenttal plum orchard in temperate climate (Potsdam, Germany), capturing 0.37 ha with 156 trees were used. The main soil consists of predominantly sandy soils, which were formed by glacial and post-glacial deposits. The generative growth of plum trees were closely analyzed and classified according to the apparent electrical conductivity (ECa) of the soil in three depths.

Results — Positive correlation with r = 0.52 was found between the soil ECa and generative tree growth in two years and planting ages, with enhanced interaction in older trees. The most influence on the generative tree growth was in this case the topsoil. Furthermore, the slope of the present orchard and soil compaction due to mechanical weed control influenced the root zone environment. Besides was shown in the soil ECa that the pattern were stable over for two years (r = 0.88).

Conclusions — The concept of precision fruticulture can provide a better insight of correlations considering tree growth and soil ECa.

Author’s contributions

I worked out the topic and content of this contribution. I developed the study idea, the experimental design, collected the data, performed the data analysis, interpreted the data, and wrote the manuscript. The visualization technique for the 3D ECa cube and the MATLAB® script for the statistical analysis were programmed by me. Prof. Dr. M. Zude-Sasse provided guidance and helped in constructing the study design, contributed to the data interpretation, and to the writing and editing of the manuscript at various stages.

MANUSCRIPT 2:

Getis-Ord's hot- and cold-spot statistics as a basis for multivariate spatial clustering of tree-based data

(Computers and Electronics in Agriculture. 2015, 111, 140-150)

Authors Aviva Peeters, Manuela Zude, Jana Käthner, Mustafa Ünlü, Riza Kanber, Amots Hetzroni, Robin Gebbers, Alon Ben-Gal

Rationale Particularly in orchards, the spatial data describe no continuous field/matrix, but represent single trees with its own features. The hot-spot analysis enables the statistical description of spatial variability found in crops and their environment.

Methods A novel approach was presented which accounts for the spatial structure of data in a multivariate cluster analysis by combining the spatial Getis–Ord $G_i^*$ statistic with aspatial *k*-means multivariate clustering. The spatial analysis partitions data into homogenus groups which is based on modeling point data, i.e. individual trees. Tested were the analyses with data from an experimental grapefruit orchard (*Citrus paradisi, cv.* Rio Red) in Mediterranean climate in Adana, Turkey.

Results For demonstration its feasibility and assess its performance in relation to the common aspatial *k*-means clustering method was applied the approach in a grapefruit orchard. Results highlight that point-based spatial-clustering methods represent a valid method to characterize the spatial structure of point-based data such as single trees in an orchard based on multiple variables, in consideration of the combination of $G_i^*$ statistic with aspatial clustering.

Conclusions Combination of the methods represents a suitable technique for identifying homogenous spatial clusters in orchards.The hot-spot analysis can be used as a tool for precision management of orchards by partitioning trees into management zones.

Author´s contributions

Dr. A. Peeters and I developed the experimental design and carried out the field measurements. I pre-processed the data for the hot spot analysis. Dr. Peeters tested the hot spot analysis with ArgGIS and evaluated the hot spot analysis with the *k*-mean clustering. I performed the approach validation using

MATLAB®. Dr. Peeters wrote the manuscript. I contributed to the data interpretation and helped with writing and editing the manuscript at various stages. The MATLAB® script was used further. A. Ben-Gal and Manuela Zude provided guidance and editing of the manuscript at various stages. With Robin Gebbers, Alon Ben-Gal, Amots Hetzroni, Robin Gebbers, and Manuela Zude were discuss the mathematical apporach. Mustafa Ünlü and Riza Kanber provided the orchard, the chemical soil probes, the yield data and weather information.

MANUSCRIPT 3:

Evaluating spatially resolved influence of soil and tree water status on quality of European plum grown in semi-humid climate

(Frontiers in Plant Science, 2017, 1-10)

Authors Jana Käthner, Alon Ben-Gal, Robin Gebbers, Aviva Peeters, Werner B. Herppich, and Manuela Zude-Sasse

Rationale Plant water status was analysed in orchard targeting spatial analysis of trees considering instantaneous and cumulative water use efficiency.

Methods Soil variability and water status of trees was spatially measured by means of leaf water potential, and thermal imaging of canopies. From thermal images, the crop water stress index was calculated for semi-humid climate. Cumulative effect of the degree of water supply was recorded as specific leaf area ratio and fruit quality. Applications of the hot-spot analysis provided extremes from the multiple tree variables.

Results Spatial variation of soil ECa, instantaneous water status of fruit tree, and water use efficiency in semi-humid climate was found. In addtion an influence on the fruit quality was observed. The hot-spot analysis resulted in 6 spots of soil ECa that was correlated with the leaf area ($R^2 = 0.78$). Extreme values of CWSI were correlated with the fruit quality and WUEc was enhanced with high crop load. Furthermore it was shown, that orchard located in semi-humid climate, irrigated throughout the vegetation period still suffered from slight drought stress.

Conclusions CWSI provided information on the instantaneous water status of fruit trees. Interaction of WUEc and CWSI pointed to considerable effects on the fruit quality.

Author´s contributions

I developed the study idea and the experimental design, collected the data, performed the data analysis, interpreted the data, and wrote the manuscript. For analysis of the thermal image and calculation of the CWSI, I developed and wrote MATLAB® scripts considering available approaches for semi-humid and humid climates. Prof. Dr. M. Zude-Sasse provided guidance and helped in constructing the study design, contributed to the data interpretation, and helped with writing and editing of the manuscript at various stages. Dr. A. Ben-Gal provided guidance and editing of the manuscript at various stages. The other authors A. Peeters and W. B. Herppich contributed with deep discussions and revisions of the manuscript.

## Abstract

Precision horticulture encompasses site- or tree-specific management in fruit plantations. Of decisive importance is spatially resolved data (this means data from each tree) from the production site, since it may enable customized and, therefore, resource-efficient production measures.

The present thesis involves an examination of the apparent electrical conductivity of the soil (ECa), the plant water status spatially measured by means of the crop water stress index (CWSI), and the fruit quality (e.g. fruit size) for *Prunus domestica* L. (plums) and *Citrus x aurantium,* Syn. *Citrus paradisi* (grapefruit). The goals of the present work were i) characterization of the 3D distribution of the apparent electrical conductivity of the soil and variability of the plant's water status; ii) investigation of the interaction between ECa, CWSI, and fruit quality; and iii) an approach for delineating management zones with respect to managing trees individually.

To that end, the main investigations took place in the plum orchard. This plantation got a slope of 3° grade on Pleistocene and post-Pleistocene substrates in a semi-humid climate (Potsdam, Germany) and encloses an area of 0.37 ha with 156 trees of the cultivar 'Tophit Plus' on a Wavit rootstock. The plantation was laid in 2009 with annual and biannual trees spaced 4 m distance along the irrigation system and 5 m between the rows. The trees were watered three times a week with a drip irrigation system positioned 50 cm above ground level providing 1.6 l per tree per event. With the help of geoelectric measurements, the apparent electrical conductivity of the upper soil (0.25 m) was measured for each tree with an electrode spacing of 0.5 m (4-point light hp). In this manner, the plantation was spatially charted with respect to the soil's ECa. Additionally, tomography measurements were performed for 3D mapping of the soil ECa and spot checks of drilled cores with a profile of up to 1 m. The vegetative, generative, and fruit quality data were collected for each tree. The instantaneous plant water status was comprehensively determined in spot checks with the established Scholander method for water potential analysis (Scholander pressure bomb) as well as thermal imaging. An infrared camera was used for the thermal imaging (ThermaCam SC 500), mounted on a tractor 3.3 m above ground level. The thermal images (320 x 240 px) of the canopy surface were taken with an aperture of 45° and a geometric resolution of 8.54 x 6.41 mm. With the aid of the canopy temperature readings from the thermal images, cross-checked with manual temperature measurements of a dry and a wet reference leaf, the crop water stress index (CWSI) was calculated. Adjustments in CWSI for measurements in a semi-humid climate were developed, whereas the collection of reference temperatures was automatically collected from thermal images.

The bonitur data were transformed with the help of a variance stabilization process into a normal distribution. The statistical analyses as well as the automatic evaluation routine were performed with several scripts in MATLAB® (R2010b and R2016a) and a free program (spatialtoolbox). The hot spot analysis served to check whether an observed pattern is statistically significant. The method was evaluated with an established *k*-mean analysis. To test the hot-spot analysis by comparison, data from a grapefruit plantation (Adana, Turkey) was collected, including soil ECa, trunk circumference, and yield data. The plantation had 179 trees on a soil of type Xerofkuvent with clay and clay-loamy texture. The examination of the interaction between the critical values from the soil and plant water status information and the vegetative and generative plant growth variables was performed with the application from ANOVA.

The study indicates that the variability of the soil and plant information in fruit production is high, even considering small orchards. It was further indicated that the spatial patterns found in the soil ECa stayed constant through the years ($r = 0.88$ in 2011-2012 and $r = 0.71$ in 2012-2013). It was also demonstrated that CWSI determination may also be possible in semi-humid climate. A correlation ($r = -0.65$, $p < 0.0001$) with the established method of leaf water potential analysis was found. The interaction between the ECa from various depths and the plant variables produced a highly significant connection with the topsoil in which the irrigation system was to be found. A correlation between yield and $ECa_{topsoil}$ of $r = 0.52$ was determined. By using the hot-spot analysis, extreme values in the spatial data could be determined. These extremes served to divide the zones (cold-spot, random, hot-spot). The random zone showed the highest correlation to the plant variables.

In summary it may be said that the cumulative water use efficiency (WUEc) was enhanced with high crop load. While the CWSI had no effect on fruit quality, the interaction of CWSI and WUEc even outweighed the impact of soil ECa on fruit quality in the production system with irrigation. In the plum orchard, irrigation was relevant for obtaining high quality produce even in the semi-humid climate.

## German abstract

*Precision horticulture* beschreibt ein neues Bewirtschaftungskonzept im Gartenbau, bei dem teilflächenspezifisch oder an den Einzelbaum angepasste Maßnahmen eine ressourcenschonende, intensitve Produktion ermöglichen. Die Datengrundlage wird aus räumlich aufgelösten Messungen aus der Produktionsanlage gewonnen, wobei sowohl kurzfristige Faktoren wie der effektive Pflanzenwasserzustand als auch langfristige Faktoren wie die Bodenvariabilität zur Informationsgewinnung genutzt werden können. Die vorliegende Arbeit umfasst eine Untersuchung der scheinbaren elektrischen Leitfähigkeit des Bodens (ECa), des Pflanzenwasserzustandes und der Fruchtqualität (zum Beispiel: Fruchtgröße) bei *Prunus domestica* L. (Pflaume) und *Citrus x aurantium,* Syn. *Citrus paradisi* (Grapefruit). Zielsetzungen der vorliegenden Arbeit waren (i) die Charakterisierung der 3D-Verteilung der scheinbaren elektrischen Leitfähigkeit des Bodens und Variabilität des Pflanzenwasserzustandes; (ii) die Untersuchung der Interaktion zwischen ECa, kumulativer Wassernutzungseffizienz (WUEc) und des crop water stress index (CWSI) bezogen auf die Fruchtqualität sowie (iii) eine Möglichkeit zur Einteilung von einzelnen Bäumen hinsichtlich der Bewässerung.

Dazu fanden die Hauptuntersuchungen in der Pflaumenanlage statt. Diese Obstanlage befindet sich in Hanglage (3°) auf pleistozänen und postpleistozänen Substraten in semi-humiden Klima (Potsdam, Deutschland) und umfasst eine Fläche von 0,37 ha mit 156 Bäumen der Kultursorte 'Tophit Plus' auf der Unterlage Wavit. Die Anlage wurde 2009 mit ein und zwei-jährigen Bäumen in einem Pflanzabstand von 4 m entlang der Bewässerung und 5 m zwischen den Reihen angelegt. Dreimal pro Woche wurden die Bäume mit einer 50 cm über dem Boden installierten Tröpfchenbewässerung mit 1,6 l pro Baum bewässert. Mit Hilfe geoelektrischer Messungen wurde die scheinbare elektrische Leitfähigkeit des Oberbodens (0,25 m) mit einem Elektrodenabstand von 0,5 m (4-point light hp) an jedem Baum gemessen. Dadurch wurde die Anlage hinsichtlich ECa räumlich charakterisiert. Zusätzlich erfolgten Tomographiemessungen zur 3D-Charakterisierung der ECa und punktuell die Beprobung von Bohrlochprofilen bis 1 m Tiefe. Die vegetativen, generativen und Fruchtqualitätsdaten wurden an jedem Baum erhoben. Der momentane Pflanzenwasserzustand wurde mit der etablierten Scholander-Methode zur Wasserpotentialanalyse (Scholander Bombe) punktuell und mit Thermalaufnahmen flächendeckend bestimmt. Die Thermalaufnahmen erfolgten mit einer Infrarot-Kamera (ThermaCam SC 500), die auf einem Traktor in 3,3 m Höhe über dem Boden montiert war. Die Thermalaufnahmen (320 x 240 Pixel) der Kronenoberfläche wurden mit einem Öffnungswinkel von 45° und einer geometrischen Auflösung von 6,41 mm x 8,54 mm aufgenommen. Mit Hilfe der Kronentemperatur aus den Thermalbildern und den Temperaturen eines nassen und trockenen Referenzblattes wurde der CWSI berechnet. Es

wurde die Anpassung des CWSI für die Messung in semi-humidem Klima erarbeitet, wobei die Erhebung der Referenztemperaturen automatisiert aus den Thermalbildern erfolgte.

Die Boniturdaten wurden mit Hilfe eines Varianz-Stabilisierungsverfahrens in eine Normalverteilung transformiert. Die statistischen Analysen sowie die automatisierte Auswertungsroutine erfolgten mit eigenen Skripten in MATLAB® (R2010b sowie R2016a) und einem freien Programm (spatialtoolbox). Die Hot-spot Analysen dienten der Prüfung, ob ein beobachtetes Muster statistisch signifikant ist. Evaluiert wurde die Methode mit der etablierten *k*-mean Analyse. Zum Testen der Hot-spot Analyse wurden ECa, Stammumfang und Ertrag Daten aus einer Grapefruitanlage (Adana, Türkei) mit 179 Bäumen auf einem Boden vom Typ Xerofkuvent mit toniger und tonig-lehmiger Textur herangezogen. Die Überprüfung der Interaktion zwischen den kritischen Werten aus den Boden- und Pflanzenwasserzustandsinformationen zu den vegetativen und generativen Pflanzenwachtumsvariablen erfolgte durch die Anwendung der ANOVA und die Ermittlung des Korrelationskoeffizienten.

In der Arbeit konnte gezeigt werden, dass die Variabilität der Boden- und Pflanzeninformationen in Obstanlagen auch kleinräumig hoch ist. Es konnte gezeigt werden, dass die räumlich gefundenen Muster in den ECa über die Jahre zwischen 2011-2012 ($r = 0.88$) beziehungsweise 2012-2013 ($r = 0.71$) stabil geblieben sind. Zum anderen wurde gezeigt, dass eine CWSI-Bestimmung auch im semi-humiden Klima möglich ist. Es wurde ein Zusammenhang ($r = -0.65$, $p < 0.0001$) mit der etablierten Methode der Blattwasserpotentialanalyse ermittelt. Die Interaktion zwischen der ECa aus verschiedenen Tiefen und den Pflanzenvariablen ergab einen hoch signifikanten Zusammenhang mit dem Oberboden, in dem das Bewässerungswasser zu finden war. Es wurde eine Korrelation zwischen Ertrag und $ECa_{topsoil}$ von $r = 0.52$ ermittelt. Durch die Anwendung der Hot-spot Analyse konnten Extremwerte in den räumlichen Daten ermittelt werden. Diese Extrema dienten zur Einteilung der Zonen in *cold-spot, random* und *hot-spot*. Die *random* Zone weist die höchsten Korrelationen zu den Pflanzenvariablen auf. Ferner konnte gezeigt werden, dass bereits im semi-humiden Klima der Pflanzenwasserstatus entscheidend zur Fruchtqualität beiträgt.

Zusammenfassend lässt sich sagen, dass die räumliche Variabilität der Fruchtqualität durch die Interaktion von Wassernutzungseffizienz und CWSI sowie in geringerem Maße durch den ECa des Bodens. In der Pflaumenanlage im semi-humiden Klima war die Bewässerung ausschlaggebend für die Produktion von qualitativ hochwertigen Früchten.

**List of abbreviation**

| | | |
|---|---|---|
| ANOVA | Analysis of variance | |
| C-H index | Calinski–Harabasz pseudo F-statistic | |
| $CO_2$ | Carbon dioxide | |
| CWSI | Crop water stress index | [0;1] |
| $CWSI_I$ | Crop water stress index according to Irmak et al.,2000 | [0;1] |
| $CWSI_R$ | Crop water stress index according to Rud et al.,2015 | [0;1] |
| $CWSI_J$ | Crop water stress index according to Jones, 1992 | [0;1] |
| $CWSI_{JB}$ | Crop water stress index according to Ben-Gal et al.,2009; Jones 2004 | [0;1] |
| DA-index | Delta absorbance index | |
| ECa or $\sigma_{soil}$ | Soil apparent electrical conductivity | [mS/m] |
| FDR | Frequency domain reflectometry | |
| Fuzzy | Clustering methods, each data point can belong to more than one cluster | |
| $G$ | Getis- Ord statistic | |
| $G_i^*$ | Getis-Ord local statistic | |
| GIS | Geographical information system | |
| GPS | Global Positioning System | |
| GVF | Goodness of variance fit | |
| GWC | Gravimetrical water content | [%] |
| Hot-spot analysis | Method for analyzing the location related tendency in the attributes of spatial data | |
| HSD | Honest significance difference (Tukey's HSD test) | |
| ISODATA | Novel method of data analysis and pattern classification | |
| *k*-mean | Aims to partition observations into k groups | |
| KM-sPC | Combined spatial principal component analysis with fuzzy *k*-means | |
| LiDAR | Light detection and ranging | |

| | | |
|---|---|---|
| Max. | Maximum | |
| Min. | Minimum | |
| $Na_4P_2O_7$ | Natriumdiphosphat | |
| NDVI | Normalized Differenced Vegetation Index | |
| NIR | Near-infrared | |
| PDWP | Predawn water potential | |
| PCA | Principal component analysis | |
| PCF | post-classification filtering | |
| PCI | prior classification interpolation | |
| pH | pondus Hydrogenii | |
| PR | penetration resistance | |
| RTK-GPS | Real Time Kinematic-Global Positioning System | |
| SLAR | Specific leaf area ratio | [$cm^2$ / g] |
| SST | Reflects between-group differences | |
| SSW | Reflects within-group similarities | |
| Std Dev. | Standard deviation | |
| SWP | Stem water potential | |
| VPD | Water vapor pressure deficit | [kPa] |
| Vis | Visual light | |
| WCSS | Within-cluster sum of squares | |
| WGS84 | World Geodetic System 1984 | |
| WUEi | Intrinsic water use efficiency | [a.u.] |
| WUEc | Cummulative water use efficiency | [g / l] |
| *z*-score | Standard score of standard deviations | |
| *p*- value | Defined as the probability of an observed | |
| F value | Ratio of two scaled sums of squares | |
| LWP or $\Psi_{leaf}$ | Leaf-water potential | [MPa] |

**Symbols**

| | | |
|---|---|---|
| $C_p$ | Specific heat of dry air at constant pressure | [J $kg^{-1}$ $K^{-1}$] |
| $d_w$ | Characteristic length of the leaves in the direction of the prevailing wind | [m] |
| D | the distance within which all locations are considered as neighbors | |
| $e_{abs}$ | Saturation vapor pressure eabs | [kPa] |
| $e_{air}$ | Actual water vapor pressure of air | [kPa] |
| i or j | Feature or index | |
| K | Number of clusters | |
| N | Is equal to the total number of features | |
| P | Pressure | [MPa] |
| $p_{air}$ | Air pressure pair | [MPa] |
| $R^2$ | Coefficient of determination | |
| R or r | Pearson correlation coefficient | |
| $r_H$ | Aerodynamic resistance to sensible heat transport $r_H$ | [s $m^{-1}$] |
| $r_{HR}$ | Resistance to sensible heat transport $r_{HR}$ | [s $m^{-1}$] |
| $R_{ni}$ | Net energy at the canopy | [$Wm^{-2}$] |
| $r_R$ | Resistance for radiative heat loss | [s $m^{-1}$] |
| $R_{sw}$ | Incoming short-wave radiation | [$Wm^{-2}$] |
| $r_v$ | Aerodynamic resistance to latent heat transport ($r_H$/1.08) | [s $m^{-1}$] |
| S | Slope of the curve relating saturation vapor pressure to temperature | |
| $S_i$ | Homogenous cluters | |
| T | Temperature | [°C] |
| $T_K$ | Absolute temperature | [K] |
| T | Time course, diurnal variation | [h] |
| $T_{air}$ | Air temperaure | [°C] |
| Tc | Current canopy temperature | [°C] |
| Td | Temperature of dry reference | [°C] |

| | | |
|---|---|---|
| Tw | Temperature of wet reference | [°C] |
| U | Wind speed | [m $s^{-1}$] |
| W | Width of the imaged area | [m] |
| $w_{ij}$ | Spatial weight for the target-neighbor i and j pair | |
| $x_j$ | Attribute value of the target feature | |
| Z | Camera-distance | [m] |
| A | Albedo of the canopy | |
| B | Opening angle of the camera | [°] |
| Γ | Thermodynamic psychrometer constant (≈0.066) | [kPa $k^{-1}$] |
| $\varepsilon_c$ | Emittance of the canopy | |
| $\mu_i$ | Mean of points | |
| P | Density of dry air | [kg $m^{-3}$] |
| Σ | Stefan-Boltzmann constant= 5.67 $10^{-8}$ | [$Wm^{-2}$ $K^{-4}$] |
| T | Osmotic value | |
| Φ | Relative humidity | [%] |
| $\Psi_p$ | Pressure potential | [MPa] |
| $\Psi_\tau$ | Osmotic potential | [MPa] |

**List of figure**

**List of tables**

# 1 Introduction

## 1.1 Present situation

At present, the approach of precision fruticulture is based on a concept from arable cultivation known as precision farming. Here, differences arise because of perennial cultures, developments specific to plant types, higher net value, and an already very high production intensity.

The prerequisites for this are spatially resolved soil and field data and information about plant growth specific to individual plants. Optimal concepts are needed, under consideration of these different local conditions and plant physiological questions in increasing yield, in order to attain an efficient and sustainable production in commercial fruit plantations. Particular attention should be paid to an efficient and targeted use of water.

### *1.1.1 History of fruticulture*

The roots of fruticulture in Germany can be traced to early history (Schuricht, 2009). According to Ritthaler (2012), the history of fruticulture in Germany can be classified by the social structures and technological progress in four eras. First, from 200 CE to 1650 CE, fruit was a semi-luxury food (Ritthaler, 2012). That said, at that time documented knowledge transfers mainly took place through monasteries and household literature (Ritthaler, 2012). The second period, from c. 1650 to c. 1830, was marked by subsistence agriculture and local use, leading into the third era of wider-ranging agriculture from c. 1830 to c. 1950 (Ritthaler, 2012). The fourth era, technically specialized operations, has only existed since around 1950 (Ritthaler, 2012). Through mechanization, irrigation, and the use of fertilizers and agricultural control chemicals, the productivity of orchards intensified (Jackson, 2005). This in turn enabled the global export of fruit products (Jackson, 2005). Precision fruticulture marks a further step in the history of cultivation. The goal is to increase the productivity of the orchard while saving resources.

### *1.1.2 Quality of fruit*

Particularly for gardening products, the quality of the harvested product is increasingly important for commercial profits. Nonetheless, in spite of the existence of a variety of quality guidelines, there is no consistent definition of fruit quality (Shewfelt, 1999). According to Eccher Zerbini (2002) and Shewfelt (1999), quality cannot be seen as a specific physiological property of fruit, but rather as a combination of factors (UNECE-NORM FFV-29, 2014; UNECE-NORM FFV-14, 2012), in particular the expectations of consumers and the needs of retailers. High market prices are attained with a high quality level of fruit (Jones and Tardieu, 1998). The most important quality parameters include, among other things, marketing norms: wholeness, cleanliness, healthiness, and the size and weight of the fruit also the fruit flesh firmness and soluble solid content (UNECE-NORM FFV-29, 2014). Thus even a few millimeters of the fruit size can strongly affect the marketability of fruit and its price (Theron, 2011).

### *1.1.3 European orchard*

Depending on climate and local consumer preferences, European orchard fruit that is in demand stems primarily from the families Rutaceaen and Rosaceaen (Faostat, 2016). This fruit includes unprocessed fruit (stone, seed, and berry fruit) from multi-year, extensive open-air cultivation of trees and bushes. Stone fruit of the genus Prunus is characterized by its pericarp in three levels (Kadereit et al., 2014). From the single fruit leaf not connected to the deeper flower bud, the three levels of tissue develop. The result is the woody, usually single-cell core (endocarp) surrounded by (mostly) edible fruit flesh (mesocarp), and enclosed by a skin barrier (exocarp) (Seifert et al., 2015). Typical examples include sweet cherries (*P. avium*), sour cherries (*P. cerasus*), plums (*P. domestica*), peaches (*P. persica*), and apricots (*P. armeniaca*). In Europe, the leader of these — with roughly 4 million metric tons — is peaches (Faostat, 2016), of which 883 t were produced in Germany. In Germany in 2015, these were followed by plums (48,536 t) and cherries (824,462 t) (Faostat, 2016).

Citrus fruits belong to the berry genus and, like the stone fruits, develop from a single (if multi-seed) fruit leaf. However, in this case the entire pericarp is fleshy (Kadereit et al., 2014). Examples of berry fruit in orchard cultivation are the citrus fruits (like grapefruit), the pomegranate, and the papaya. The citrus fruit most produced in Europe is the orange (6.2 million metric tons), clementines (3.1 million t), lemons (1.1 million t), and grapefruit (80,000 t).

### *1.1.4 Fruit consumption*

Fruit consumption in Germany has risen by 6% in the past 17 years (Gracia and Albisu, 2001). According to a 2015 study, the annual per capita consumption of marketed fruit is about 67.3 kg (BMEL, 2016). In comparison to the previous year, 0.7 kg more were consumed. Commercial fruticulture plays an increasing role in securing nutrition, but also an important role in physical and psychological health in urban and rural areas (Beddington et al., 2008).

### *1.1.5 Cultivation area*

In 2013, 21.3% of Europe's land area was under cultivation. This translates into roughly 470 million hectares. Of that, 15 million are used for fruticulture (Faostat, 2016). Therefore commercial fruticulture plays an important role in Europe. This is further indicated by the increased production of fruit — up to 130.5 t/ha in recent years (Faostat, 2016). At a continental level worldwide, Europe (10.9%) is in third place behind Asia (52.8%) and North and South America (21.7%) in fruit production (Faostat, 2016). Some of the best-known fruticulture areas in Germany are the Alte Land in parts of the lower Elbe River in Hamburg and Lower Saxony, the Lake Constance region, and the Havel River region west of Berlin in Brandenburg state. Further important fruticulture regions in Europe include the Steiermark in Austria, northeastern Switzerland, and large parts of Moldova (Faostat, 2016).

## 1.2 State of the art

### *1.2.1 Precision agriculture*

The concept behind precision fruticulture is derived from the established concept of precision agriculture (Auernhammer, 2001; Sadler et al., 1998; Srinivasan, 2006; Stafford et al., 2000). In precision agriculture, it is already possible to create, evaluate, and react to georeferenced maps from automatically measured and collected data. (Blackmore et al., 2003; Auernhammer 2001). This management leads to a significant increase in yield (Fountas et al., 2011). The spatial variability of the yield makes it possible to identify areas in the crop that are over- or undersupplied with water or fertilizer (Gebbers and Adamchuk, 2010). Using this, the growth factor like chemical soil properties can be adjusted and the operations optimized for their economy and sustainability (Auernhammer 2001; Zhang et al, 2002; Bongiovanni and Lowenberg-Deboer 2004).

In fruit production, Zude-Sasse et al. (2016) assume that fruit trees are influenced by changes in supply of light, water, and nutrients, and further that the plants will likely adjust to those changed conditions.

Site-specific management in field cultures includes the analysis of yield maps, while taking into account the relevant soil variables (Hedley, 2015). These parameters are, for example, soil texture and chemical properties, especially the pH value (Schirrman et al., 2011, Leinweber et al 1996). To get the necessary spatial resolution of soil variability, tried and tested sensors were used which were also usable for fruticulture (Corwin und Lesch, 2003), taking the structure of the orchard into account (Winter und Link, 2002).

All sensors currently available differ not just in the way they work, but also in their depth range and sensitivity (Gebbers et al, 2009). A commonly used method for analyzing the variability of the soil is its electrical conductivity (ECa) using direct current geoelectricity (Allred et al., 2008). The ECa is the ability of a material to conduct electric current (Telford et al., 1990). Using the ECa, it is possible to image the variability of the soil, showing parameters like texture, water saturation, fluid conductivity, changes in density, and organic substances (Lück et al., 2009). The soil's conductivity depends on many factors, such as saturation, activity, and the mixture of soluble salts, as well as the clay content (Corwin und Lesch, 2003). Furthermore, the soils are also influenced by variations in how they were created, developed, and influenced, for example through glaciation (Richard et al., 2001; Kleber, 1992; Kutílek and Nielsen, 1994; Bouma et al., 1990).

### *1.2.2 Precision fruticulture*

According to Zude-Sasse et al. (2016), "precision fruticulture" is to be understood as follows:

They consider every approach that uses in-situ information of soil and plant aiming to manage the orchard more precisely as PRECISION HORTICULTURE.

This includes on-site sensor-controlled process solutions for environmentally friendly and competitive production of quality fruit (Zude-Sasse et al., 2016). To that end, spatially differentiated data about the multi-year plants and soils are collected directly by the apparatus, which makes it possible to adjust the work processes and optimize production and harvest (Zude-Sasse et al., 2016, Peeters et al., 2015; Fereres and Soriano, 2007).

Currently, the possibilities of automated data collection include the use of autonomous vehicular platforms, unmanned drones, and wireless sensor networks (Bendig, 2015; Nink et al., 2015; Fukatsu et al., 2014). The number of automated measurements for the various fruit cultures is increasing constantly (Zude-Sasse et al., 2016). This data is then transferred to the spatial decision support system (Fountas et al., 2006).

As with precision agriculture, precision fruticulture can be considered a cycle system (Gebbers and Adamchuk, 2010). Figure 1 shows the modified version of the cycle system with the following steps: data collection and localization, data analysis, management decisions on applications, implementation, and evaluation of management decisions (Zude-Sasse et al., 2016).

Data collection is taken on each single tree. Taking into account that measures such as flower thinning (Link, 2000; Jafari et al 2014) must be performed in orchards, data such as the number of flowers must be collected several times. The data localization is determined by the established GNSS method and brought into relation to the boniture data (e.g. manuel count of the number of flowers). Furthermore, the data localization is used for measuring spatial data. All data collected will be analyzed and the results brought into management

decisions on implementations, where they will be implemented and evaluated before the cycle system is started new.
In contrast to precision agriculture, not all steps in precision fruticulture are fully established yet (green). The management decisions for implementations are currently the latest research question (blue), with the challenge being to record high-resolution spatial data in orchards. The steps implementation and evaluation of management decisions are currently still challenging (gray).

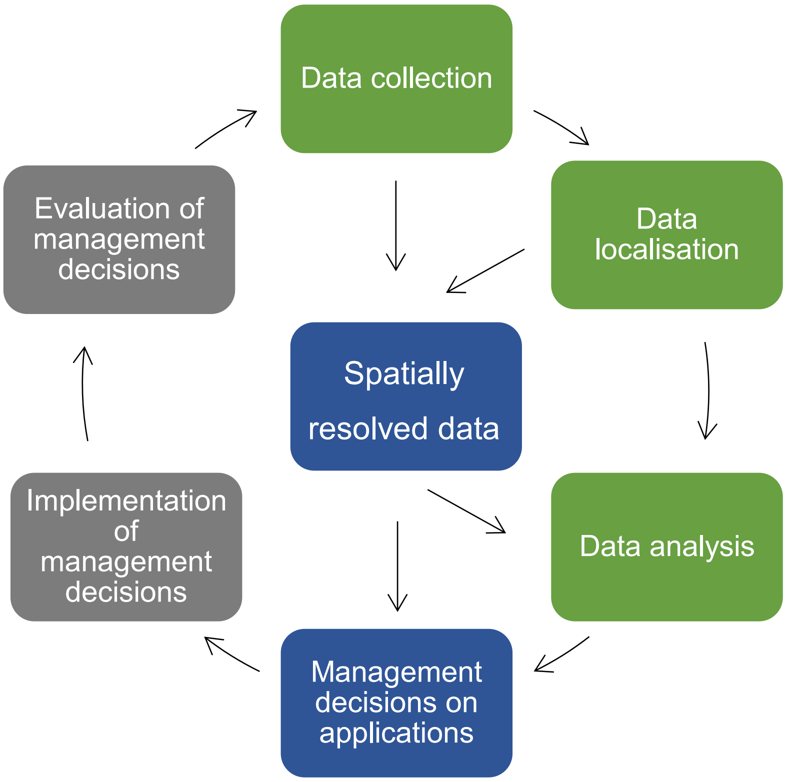


Figure 1. Shows the circle system of precision fruticulture modified from the concept of precision agriculture. The different colors symbolize the stage of the steps (green: established, blue: ongoing research, grey: future work) related to applications in fruit production.

As according to the concept of precision fruticulture, information about yields in tons per hectare are probably not enough to react appropriately and save resources (Aggelopoulou et al., 2011; Aggelopoulou et al., 2013). The quality of the harvested product must be much more intensively considered (Konopatzki et al., 2015, Scharf, 2015; Cohen et al, 2012; Ehsani and Karim, 2010). This is the most important challenge in precision fruticulture (Zude-Sasse et al., 2016).

Furthermore, necessary production methods like thinning (Link, 2000; Jafari et al., 2014), pruning, irrigation (Ben-Gal et al., 2009; González-Dugo et al., 2015; Goodwin et al, 2008; Fereres et al., 2003), harvesting (Zude et al., 2008) present possible macro paths to optimization, whereas site-specific management is plausible for individual trees or areas (Zude-Sasse et al., 2016).

This type of data-driven management with the aid of soil and plant information in fruit orchards has so far only been discussed in very few scientific papers. Bramley and Hamilton (2004) identified yield zones in vineyards. Zaman and Schumann (2006), Nadler (2004), Gebbers and Zude (2008), Bramley and Hamilton (2004), and Ben-Gal et al. (2008) observed high variability in the soil in between fruit trees. They found that the soil properties could be connected to describe plant growth, yield, and fruit quality. Nadler (2004) used a portable electric conductivity meter to check variations in water in the soil ~~and to measure the root water potential~~. Zude and colleagues (Zude et al., 2008) analyzed spatial patterns of fruit quality in citrus fruit. For apples, Gebbers and Zude (2008) and Aggelopoulou et al. (2013) measured temporal and spatial changes in fruit quality as related to electrical conductivity of the soil.

For spatial analyses, the use of remote sensing technology makes it possible to quickly gather data for soil and plant information in a contact less blanket method (Thorp and Tian, 2004; Panda et al., 2010). During the past 20 years the development of different electrical sensors for determining soilmoisture at a point has advanced considerably (Robinson et al., 2008). Among others, tensiometers were used for long-term monitoring (Ling, 2004).

The variability of chemical properties of the soil can be comprehensively estimated using on-the-go sensors for visual light and near-infrared (Vis/NIR) spectroscopy (Schirrman et al, 2011; Schirrmann and Domsch, 2011), electromagnetic induction (Hartsock et al, 2000), or apparent resistance measurements (Allred et al., 2008). For the measurement of ECa on large fields, various methods and tools from geophysics can be used (Gebbers and Lück, 2008; Halvorson and Rhoades 1976; Lück and Rühlmann 2013, Lück et al., 2009). Using optical multi- and hyperspectral settings, the electromagnetic spectrum can be observed (Usha and Sigh, 2013).

By measuring light reflected from the soil or from plants using the Normalized Difference Vegetation Index (NDVI), one can derive useful information about the chlorophyll content of the plants and of the harvested product (Govender et al., 2007; Hall et al., 2002; Zude, 2003). This is reinforced by the work of Ač et al. (2015). This workgroup estimated the chlorophyll and water content of the canopy with the help of fluorescence (Ač et al., 2015). Liakos et al. (2011) showed a connection between NDVI and yield in apples. Furthermore, Tucker et al. (1980) demonstrated a process with near-infrared to find leaf water potential.

Xujum et al. (2007) demonstrated potential in selective harvesting of citrus fruit with the aid of hyperspectral imaging.

However, the use of nondestructive soil and plant sensors in fruticulture is limited. Open field fruit cultivation is characterized by established growth factors like $CO_2$ concentration, air and soil temperatures, the chemical and physical soil properties, but also changeable factors like microclimate, water supply, and the endogenic distribution of substances (Blume et al., 2010).

For long-term cultures, the climate and growth factors of geographic location present a challenge. Here is where the potential for precision fruit cultivation lies. The properties of the climate for the location may be viewed as fixed, but are not steady-state. The micro climate can change through pruning and cutting; this influences other parameters like pests, water use, and metabolic activity — in particular the respiration rate (Kang et al., 2002; Simon et al., 2006; Schneider and Childers, 1941).

### *1.2.3 Growth factor water*

One of the most important and changeable growth factors is water. The freshwater needed for irrigation is a limited resource (Naor et al., 2006). Among other things, a water shortage causes reduced yield and equality in the harvested products (Berman and DeJong, 1996). In particular, it is important to note the total amount of fruit per liter of water while considering the fruit quality (Moriana et al., 2003). Therefore it is necessary to irrigate efficiently. In current practice, the irrigation amounts and intervals are regulated through taking measurements with tensiometers or evaluating climate data (Nadler, 2004). However, the actual water requirements of the plants, which show in stress indicators, are not taken into account in commercial fruit production (Naor et al., 2006; Maes and Steppe, 2012; Sadeghi et al. 1994). Stress indicators include a rise in leaf temperature (Jones et al., 2002), closed stomata (Scholander et al., 1965), and an impaired flow in the xylem (Tromp, 1984). Even a small drought stress causes changes in physiological parameters like the leaf water potential and stomatic conductivity (Elsayed-Farag and Melgar, 2015).

For pears, Naor et al. (2006) demonstrated that leaf analysis of water potential, transpiration rate, and the maximum change in stem thickness can be used as stress indicators. Meanwhile they showed that, for apples and nectarines, soil moisture is a better stress indicator (Naor et al., 2006). This is especially true of young tress (Moriana and Fereres, 2003).

With the aid of established water potential measurements, trials in fruit cultivation have spot tested current water deficits of plants (Choné et al., 2001, Scholander et al., 1965). By using pressure chamber technology, the leaf potential (LWP), the predawn water potential (PDWP), as well as the stem water potential (SWP) may be determined (Herroero-Langreo et al., 2013).

This method is based on a high correlation between the LWP and the soil water content (Williams and Araujo, 2002). This is true for various fruit (citrus, apples, olives, wine grapes) in the subtropics as well as temperate zones (Williams and Araujo, 2002; Jones 2007; Ünlü 2014; Nadler 2004). Ünlü et al. (2014) further showed the connections between yield and LWP ($R^2$= 0.68) and between yield and soil water depletion ($R^2$= 0.66) in grapefruit. Top of this, Naor (2000) investigated apples, grapevines, litchi, and nectarines, and found that the stem water potential was a better water stress indicator than LWP. This was supported by continuing work by Naor and Cohen (2003). Gómez-del-Campo (2013) showed that a reduced stem water potential also is a positive influence on the fruit size (Naor et al., 2001). Leib et al. (2006) showed the same for apples and Mahhou et al. (2006) did as well for peaches.

For grapevines, Griona et al. (2006) investigated the connection between water potential and the fruit quality. The workgroup showed that drought stress was a negative influence on the size of the fruit as well as the water content and sweetness of the grapes. That said, Herroero-Langreo et al. (2013) had a better result with a higher correlation to fruit quality, while the type of water potential measurement was irrelevant.

In addition, the plant temperature can nondestructively record the plant's water availability (Gates, 1964). This is founded on the work of Ido and Jackson (Ido, 1982; Jackson 1981) and is termed the Crop Water Stress Index (CWSI). In 1982, Ido examined various crop non-water stress baselines using the vapor pressure deficit (VPD), although air temperature (Tair) and canopy temperature (Tc) were manually recorded. According to Fuchs (1990), the manual measurement of leaf temperature is not possible, since atmospheric influences such as air temperature, humidity, wind speed, and solar radiation lead to different conditions within each measurement. Jones (1992, 2004) expanded on this approach by taking into account variable climactic conditions for arid and semi-arid regions. In 2013, González-Dugo et al. investigated water status for five different fruit types (almonds, apricots, peaches, lemons, and oranges) with the help of thermal imaging. They were able to show that the stem water potential does well with Tair-Tc. Sepaskhah and Kashefipour (1994) reached the same conclusions with sweet limes.

As the plant water status is further influenced by soil, canopy dimension, topography, and irrigation intervals, only a few trees could be measured in open field conditions (Cohen et al., 2005; Berni et al., 2009). With thermal imaging is it possible to remotely and comprehensively collect CWSI data for an entire plot (Jones, 2002; Acevedo-Opazo et al., 2008; González-Dugo et al., 2006; Bellvert et al., 2014a). A further advantage is the possibility of automated measurement, which makes CWSI a cost-effective method (González-Dugo et al., 2006). At the same time, the modification of the equation for different reference points for wet and dry leads to the CWSI becoming ever closer to the mark (Irmak et al. 2000; Jones 1999, Meron et al. 2010). For example, Meron et al. (2010) adjusted the equation for the artificially wet reference plot, and Irmak et al. (2000) used the dry reference Tair + 5°C. Cohen et al. (2015) connected the method used by Meron et al. (2010) and Irmak et al. (2000) and showed a connection ($R^2$= 0.82) between LWP and CWSI in various development stages of cotton. For grapevines, Bellvert et al. (2014b) found the same. Aside from that, Möller et al. (2007) used an adjusted equation for grapevines that the connection between CWSI and leaf conductivity is robust. Rud et al., (2015) supported this with their work on salt-induced effects in olives. The work of Cohen et al. (2005) showed that the connection between CWSI and LWP is stable. Furthermore, Agam et al. (2014) were able to document less distinctive water stress in olives in arid areas with the help of thermal images. This group showed further that differences in tree volume were expected to produce varied stress level of $r^2$ = 0.88.

Long-term water stress is reflected in the leaf surfaces of the tree (Käthner et al., 2014). This can be automatically measured with Light detection and ranging (LiDAR) (Zaman and Schuhmann, 2006; Zaman and Salyani, 2004). Rosell et al. (2009) showed that this method shows a good correlation between manual and sensor-based measurements of vegetative volume in tree row plantations of apples, pears, and grapevines. Acevedo-Opazo et al. (2010) were further able to show in their study of a non-irrigated vineyard in France that trunk circumference and leaf area are mainly influenced by vine water status. The work of Intrigliolo and Castel (2006a) supported this, as they found that reduction in leaf area is caused by water stress.

All these researches were primary performed in arid to semi-arid areas, while most of the trial plots in semi-humid climates were artificially irrigated. This study is focused on the use of these methods in a semi-humid area. The authors took into account yield maximization, sparing resources, and quality optimization.

## 1.3 Statement of the hypothesis and research objectives

It is hypothesized that:

1. There is soil variability in our region's fruit plantations. The soil was formed by different glacial events during the upper pleitocene. As a consequence different grain size distribution and different water saturation was developed. And this influence the water and nutrient supply into the soil. Thus it could be an influence of the fruit quality
2. The water status of the trees could show spatial differences.
3. Both factors could affect the fruit quality.

To test the previous hypothesizes, the following research objectives were established.

i) Characterization of the 3D distribution of the apparent electrical conductivity of the soil and variability of the plant's water status

The present study is intended to characterize a plot based on apparent electrical conductivity, land topography, and the trunk water status. For this, a plum orchard in a semi-humid climate in Marquardt, Germany was tested. The apparent electrical conductivity of the soil should be used to see which depth has the most influence on the generative growth, e.g. flower set and fruit set, of the fruit tree. To that end, a 3D model of the conductivity of the soil over the entire orchard is to be recorded. Aside from that, various monitoring data and fruit quality parameters will be recorded for each individual tree. The characterization of the connections between the chosen variables shall be determined.

ii) Investigation of the interaction between ECa, the crop water stress index (CWSI), and fruit quality

The water availability of the tree should be of particular interest, which plays an important role in product quality. For this, water content of the soil and plant will be determined with an established measurement method. A sensor to monitoring of soil matric potential is called pF-meter and a Scholander pressure bomb are particularly effective, since the water potential of a plant is recorded. Additionally, the sensor-provided data will be compared to the gravimetric tests. With a commercial technique, the Scholander bomb, for measuring the median plant water potential, the current plant water deficit should be destructively determined. Furthermore, with the aid of thermographic data, the study will seek to find a non-destructive and spatially resolved method for determining the plant water status for individual trees. From the thermal data, the CWSI of the tree in a semi-humid climate should be determined.

iii) Possibility of division of management zones with respect to irrigation.

Various evaluation methods should help determine how the spatially resolved plant and soil data relate to one another. For example, the fruit quality, monitor data, and optical fruit data will be employed. The statistical analysis will be performed with the statistics package of MATLAB® (R2010b & R2016b, MathWorks, USA).

An evaluation process should be found that makes possible a spatial analysis of soil and plant. A free “spatial toolbox” program with algorithms for hotspot analysis shows the potential for this.

# 2 Interaction of 3D soil electrical conductivity and generative growth in *Prunus domestica* L.

(European Journal of Horticultural Science. 2015, 80 (5): 231-239, DOI: 10.17660/eJHS.2015/80.5.5)

Correctio: page 17 para 1 were inserted: per tree

page 20: # fruit instead of yield

## 2.1 Summary

Examination of spatial soil heterogeneity within orchards may provide an approach for precise, more sustainable production processes. In predominantly sandy soil, which was formed by glacial and post-glacial deposits, generative growth of plum trees (*Prunus domestica* 'Tophit plus', n=156) were closely analyzed (flower set, fruit set, fruit drop, fruit size, fruit pigments, and yield), and classified according to the apparent electrical conductivity (ECa) of the soil in three depths (topsoil, root zone, subsoil). The soil ECa showed small scale variability between 1.3 mS/m and 76.7 mS/m with stable pattern for two years ($r = 0.88$). The ECa in different depths corresponded to the compaction profile and water content of the sandy soil. The ECa in the root zone correlated to tree growth. However, the ECa of topsoil and the elevation (slope = 3.15°) of the terrain had a similar or enhanced impact. The ECa in the topsoil and elevation were correlated with fruit set at $r = 0.17$ ($p = 0.011$) and $r = -0.45$ ($p = 0.133$), and fruit size at $r = 0.06$ ($p < 0.001$) and $r = 0.05$ ($p < 0.001$) respectively. Such findings are particularly interesting for orchards with graded elevation gradient or soil compaction from mechanical weed control.

Keywords: electrical conductivity, fruit, plum, precision fruticulture, spatial variability

## 2.2 Introduction

The concept of precision fruticulture follows the knowledge achieved in site-specific farming over the last decades. Using spatial information of soil and variability of plant phenotype, zones can be marked that are under- or over-supplied with a certain growth factor. This information can be used to optimise farm profitability and sustainability (Auernhammer, 2001; Zhang et al., 2002). However, for management charting of orchards, the approach may need hedging due to more complex root system responding to the environment in perennial plants.

In orchards, methods for spatial soil analysis such as georadar, electromagnetic, and seismic readings are either not suitable to provide the necessary spatial resolution or interfere with machinery and constructions in the orchards such as drip irrigation. Therefore, electrical conductivity (ECa) is frequently used for spatially analyzing soil pattern in orchard and vineyard. ECa is measured by means of apparent resistance readings (Allred et al. 2008). To map the soil ECa, set-ups as rolling system are unsuitable, again due to interference with trees and machinery in the orchard (Gebbers et al., 2009; Lück and Rühlmann, 2013). Instead, direct current geoelectric readings can be applied using four electrodes on a mobile frame, with the measurement spot close to the tree (Wenner, 1915; Pozdnyakov and Pozdnyakov, 2002). Direct current is coupled to the soil and as a function of spatial distribution of resistivity; an electrical field is built up. The strength and direction of direct current remains equal for each measurement. Using Ohm's law, ECa can be measured (Telford et al. 1990). By setting the distance of electrodes, the desired measuring depth can be addressed (Mancuso, 2012). The relative depth response of the signal with a electrode spacing of 0.5 m shows a peak at 0.17 m depth (Joschko et al., 2009), where 100% of the signal is contributed by this setup. By means of a multi-electrode array, a 3D cube of soil ECa can be mapped, providing enhanced spatial resolution by decreasing the electrode spacing (Loke and Barker, 1996; Reynolds, 1997). ECa appears to be feasible for delineating soil heterogeneity, even if it provides a merged signal for texture, water content, and pH, as well as fluid conductivity and organic matter (Lück et al., 2009). In areas with high spatial variability, ECa is a qualitative indicator for soil texture (Molin and Faulin, 2012), while in particular for low variability, the influence of soil moisture, activity, or composition of dissolved ions as well as clay content determine the lead of the current in the soil (Corwin and Lesch, 2003; Telford et al., 1990). Consequently, low, but small scale variability of soil ECa points to varying root environment caused by natural soil development or production measures as mechanical weed control.

Rodriguez-Perez et al. (2011) applied a soil electrical conductivity meter in a vineyard to characterize spatial distribution of soil with high clay content. It was pointed out that ECa data can be used to obtain a cartographic representation of spatially complex soil at different depths. Mc Bratney et al. (2005) showed that ECa can be used for delineating management zones in different parts of New South Wales Australia. The work from Hartsock and co-workers, which was carried out in an orchard, shows that absolute ECa varied, but spatial pattern of ECa were stable over two seasons (Hartsock et al., 2000).

By means of correlation analysis regarding soil and plant parameters in vineyards, ECa was indicated to be useful for describing soil-plant-interaction with respect to trunk circumference, and yield (Bramley et al., 2011; 2004). Findings were presented for soil showing high variability of ECa. Furthermore, several studies carried out in the Marlborough region of New Zealand revealed that plant variability in vineyards was influenced by variation in the soil (Bramley and Hamilton, 2004; Trought et al., 2008). Here, pattern of silty hollows, sand, and some gravel was interesting for vintners in parceling and harvest scheduling (Trought and Bramley, 2011). Furthermore, Cortell et al., (2005) have shown that soil depth and corresponding water-holding capacity have both direct effects on vine vigor as well as indirect effects on vine microclimates. As a result, accumulation of phenolic compounds in the fruit appeared in spatial pattern. Reynolds et al., (2007) described the interaction of chemical composition of grapes and soil texture as well as chemical composition of the soil.

In fruit trees, soil properties were correlated to plant growth and fruit quality, mainly in studies on citrus and pip fruits: Zaman and Schumann (2006) measured spatial pattern of yield and its spatial correlation with respect to different soil zones for *Citrus × sinensis* L. (oranges). The influence of spatial variability of chemical soil properties on *Pyrus communis* L. (pears) fruit trees was analyzed by monitoring spatial pattern of fruit diameter (Konopatzki et al., 2008). In commercial production of *Malus × domestica* Borkh. (apples), it was pointed out that fruit development and soil ECa correlated (Gebbers and Zude, 2010; Türker et al., 2011). High-value stone fruits have so far been rarely studied. The impact of tomography on soil properties including ECa has been described for several landscapes resulting in sometimes opposite conclusions. However, elevation was even considered for delineating management zones in citrus production (Siqueira et al., 2010).

The present study is aimed at evaluating the interaction of small-scale variations in soil ECa pattern and tree growth. The objectives were (i) to characterize the orchard considering spatial variability of soil ECa in different depths and the slope of the terrain, and (ii) to evaluate its correlations to generative growth in plum trees.

## 2.3 Material and Methods

### *2.3.1 Experimental design*

In 2011 and 2012, measurements were carried out in plum (*Prunus domestica* L.) orchard with a size of 0.37 ha located in Potsdam, Germany. The climate is temperate and the terrain is 42 m above sea level. The main soil consists of predominantly sandy soils, which were formed by glacial and post-glacial deposits after the last ice age about 10000 years ago. Drip irrigation with 0.5 m spacing in the row was maintained in the entire orchard with one application level: Each dripper delivered 1.6 ±0.1 liters within 30 min. Irrigation was performed every three days from April to September. Weed control in the rows was carried out using a rotary cultivator three times per year since 2009.

The plantation consisted of six rows with a total of 180 plum trees, with 5 m between rows and 4 m between plants in each row. Trees were planted at two ages, both in the dormancy period 2008 – 2009. Consequently, trees were five and six years old in 2012. All measurements were carried out in 2011 and 2012 on each of the 180 plum trees. The cultivar used in the experiment is 'Tophit plus' budded on Wavit, while 24 pollinator trees ('Jojo' on Wavit) were excluded from the data set. All trees had an adventitious root system. The unripe fruits are green, while ripe fruit appear as large blue fruits with a yellow flesh.

#### *2.3.2 Topographic readings*

Tree positions were recorded by an RTK-GPS system (HiPer Pro, Topcon Corporation, Japan), while providing geographical data using the WGS 84 System. Horizontal data was used for linking ECa and tree data. Vertical data provided the elevation of each tree, where the positions of highest and lowest trees were used to calculate the slope of orchard.

The horizontal and vertical margins of error for this system were less than 0.03 m and 0.04 m, respectively. Topographical data was captured with 5 m measuring intervals in x and 0.50 m in y-axis. The topographical model was created using a combination of natural nearest neighbor interpolation and a triangulation tool from MATLAB® (R2010B, MathWorks, U.S.), then converted to grid surface map with 0.50 m grid resolution.

#### *2.3.3 Soil analyses*

##### *2.3.3.1 ECa tomography*

Apparent soil ECa was analyzed using electrode configuration as a Wenner array (4-point light hp, LGM, Germany), in which four electrodes are arranged in line equally spaced. Two outer electrodes are current electrodes and two inner electrodes are potential electrodes (Mancuso, 2012). All measurements were taken with one additional ground electrode in one place in order to obtain more stable data. Measurements were carried out in two seasons (2011, 2012) on each tree with an electrode spacing of 1 m, and additionally in 2011 with an electrode spacing of 0.25 m at right angles to tree rows. When measuring electrical resistance, the penetration depth depends on the spacing of transmitting electrodes, which were adjusted in the range from 0.75 m up to 20 m. As a result, penetration depth was at minimum 0.08 m and at maximum 2.20 m. An area of 192.0 m x 37.5 m was analyzed with 1.0 m measuring intervals in the x- and 0.5 m in the y-axis.

The values of electrical resistance were inverted and pre-analyzed in RES2DINV (Geotomo software, allied associates geophysical LTD, United Kingdom). Inversion of resistivity was conducted by a least-square method involving finite-element and finite-difference methods (Loke and Barker, 1996). With these steps, 132 profiles in the y-axis were obtained and, by using the tree position, tree-specific ECa values were calculated.

#### *2.3.3.2 Boreholes*

Additionally, geoelectric (4-point light hp, LGM, Germany) measurements were carried out in boreholes located 0.10 m north to the stem of 37 randomly selected trees in order to measure the depth profiles of soil variability with enhanced spatial resolution. ECa was analyzed at every 0.05 m for the uppermost 1 m depth by using the Wenner electrode configuration with electrode (0.30 m diameter and 0.03 m thickness) distance of 0.25 m.

The distribution of water infiltration was recorded at the trees, where borehole analysis was applied. Mimicking irrigation, over a period of 30 minutes 1.6 liters were deposited at an incident point and the profile was cut off with a spade, perpendicular to the irrigation tube. Visually wet areas were manually measured with 2 cm resolution in x- and y-axis.

Also, soil texture was recorded by wet-sieving and sedimentation with the Köhn-Pipette method using $Na_4P_2O_7$ (Hartge and Horn, 1992). The content of fine particles was calculated from total clay content plus content of fine silt (< 0.0063 mm). The soil texture classification was carried out according to Bouyoucos (Bouyoucos, 1951) at five different depths (0-5 cm, 15-20 cm, 20-30 cm, 30-60 cm, and 60-100 cm).

At same positions, penetration resistance (PR) of soil was measured with a hand-held penetrometer (06.01.SA, Eijkelkamp, Netherlands) equipped with a probe cone of 3.3 cm and an opening angle of 60°. The ratio between measured value and probe cone provides the PR [kN/cm²]. The PR was measured along the rows, twice on opposite sides of trees at 0-5 cm, 15-20 cm, 20-30 cm, 30-60 cm and 60-100 cm.

Soil samples (n=10) were taken randomized for chemical analysis of organic matter, pH, salinity, phosphorus, potassium, magnesium, calcium, sodium, and chlorine according to standardized methods (VDLUFA, 2003).

### *2.3.4 Location of roots*

By the end of the experiment, 31 trees were excavated and the number of roots was counted to estimate the root zone. Roots were found between 0 and 60 cm depth with marginal number of roots above 25 and below 50 cm, which was defined as root zone in the present study. Trees showed their maximum root density between 25 and 30 cm.

### *2.3.5 Plant readings*

Measurements were carried out in phenological stages 6, 7, and 8 (Meier, 2001). On each of the 180 plums the following indicators of generative growth were measured: flower set [#flowers/tree], fruit set [#fruit/tree], fruit drop [#fruit/tree], yield [#fruit/tree] and [kg/tree], fruit size [mm/fruit]. Flower set was measured as inflorescences as well as individual flowers per tree, with an average of 1.3 flowers per inflorescence. Fruit size was measured by height considering the length of fruit in the peduncle plane on all fruit. Fruit development and ripening were followed in weekly measurements on 10 fruit per tree. Two non-destructive optical fruit sensors were employed, both addressing the chlorophyll content of fruits by means of indices established for peach and apple (Zude, 2003; Ziosi et al, 2008). One multispectral sensor (DA-Meter, Sintéleia, Italy) used light-emitting diodes and a photodiode detector with a filter to measure the absorbance at 670 nm and 730 nm. The DA-index is calculated as intensity difference of these two wavelengths. Also, a spectrophotometer capturing the wavelength range of 500-1100 nm (Pigment Analyzer, CP, Germany) was applied. The variable of note was the normalized difference vegetation index (NDVI) that was calculated from remittance (R) intensities at indexed wavelengths (CP, 2002) by NDVI = $(R_{780} – R_{660}) / (R_{780} + R_{660})$.

### *2.3.6 Statistical analyses*

Growth data were transformed into a normalized distribution using a variance-stabilizing method by processing the root of raw data. The multiple-path analysis of variance, ANOVA, was applied (i) to identify the most suitable number of classes of soil ECa and (ii) to test the effect of ECa depths and elevation on the means of tree data (Webster and Oliver, 1990). Linear correlation analysis and ANOVA were carried out in the statistical package for MATLAB® (R2010B, MathWorks, U.S.).

## 2.4 Results and Discussion

### *2.4.1 Correlation of soil ECa and tree data in two growing seasons*

Geoelectrical readings of soil ECa revealed spatial pattern ranging from 1.3 mS/m to 76.7 mS/m (Figure 2). Small-scale differences resulted in variations in soil conditions even for neighboring trees. Soil ECa in the root zone, measured in 2011 and 2012, resulted in a linear correlation coefficient of r = 0.884, which points to a temporally stable soil pattern over time. Also, readings at different soil depths correlated highly with r = 0.917, 0.898, and 0.985 for topsoil and root zone, for topsoil and subsoil, and for root zone and subsoil, respectively.

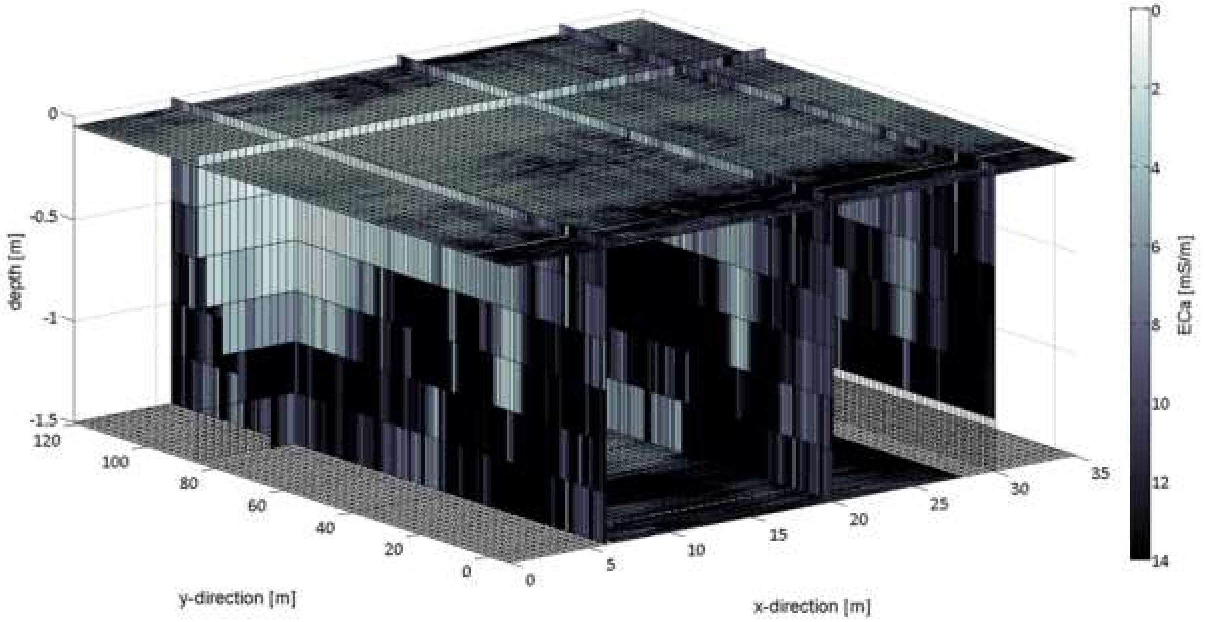


Figure 2. 3D soil ECa cube with 35 m in the x- axis, 132 m in the y-axis and 1.5 m in the depth. The ECa values of the cube range from 1.3 mS/m to 76.7 mS/m. Legend was cut at 16 mS/m to increase the contrast in the low variability relevant in the topsoil and root zone.

In 2011, trees, planted as one-year budded material, only approached maturation. The mean data for flower set and yield per tree were 1561.28 (+/-493.64) and 240.17 (+/-98.34), respectively. The Pearson correlation of soil ECa and tree data measured in 2011 was r = 0.521 for yield and r < 0.400 for remaining variables (Table 1). In 2012, mean values for flower set and yield were increased to 1075.68 (+/-329.20) and 970.49 (+/-190.43), respectively. Correlations were found for soil ECa and yield as well as fruit quality considering fruit size and fruit pigmentation (NDVI and DA-Index). However, compared to data of 2011, in 2012 the correlation coefficient slightly decreased for all variables including yield and fruit size, but results are significant only in 2012 due to larger data sets and reduced variance in mature trees (Figure 3a). Due to the significance of this, the second year of experiments will be presented in further detail.

Table 1. Pearson correlation coefficients (r) of generative tree data and soil electrical conductivity, ECa, at three depths measured in a Prunus domestica orchard. Fruit data was measured on 10 fruit per tree and are given as mean values for each tree (n). The presented trees were planted as one-year old budded material and were 4 years old in 2011.

| Tree data (n) | $ECa_{topsoil}$ | $ECa_{root\ zone}$ | $ECa_{subsoil}$ |
|---|---|---|---|
| Flower set (104) | 0.10* | 0.05* | 0.04* |
| Fruit set (96) | 0.20* | 0.14* | 0.11* |
| Fruit drop (96) | -0.06* | 0.02* | 0.02* |
| # Fruit (71) | 0.36* | 0.40* | 0.40* |
| Fruit height (251[1]) | 0.08* | 0.18* | 0.19* |
| Yield (12[2]) | 0.52* | 0.33* | 0.34* |

[1] fruit basis, while all other values were measured on a tree basis; [2] note that only 12 trees were recorded, since most trees lost their fruit already by pre-harvest fruit drop
* significance level of 0.05

### *2.4.2 Interaction of soil ECa in different depths and tree data in the second year of the experiment*

F values for classes according to ECa values of topsoil and subsoil were calculated. However, F values showed no significance apart from flower set ($ECa_{topsoil}$: F = 1.43 and p = 0.21; $ECa_{subsoil}$: F = 4.02 and p = 0.02). The F values for tree data from ANOVA, resulting from classes based on ECa in the root zone, ranged from 0.01 to 8.2 with different number of soil classes (Figure 4). As a result, ECa values in the root zone were used to group the data into 8 classes according to the highest F values. Nevertheless, a test was carried out on classes with respect to ECa in other depths (data not shown). In this approach, classes of topsoil were evaluated for analyzing the root zone and subsoil; then the classes of root zone were applied for analyzing topsoil and subsoil; and subsoil classes were used for analyzing root zone and subsoil interaction with yield parameters. For each of these three variants, an ANOVA calculation was performed. This approach revealed that only the group related to the root zone shows a dependency between tree data and ECa values. Consequently, all subsequent calculations of ANOVA were carried out according to 8 soil classes based on ECa in the root zone. In the orchard, class 8 is the most frequent, but this disproportion has had no effect on the ANOVA results obtained.

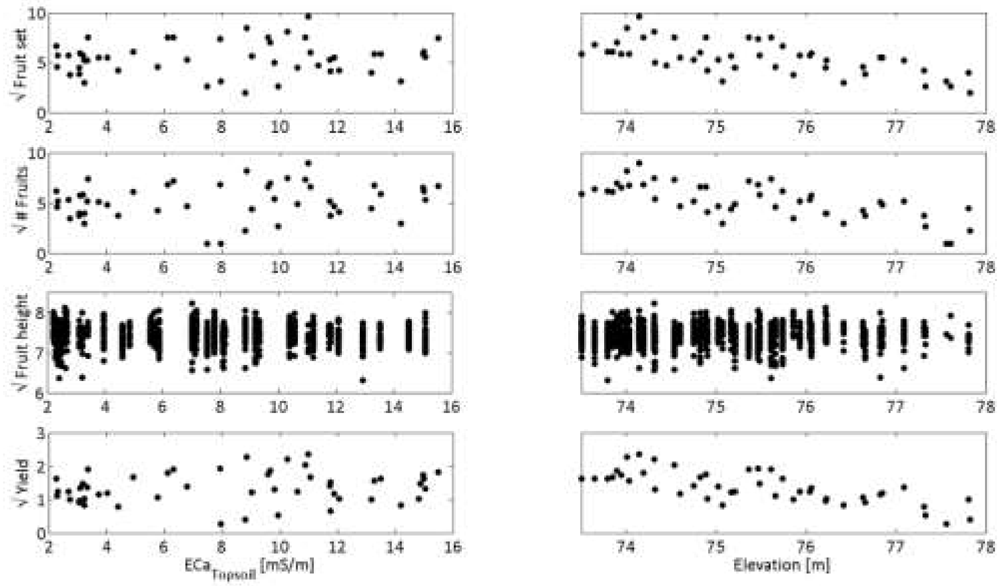


Figure 3. Scatter plot Scatter plots from six-year-old trees in the second year of the experiment, where the root of values of fruit set (n = 97, r = 0.17 for $ECa_{topsoil}$; and -0.45 for elevation), # fruits/tree (n = 83, r = 0.18; -0.45), fruit height (n = 1378, r = 0.06; -0.05), and yield in kg/tree (n = 87, r = 0.04; -0.54) are plotted over $ECa_{topsoil}$ (a) and elevation (b).

Interaction of tree data and ECa at different soil depths was found (Table 2). In 2012, soil $ECa_{root\ zone}$ showed an interaction with flower set and fruit set in trees planted as one-year old budded material. Such findings were confirmed on trees planted as 2-year budded material and a resulting age of six years (Table 2).

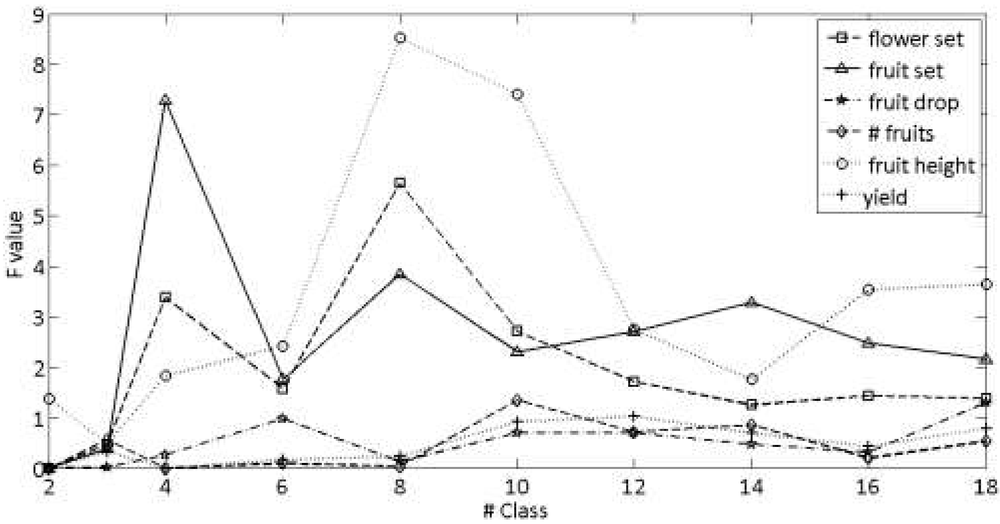


Figure 4. The F values of normalized plant parameters (flower set, fruit set, fruit drop, # fruit per tree, fruit height in mm per fruit, yield in kg per tree) for a different number of classes considering ECa in the root zone.

Table 2. ANOVA results showing F- and p-values of plant parameters in 2012 for trees planted in winter 2008/2009 as one- and two-year-old budded material. ANOVA was carried out on the classed tree data after transformation to normal distribution by the root of raw data.

| Plant parameter | | $ECa_{topsoil}$ | | $ECa_{root\ zone}$ | | $ECa_{subsoil}$ | |
|---|---|---|---|---|---|---|---|
| | | F | p < F | F | p < F | F | p < F |
| 5-year old trees | Flower set | 1.87 | 0.084 | 5.65 | **0.005** | 9.54 | **0.003** |
| | Fruit set | 1.58 | 0.153 | 3.84 | **0.025** | 0.01 | n. s. |
| | Fruit drop | 1.17 | n. s. | 0.12 | n. s. | 2.57 | n. s. |
| | # Fruits | 1.26 | n. s. | 0.03 | n. s. | 0.02 | n. s. |
| | Fruit height* | 5.11 | **< 0.001** | 2.52 | 0.113 | 1.47 | n. s. |
| | Yield | 0.93 | n. s. | 0.22 | n. s. | 0 | n. s. |
| | Fruit NDVI* | 1.87 | 0.152 | 1.47 | 0.242 | 0 | n. s. |
| | DA-index* | 3.27 | **0.032** | 1.96 | 0.157 | 0 | n. s. |
| 6-year old trees | Flower set | 14.25 | **0** | 5.64 | **0.022** | 0.05 | n. s. |
| | Fruit set | 9.61 | **< 0.001** | 4.55 | **0.039** | 1.82 | n. s. |
| | Fruit drop | 4.37 | **0.009** | 1.65 | n. s. | 2.15 | 0.129 |
| | # Fruit | 6.70 | **0.001** | 0.27 | n. s. | 1.13 | n. s. |
| | Fruit height* | 13.77 | **< 0.001** | 21.32 | **< 0.001** | 0.95 | n. s. |
| | Yield | 2.20 | 0.125 | 0.91 | n. s. | 1.35 | n. s. |
| | Fruit NDVI* | 0.39 | 0.540 | 0.08 | 0.916 | 4.68 | **0.042** |
| | DA-index* | 0.50 | 0.486 | 0.35 | 0.708 | 1.83 | 0.190 |

* means on each tree was considered, calculated from readings on all fruit per tree for fruit height and 10 fruits per tree for pigmentation (NDVI, DA-Index)

In these older trees, flower set and yield were enhanced with mean 2091.39 (+/-660.93) and 1889.89 (+/-343.38), respectively. Here, the yield was also significantly increased along with enhanced soil $ECa_{root\ zone}$.

Fruit height appears highly significant (< 0.001) for topsoil and root zone. This is particularly notable because fruit size is the main quality parameter for small stone fruits (cherry, plum, apricots). The highest F value of 21.32 was calculated in older trees for $ECa_{root\ zone}$. A similar impact of soil properties on fruit size was reported for pears earlier (Konopatzki et al., 2008). Flower set and fruit set show high values for F in $ECa_{topsoil}$ and $ECa_{root\ zone}$. In older trees, the # fruit depends significantly on the ECa in the topsoil. The maturity-dependent fruit chlorophyll was marginally influenced by soil ECa in five-year old trees, for NDVI (F = 1.87 and p = 0.152) and DA-index (F = 3.27 and p = 0.032). Under the principles of precision agriculture, numerous methods exist for spatial analysis (Gelfand et al., 2010). In practice, statistics were developed for small-scale variability in orchard hot spots. Such an approach addresses point based data instead of zonal data (Peeters et al., 2015).

For interaction of soil ECa and tree data, no significant influence was found regarding the ECa of subsoil. Flower set appears to be $p = 0.003$, but this may be assumed to be caused by a high correlation between the soil ECa pattern of subsoil, root zone, and topsoil. Surprisingly, ECa of topsoil sometimes showed enhanced significance level in comparison to ECa of root zone. We assume that in particular the short-term influence of soil moisture in cases of low precipitation and irrigation rates result in an increased impact of the ECa of topsoil on tree variables.

### *2.4.3 Impact of $ECa_{topsoil}$ and elevation on generative tree growth*

In the plum orchard, the elevation gradient from the highest (117, 25) to the lowest (1, 1) point is 6 meters, resulting in a slope of 3.15°. In higher elevations, the soil showed decreased soil ECa. For elevation, negative correlation was found with generative growth (flower set, fruit set, yield) and fruit quality (Figure 3b). Such negative correlation of yield and elevation was already found earlier in citrus production (Mann et al., 2011).

Concluding from ANOVA results using 8 soil classes (Figure 4), the ECa of topsoil was studied further (Table 2) and compared to the dependencies of elevation gradient. By assessing elevation, ANOVA revealed decreased significance levels for $ECa_{topsoil}$, but indicates a dependency on elevation (Table 3). Fruit quality, namely fruit height, is strongly significantly influenced by $ECa_{topsoil}$ as well as by elevation. The indicators for maturity-related chlorophyll content, NDVI and DA-Index, point to no dependencies at any soil depth or elevation for older trees (Table 3). Flower set, fruit set, and fruit drop show a higher level of significance in older trees compared to less mature trees (data not shown), again due to more homogeneous bearing in more mature trees. Concluding, for all tree variables, $ECa_{topsoil}$ showed an enhanced impact in comparison with elevation in the situation of 3° slope (Table 3).

Table 3. ANOVA results regarding electrical conductivity (ECa) in the topsoil and elevation of terrain, showing F- and p-values of tree data in 2012. ANOVA was carried out on the classed tree data after transformation to normal distribution by the root of raw data.

| | Plant parameter | $ECa_{topsoil}$ | | Elevation | |
|---|---|---|---|---|---|
| | | F | p < F | F | p < F |
| 6-year old trees | Flower set | 3.78 | **0.007** | 2.63 | **0.038** |
| | Fruit set | 3.46 | **0.011** | 1.80 | 0.133 |
| | Fruit drop | 3.78 | **0.007** | 0.47 | n. s. |
| | # Fruit | 9.75 | 0 | 0.58 | n. s. |
| | Fruit height* | 10.72 | **< 0.001** | 8.20 | **< 0.001** |
| | Yield | 1.84 | 0.128 | 0.65 | n. s. |
| | Fruit NDVI* | 0.46 | 0.800 | 1.72 | 0.184 |
| | DA-index* | 0.70 | 0.630 | 0.98 | 0.441 |

* means on each tree were considered, calculated from readings on all fruit per tree for fruit height and 10 fruit per tree for pigmentation (NDVI, DA-Index)

It can be assumed that the impact of elevation is due to the merged effects of variations in micro-climate in the canopy as well as the water-holding capacity of the soil – the later potentially also covered by ECa readings. In the present and former studies (Siqueira et al., 2010; Mann et al., 2011), generative growth was negatively correlated with elevation, and oppositely correlated with ECa, due to a higher percentage of low soil quality uphill and presumably decreased water supply due to water transport down-hill.

### *2.4.4 Interpretation of soil ECa data by means of two characteristic profiles*

Using geoelectric analyses of boreholes, variability of ECa of topsoil and root zone was measured with an enhanced spatial resolution. Results reveal no extreme values. The ECa of subsoil appeared to be rather homogeneous in the entire orchard. Two characteristic ECa profiles are presented out of 37 profiles to achieve a better insight into the soil characteristics (Figure 5) and interaction with tree growth. The profiles were measured at trees representing the classes 1 and 5, considering the ECa values (Figure 2) classed by ANOVA (Figure 4).

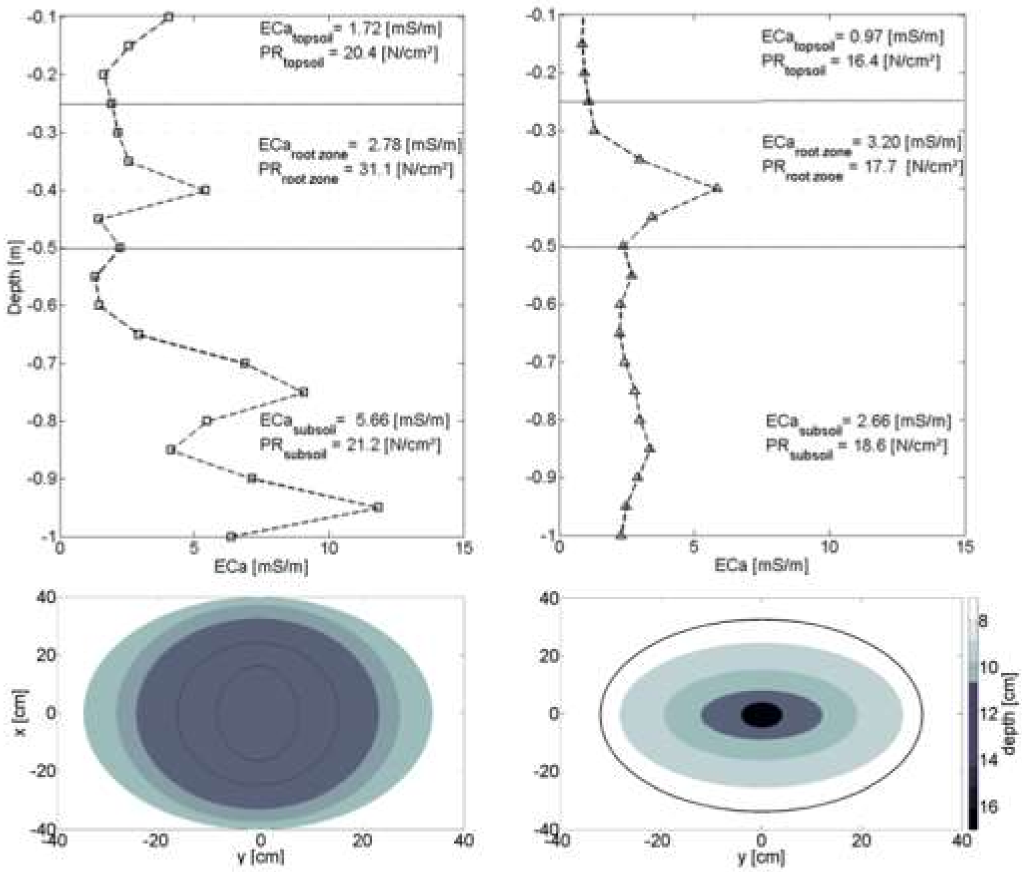


Figure 5. Two representative ECa profiles measured by borehole geoelectric including corresponding penetrometer resistance and infiltration figures. The symbols indicate the measuring depths, while the line represents the interpolated curve. In addition, zone border are shown with a solid line: topsoil (0.0-0.25 m), root zone (0.25-0.5 m), and subsoil (1.00-1.25 m). Borders were set according to the root distribution measured the 31 trees, which were removed from the orchard after the experiment.

The ECa profile of class 5 ranged from 1.3 to 11.8 mS/m (Figure 5, left). Here, the ECa values of the root zone increased at the depth of 0.4 m up to 6 mS/ m and then fell back to 1.4 mS/m. The data represent soil lenses in which loam nourishment is enhanced compared to the surrounding environment. In the subsoil, ECa values increased to 3.5 mS/m at a depth of 0.75 m. The enhanced ECa indicates higher loam content with increasing depth disturbed again by a small sand lens. The subsequent increase of ECa values to 11.8 mS/m suggests the appearance of a silt lens or at least enhanced silt content in the soil.

The ECa profile of class 1 (Figure 5, right) revealed relatively low ECa values ranging from 0.9 to 5.8 mS/m. The minimum value for this reading with enhanced spatial resolution exceeds results from geoelectrical tomography (Figure 2). The low values can be interpreted as sandy sand. An increase in ECa values from 1.9 mS/m to 4.1 mS/m appeared from topsoil to root zone, indicating reduced percentage of sandy soil at the root zone and the center of horizon A. From root zone to subsoil, ECa values increased to 5.8 mS/m, suggesting a marginal increase of silt content in the sandy soil.

The center of horizon A is visible in both profiles. It may be derived from the sudden increase in ECa at 0.40 m and is further supported by texture analysis, showing a transition to smaller particles at the same depth. The average percentage of silt content with a particle size between 2 µm and 63 µm in the topsoil is at 14.77%, and sand content with a particle size > 63 µm is at 85.01%. In the root zone, silt content of 14.95% and sand content of 84.74% was found. Clay content in all profiles were below 1.27% for topsoil, but showed increasing amounts in the root zone with 2.57%.

The unexpected impact of $ECa_{topsoil}$, therefore, can be characterized by enhanced ECa values in this zone. However, increased ECa in the topsoil can only partly be explained by soil texture showing a slightly elevated amount of clay. The cone penetrometer resistance (PR) can readily explain the water infiltration measured in opposite classes – represented in the bottom of figure 5. High PR in the upper zones (Figure 5 left) hinders the vertical water flow and water infiltration appears shallow. As a result, water was stored in the topsoil. It can be assumed that enhanced soil compaction was the result of mechanical weed control by means of rotary cultivation (Fountas et al., 2011).

In profiles not showing increased PR values, the water infiltration appears as expected for sandy soil with water rapidly infiltrating the soil. In earlier studies, no or low correlation was found for penetrometer values and ECa (Jabro et al., 2006), while ECa and soil water content correlate highly. Since water transport is hindered by enhanced PR values, we may suggest an indirect correlation of ECa and PR in the present study.

Chemical soil analyses pointed to a normal range for all elements (Schäfer and Grantzau, 1999), excluding phosphorus and potassium, which appeared slightly elevated. However, no impact of the chemical data on the plant growth is assumed for the present study.

The next step would be to delineate management zones in the orchards. Excellent geostatistical methods to analyze spatial data were adapted to this application in fruticulture (e.g. Aggelopooulou, et al., 2013; Peeters et al., 2015). However, an additional further look into plant interaction with spatially measureable soil properties seems to be reasonable before.

## 2.5 Conclusions

Consistent with findings in precision agriculture of field crops, correlation was found between soil electrical conductivity, terrain elevation, generative tree growth, and fruit size. An increasing interaction was found in older trees. Considering the depth of the ECa readings, ECa in the root zone showed high correlation coefficients for generative tree growth. Furthermore, the slope (elevation gradient) of the present orchard and soil compaction influenced the root zone environment. Such findings are based on data sets from an orchard with relatively small-scale variation in soil ECa due to glacial and post-glacial imprinting and soil compaction due to mechanical weed control within the topsoil.

## 2.6 Acknowledgments

Research has been carried out in the framework of the 3D-*Mosaic* Project (FP7, ICT-AGRI, 2810ERA095), targeting the Advanced Monitoring of Tree Crops for Optimized Management.

## 2.7 References

Aggelopooulou, K., Castrignano, A., Gemtos, T., and de Benedetto, D. (2013). Delineation of management zones in an apple orchard in Greece using a multivariate approach. Computers and Electronics in Agriculture. 90, 119-130.

Allred, B.J., Ehsani, M.R., and Daniels, J.J. (2008). Chapter 1 – General considerations for geophysical methods applied to agriculture. In: Handbook of Agricultural Geophysics, edited by Allred, B.J., Daniels, J.J., and M.R. Ehsani. CRC Press LLC. Boca Raton, Florida. 3-16.

Auernhammer, H. (2001). Precision farming – the environmental challenge. Computers and Electronics in Agriculture. 30, 31- 43. http://dx.doi.org/10.1016/S0168-1699(00)00153-8.

Bouyoucos, G.J. (1951). Hydrometer method improved for marking particle size analysis of soils. Agronomy J. 54, 464–465.
http:// dx.doi.org/10.2134/agronj1962.00021962005400050028x.

Bramley, R.G.V., Trought, M.C.T., and Praat, J.P. (2011). Vineyard variability in Marlborough, New Zealand: characterising variation in vineyard performance and options for the implementation of Precision Viticulture. Australian Journal of Grape and Wine Research. 17, 83-89. http://dx.doi.org/10.1111/j.1755-0238.2010.00119.x.

Bramley, R.G.V. and Hamilton, R.P. (2004). Understanding variability in vinegrape production systems 1. Within vineyard variation in yield over several vintages. Australian Journal of Grape and Wine Research. 10, 32–45. http://dx.doi.org/10.1111/j.1755-0238.2004.tb00006.x.

Control in applied Physiology (2002). Manual Pigment Analyzer. 2, 1-45.

Cortell, J.M, Halbleib, M., Gallagher, A.V., Righetti, T.L., and Kennedy, J.A. (2005). Influence of vine vigor on grape (Vitis vinifera L. Cv Pinot Noir) and wine proanthocyanidins. Journal of Agriculture Food Chemistry. 53, 5798-5808. http://dx.doi.org/10.1021/jf0504770.

Corwin, D.L., and Lesch, S.M. (2003). Application of soil electrical conductivity to precision agriculture: Theory, Principles and Guidelines. Agronomy Journal. 95, 455-471. http://dx.doi.org/10.2134/agronj2003.0455.

Faostat (2014). FAO Statistics Division, May 03, 2014. Available at http://faostat3.fao.org/faostat-gateway/go/to/download/Q/QC/E.

Fountas, S., Aggelopoulou, K., Bouloulis, C., Nanos, G.D., Wulfsohn, D., Gemtos, T.A., Paraskevopoulos, A., and Galanis, M. (2011). Site-specific management in an olive tree plantation. Precision Agriculture. 12, 179-195. http://dx.doi.org/10.1007/s11119-010-9167-4.

Gebbers, R., Lück, E., Dabas, M., and Domsch, H. (2009). Comparison of instruments for geoelectrical soil mapping at the field scale. Near Surface Geophysics. 88, 179-190. http://dx.doi.org/10.3997/1873-0604.2009011.

Gebbers, R., and Zude, M. (2010). Spatially resolved monitoring of fruit development in an apple orchard by means of sensor fusion. Acta Horticulture. 880, 217-221. http://dx.doi.org/10.17660/actahortic.2010.880.24.

Gelfand, A.E., Diggle, P., Guttorp, P., and Fuentes, M. (Eds.). (2010). Handbook of spatial statistics. CRC Press. http://dx.doi.org/10.1201/9781420072884.

Hartge, K.H. and Horn, R. (1992). Bodenphysikailsches Praktikum. 3rd ed., enkeverlag, Stuttgart, Germany.

Hartsock, N.J., Mueller, T.G., Thomas, G.W., Barnhisel, R.I., Wells, K.L., and Shearer, S.A. (2000). Soil electrical conductivity variability. In Proceedings 5th International Conference on Precision Agriculture, P.C. Robert et al., eds. (Madison, WI.: ASA Misc. Publ., ASA, CSSA, and SSSA).

Jabro, J.D., Evans, R.G., Kim, Y., Stevens, W.B., and Iversen, W.M. (2006). Characterization of spatial variability of soil electrical conductivity and cone index using coulter and penetrometer type sensors. Soil Science. 171, 627-637.

http://dx.doi.org/10.1097/01.ss.0000228037.80270.1d.

Joschko, M., Gebbers, R., Barkusky, D., Rogasik, J., Hohn, W., Hierold, W., Fox, C.A., and Timmer, J. (2009). Location-dependency of earthworm response to reduced tillage on sandy soil. Soil & Tillage Research. 102, 55-66. http://dx.doi.org/10.1016/j.still.2008.07.023.

Konopatzki, M.R.S., De Souza, E.G., Nóbrega, L.H.P., Uribe-Opazo, M.A., Suuszek, G., and Rodrigues, S. (2008). Spatial variability of the soil properties in a pear tree. Proceedings CIGR International Conference of Agricultural Engineering, XXXVII Congress Brasileiro de Engenharia Agricola.

Loke, M.H., and Barker, R.D. (1996). Rapid least-squares inversion of apparent resistivity pseudosections by a quasi-Newton method. Geophysical Prospecting 44, 131–152. http://dx.doi. org/10.1111/j.1365-2478.1996.tb00142.x.

Lück, E., Gebbers, R., Ruehlmann, J., and Spangenberg, U. (2009). Electrical conductivity mapping for precision farming. NearSurface Geophysics 7, 15–25. http://dx.doi.org/10.3997/1873-0604.2008031.

Lück, E., and Rühlmann, J. (2013). Resistivity mapping with GEOPHILUS ELECTRICUS – Information about lateral and vertical soil heterogeneity. Geoderma 119, 2–11. http://dx.doi.org/10.1016/j.geoderma.2012.11.009.

Mann, K.K., Schumann, A.W., and Obreza, T.A. (2011). Delineating productivity zones in a citrus grove using citrus production, tree growth and temporally stable soil data. Precision Agriculture 12, 457–472. http://dx.doi.org/10.1007/s11119-010-9189-y.

Mancuso, S. (2012). Measuring Roots – An Updated Approach (New York: Springer), pp. 151–168. http://dx.doi.org/10.1007/978-3-642-22067-8.

Mc Bratney, A.B., Minasny, B., and Whelan, B.M. (2005). Obtaining 'useful' high-resolution soil data from proximally-sensed electrical conductivity/resistivity (PSEC/R) surveys. Proceedings 5$^{th}$ Conference on Precision Agriculture, pp. 503–510.

Meier, U. (ed.) (2001). Growth stages of mono-and dicotyledonous plants. BBCH Monograph, 2nd edn., (Braunschweig, Germany: Federal Biological Research Centre for Agriculture and Forestry), pp. 1–158.

Molin, J.P., and Faulin, G.C. (2012). Spatial and temporal variability of soil electrical conductivity related to soil moisture. Scientia Agricola 70(1), 1–5.

Peeters, A., Zude, M., Käthner, J., Ünlü, M., Kanber, R., Hetzroni, A., Gebbers, R., and Ben-Gal, A. (2015). Getis-Ord's hot- and cold-spot statistics as a basis for multivariate spatial clustering of treebased data Computers and Electronics in Agriculture. Computers and Electronics in Agriculture 111, 140–150. http://dx.doi.org/10.1016/j.compag.2014.12.011.

Pozdnyakov, A., and Pozdnyakov, L. (2002). Electrical fields and soil properties, 17th World Congress of Soil Science, Symposium no. 53, Proceeding, Thailand, Paper No. 1558, 1-11.

Reynolds, J.M. (1997). An Introduction to Applied and Environmental. Geophysics: Chichester, England, John Wiley & Sons Ltd. 796 pp.

Reynolds, A.G., Senchuk, I., and De Savigny, C. (2007). Use of GPS and GIS for elucidation of the basis for terroir. Spatial variation in an Ontario Riesling vineyard. American Journal of Enology and Viticulture. 58, 145–162.

Rodriguez-Perez, J.R., Plant, R.E., Lambert, J., and Smart, D.R. (2011). Using apparent soil electrical conductivity (ECa) to characterize vineyard soils of high clay content. Precision Agric. 12, 775-794. http://dx.doi.org/10.1007/s11119-011-9220-y.

Schäfer, B., and Grantzau, E. (1999). Chemische Analysen von Böden und Substraten (4). Deutscher Gartenbau 53, 45-46.

Seifert, B., Pflanz, M., and Zude, M. (2014). Spectral shift as advanced index for fruit chlorophyll breakdown. Food Bioprocess Technology. 7, 2050-2059.
http://dx.doi.org/10.1007/s11947-013-1218-1.

Siqueira, D.S., Marques, J., and Pereira, G.T. (2010). The use of landforms to predict the variability of soil and orange attributes. Geoderma 155, 55-66.
http://dx.doi.org/10.1016/j.geoderma.2009.11.024.

Telford, W.M., Geldart, L.P., and Sheriff, R.E. (1990). Applied Geophysics, second edition, Cambridge University press 1990, Cambridge (0-521-32693), 343-577.

Trought, M.C.T., Dixon, R., Mills, T., Greven, M., Agnew, R., Mauk, J.L., and Praat, J.P. (2008). The impact of differences in soil texture within a vineyard on vine vigour, vine earliness and juice composition. Journal International Des Sciences De La Vigne Et Du Vin. 42, 67-72.

Trought, M.C.T., and Bramley, R.G.V. (2011). Vineyard variability in Marlborough, New Zealand: characterising spatial and temporal changes in fruit composition and juice quality in the vineyard. Australian journal of grape and wine research. 17, 72-82.
http://dx.doi.org/10.1111/j.1755-0238.2010.00120.x.

Türker, U., Talebpour, B., and Yegül, U. (2011). Determination of the relationship between apparent soil electrical conductivity with pomological properties and yield in different apple varieties. Žemdirbystė =Agriculture. 98, 307-314.

VDLUFA: Federal Compost Quality Assurance Organisation (FCQAO), Bundesgütegemeinschaft Kompost e.V. (BGK) (2003). Methods Book for the Analysis of Compost. 3rd edition. Germany. ISBN 3-928179-33-0, 14-60.

Webster, R., and Oliver, M.A. (1990). Statistical methods in soil and land resource survey. Oxford University Press, Oxford. ISBN0-19-823316-7, pp. 316.

Wenner, F. (1915). A method of measuring earth resistivity. Bull, Bureau of Standards. 12, 258, 469-478. http://dx.doi.org/10.1016/ s0016-0032(15)90298-3.

Zaman, Q.U., and Schumann, A.W. (2006). Nutrient management zones for citrus based on variation in soil properties and tree performance. Precision Agric. 7, 45–63. http://dx.doi.org/10.1007/s11119-005-6789-z.

Zhang, N., Wang, M., and Wang, N. (2002). Precision agriculture- a worldwide overview. Computers and Electronics in Agriculture. 36, 113- 132. http://dx.doi.org/10.1016/S0168-1699(02)00096-0.

Ziosi, V., Noferini, M., Fiori, G., Tadiello, A., Trainotti, L., Casadoro, G., and Costa, G. (2008). A new index based on vis spectroscopy to characterize the progression of ripening in peach fruit. Postharvest Biology and Technology. 49, 319–329. http://dx.doi. org/10.1016/j.postharvbio.2008.01.017.

Zude, M. (2003). Comparison of indices and multivariate models to non-destructively predict the fruit chlorophyll by means of visible spectrometry in apple fruit. Analytica Chimica Acta. 481, 119-126. http://dx.doi.org/10.1016/S0003-2670(03)00070-9.

## 3 Getis-Ord's hot- and cold-spot statistics as a basis for multivariate spatial clustering of orchard tree data

(Computers and Electronics in Agriculture. 2015, 111: 140-150, DOI: 10.1016/j.compag.2014.12.011)

### 3.1 Abstract

Precision agriculture aims at sustainably optimizing the management of cultivated fields by addressing the spatial variability found in crops and their environment. Spatial variability can be evaluated using spatial cluster analysis, which partitions data into homogeneous groups, considering the geographical location of features and their spatial relationships. Spatial clustering methods evaluate the degree of spatial autocorrelation between features and quantify the statistical significance of identified clusters. Clustering of orchard data calls for an approach which is based on modeling point data, i.e. individual trees, which can be related to site-specific measurements. We present and evaluate a spatial clustering method using the Getis–Ord $G_i^*$ statistic to the analysis of tree-based data in an experimental orchard. We examine the robustness of this method for the analysis of ‘‘hot-spots’’ (clusters of high data values) and ‘‘cold-spots’’ (clusters of low data values) in orchards and compare it to the *k*-means clustering algorithm, a widely-used aspatial method. We then present a novel approach which accounts for the spatial structure of data in a multivariate cluster analysis by combining the spatial Getis–Ord $G_i^*$ statistic with *k*-means multivariate clustering. The combined method improved results by both discriminating among features values as well as representing their spatial structure and therefore represents a superior technique for identifying homogenous spatial clusters in orchards. This approach can be used as a tool for precision management of orchards by partitioning trees into management zones.

Keywords: GIS; hot-spot analysis; *k*-means clustering; management zones; precision agriculture; spatial clustering

### 3.2 Introduction

The growing challenge to diminish the environmental footprint of farming while ensuring food security and economic viability of agricultural practices has resulted in the development of precision agriculture. Precision agriculture aims to sustainably optimize the management of cultivated fields by addressing the spatial variability found in crops and their environment. Soil properties and past and present yield distributions are common examples of spatially variable data with potential value for precision agriculture (Zhang et al., 2002). Knowledge regarding the form of distribution and the extent of spatial variability of data can support site-specific management of agricultural crops.

A well-established approach to recognize homogenous groupings in data uses *clustering* or *cluster analysis*. This approach has been extended to the analysis of spatial variability in agricultural environments. Clustering consists of a group of methods which aim at partitioning data into coherent or natural groups based on measures of similarity by maximizing within-cluster similarities as well as between-cluster differences (MacQueen, 1967). In general, clustering methods can be defined as either *partitioning* or *hierarchical*. Partitioning methods operate by dividing the entire dataset into *n* clusters, and hierarchical methods work by pairing individual data points in a bottom-up or agglomerative process (Jain, 2010). Various clustering methods have been developed and adopted from other scientific fields to recognize homogenous groupings in spatial agricultural data. Existing methods use either a univariate or multivariate approach of yield-defining variable(s) for recognizing homogenous groups in field data.

One of the most popular and well-established algorithms, widely applied in research domains such as data mining and pattern recognition, is *k*-means clustering (Ball and Hall, 1965; Lloyd, 1982; McQueen, 1967; Steinhaus, 1956; Theodoridis et al., 2010). While *k*-means has been used extensively in agriculture (Mucherino et al., 2009; Ortega and Santibáñez, 2007), its standard algorithm is not very flexible and *fuzzy* clustering variants to improve its use have therefore been developed (Fridgen et al.,2004; Fu et al., 2010; Kitchen et al., 2005; Vitharana et al., 2008; Yan et al., 2007). Additional clustering methods for agricultural data include the ISODATA method (Fraisse et al., 2001; Guastaferro et al., 2010), a non parametric approach developed by Aggelopoulou et al. (2013) and a hierarchical approach presented by Fleming et al. (2000). A number of researchers have integrated *k*-means or *fuzzy* clustering with other algorithms (Córdoba et al., 2013; Davatgar et al., 2012; Fridgen et al., 2004).

In spite of the different clustering approaches that have been developed, only a few make use of spatial constraints. Clustering approaches commonly rely only on the data attributes to recognize natural groupings and partition data observations. To consider the spatial structure of data, clustering methods must integrate the geographical location of objects and the spatial relationships between them directly into their mathematics (Cressie and Wikle, 2011; Lloyd, 2010; Mitchell, 2005). By accounting for both the differences in attribute values between features as well as for spatial location and relationships, spatial clustering methods model spatial variability and uncertainties by quantifying the statistical significance of recognized patterns and evaluate the degree of clustering of observed spatial distribution.

Since agriculture is inherently a spatial phenomenon, in which yield defining variables such as soil conditions, topography and microclimate vary in space, processes related to agricultural crops and environments should be modeled using spatial methods. Some studies, have introduced spatially constrained clustering methods, which limit class association to contiguous or proximal features in order to form homogenous management zones. Spatially constrained clustering uses aspatial clustering algorithms which are modified by introducing constraints of spatial contiguity, for example by introducing spatial coordinates, Delaunay triangulation or *k* nearest neighbors (Gordon, 1996; Legendre and Legendre, 2012; Shatar and McBratney, 2001).

Other studies have examined different approaches to spatial clustering. Pedroso et al. (2010) for example, used a segmentation algorithm, adopted from image processing, and compared it to *k*-means clustering and to spatially constrained *k*-means clustering with promising results, and Ping and Dobermann (2003) used a prior classification interpolation (PCI) approach preceding the cluster analysis and a post-classification filtering (PCF) approach to improve spatial contiguity of yield classes. Perry et al. (2010) have shown that tree properties in orchards exhibit spatial autocorrelation and that clustering results could be improved considerably by introducing spatial methods. A recent study by Córdoba et al. (2013), for example, compared the aspatial *k*-means algorithm with spatial clustering techniques, when applied to wheat and soybean crops. Their proposed approach combined spatial principal component analysis with *fuzzy k*-means (KM-sPC) to classify elevation, soil and yield into spatial clusters. They assessed the degree of within-field spatial variation (spatial autocorrelation) and came to the conclusion that adding the spatial dimension improved the clustering results and produced more contiguous groups. Moreover, they concluded that under spatial autocorrelation, unconstrained *fuzzy k*-means clustering and classical principal component analysis (PCA) were insufficient and were likely to less successfully recognize spatial structure.

The majority of relevant agricultural research has concentrated on the use of aspatial clustering methods and particularly on their application to field crops (Perry et al., 2010). While spatial clustering methods have been applied in agriculture to address various issues such as, crop disease (Cohen et al., 2011), yield potential (Lark, 1998; Perry et al., 2010) and soil fertility (Cohen et al., 2013; Yan et al., 2007), contributions attempting to apply spatial clustering techniques to tree-based data in orchards, are few and rather recent (Aggelopoulou et al., 2010, 2013; Kounatidis et al., 2008; Mann et al., 2010; Perry et al., 2010; Zaman and Schumann, 2006).

Since existing clustering approaches have been mainly developed for annual crops they are based on either sampling continuous data, or on zonal data, such as yield per area, and do not necessarily consider point-based data, such as from individual trees. Attributes associated with tree crops can be either discrete or continuous. For example, tree size, flowering level and fruit yield are examples of discrete variables associated with single trees only, while soil properties and consequential variables including water or nutrient availability are continuous and occur throughout the entire orchard, even where trees are not present. Therefore, clustering of orchard data calls for an approach which is based on modelling point-based data i.e. individual trees and which can be related to site-specific measurements.

We further investigated the conclusions on the significance of spatial clustering in agriculture presented by studies such as Córdoba et al. (2013) and examined the application of spatial clustering to data gathered from individual trees in an orchard. We begin by presenting a comparative study between two clustering methods; one aspatial and extensively-used and the other spatial and often applied to the analysis of point-based data such as crime events, rainfall modeling and disease cases, but rarely used in agriculture, to recognize hot-spots (clusters of high data values) and cold-spots (clusters of low data values) in orchard data. We then present a novel approach which combines spatial and aspatial methods, particularly suitable for point-based data, and we evaluate its appropriateness for contiguous spatial cluster recognition in orchards.

### 3.3 Spatial vs. aspatial clustering

Aspatial clustering considers only the values of data points, in partitioning the data into clusters. It does not account for the geographical spatial context (spatial location and neighborhood), or for the extent of spatial autocorrelation among data points (Aggelopoulou et al., 2013; Córdoba et al., 2013). However, spatial autocorrelation which measures the degree of similarity between neighboring features (data points), is an important concept in the analysis of spatial data as it indicates whether features are spatially dependent or independent (Cressie and Wikle, 2011; Lloyd, 2010). If features closer to each other tend to be more similar than features farther apart, they are considered to be spatially dependent and form a cluster (Lloyd, 2010). Another important aspect in the analysis of spatial data is the representation of the spatial structure of the data in the actual computation of clusters. In order to compare the attribute values of each feature to the attributes of neighboring features the extent of the neighborhood surrounding each feature and the type of spatial interactions among features needs to be quantified. For example, if the influence of a feature on neighboring features decays with distance, or if there is a sphere of influencebeyond which features are not impacted, it should be represented in the computation (Mitchell, 2005).

Traditional aspatial statistics is based on the assumptions that observations are independent of one another and identically distributed (Chun and Griffith, 2013), and that relationships modeled are constant across the study area. However, spatial phenomena exhibit both spatial dependence among features, and non-stationarity, i.e. spatial processes and relationships vary across the study area (Mitchell, 2005). Spatial statistical methods offer a range of inferential tests that measure the degree to which the value of a feature's attribute is similar to the attribute value of neighboring features and can be used to quantify how spatial autocorrelation varies locally and recognize spatial clusters. Similar to aspatial inferential statistics, spatial methods are evaluated within the context of a null hypothesis which states that attribute values do not exhibit local spatial clustering and can be rejected only if results can be considered statistically significant within a defined confidence level. Since a statistical index is calculated for each feature in the dataset, these can be mapped to indicate both the spatial variability in local autocorrelation, and which features have statistically significant relationships with their neighbors. The contribution of individual features on the identified pattern can be evaluated, thus enabling the recognition of outliers in the data.

The following presents the two clustering methods examined in the current research: the aspatial *k*-means algorithm and the spatial Getis–Ord $G_i^*$ statistic (Getis and Ord, 1996; Mitchell, 2005; Ord and Getis, 1995).

### *3.3.1 Aspatial k-means clustering*

The *k*-means algorithm is an iterative algorithm for partitioning a set of *n* data observations ($x_1$, $x_2$, …, $x_n$) into homogenous *k* clusters ($k \leq n$) S = {$S_1$, $S_2$, …, $S_k$}. *k*-means minimizes the within-cluster sum of squares (WCSS) and uses the squared Euclidean distance metric (the distance between attribute values) as the measure of similarity - Eq. (1) (Theodoridis et al., 2010):

$$S = arg\,min_s \sum_{i=1}^{k} \sum_{x_j \in S_i}^{n} \left\| x_j - \mu_i \right\|^2 \tag{1}$$

where $x_j$ is the attribute value of the target feature, and $\mu_i$ is the mean of points in $S_i$.

At its most basic form, *k*-means uses an iterative refinement process in which observations are assigned to a cluster with the objective that each data observation will belong to the cluster with the nearest mean (Jain, 2010). The centroid of each cluster subsequently becomes the new mean and the process is repeated again until convergence to a local minimum is reached. The *k*-means method is fast, straightforward and simple to implement, however, it suffers from a few drawbacks. The algorithm cannot assure convergence to the global minimum of *S*. Consequently, different initializations of the algorithm might result in different final clusters. Another critical drawback is the prerequisite for a userdefined parameter of the number of clusters (*k*) to be partitioned. A poor estimate will prevent the algorithm from recognizing the underlying structure. The algorithm additionally is sensitive to the presence of outliers (Theodoridis et al., 2010).

### *3.3.2 The spatial Getis-Ord $G_i^*$ statistic*

The Getis–Ord $G_i^*$ statistic ($G_i^*$), known also as hot-spot analysis (Getis and Ord, 1992, 1996; Mitchell, 2005; Ord and Getis, 1995) is a method for analyzing the location related tendency (clustering) in the attributes of spatial data (points or areas). Developed in the mid 1990s, this method has commonly been used in rainfall and epidemic modeling and has been applied in recent years in agriculture as well (Chopin and Blazy, 2013; Kounatidis et al., 2008; Rud et al., 2013). The method is an adaptation of the General *G*-statistic (Getis and Ord, 1992), a global method for quantifying the degree of spatial autocorrelation over an area. The General *G*-statistic computes a single statistic for the entire study area, while the $G_i^*$ statistic serves as an indicator for local autocorrelation, i.e. it measures how spatial autocorrelation varies locally over the study area and computes a statistic for each data point. The method evaluates the degree to which each feature is surrounded by features with similarly high or low values within a specified geographical distance (neighborhood) - Eq. (2).

$$G_i^*(d) = \frac{\sum_j w_{ij}\ (d)\ x_j}{\sum_j x_j} \tag{2}$$

where $G_i^*(d)$ is the local *G*-statistic for a feature *(i)* at a distance *(d)*, $x_j$ is the attribute value of each neighbor, and $w_{ij}$ is the spatial weight for the target-neighbor *i* and *j* pair. Typically, the spatial distances between observations at points are calculated by the Euclidean norm. The spatial weights $w_{ij}$ are the *n x n* elements of the spatial weight matrix *W*, where *n* is the number of observations. There are several possible types of *W* (Haining, 2003). A simple form, commonly used in the $G_i^*$ statistic is a matrix derived from a threshold *(d)* for the distance between $x_i$ and $x_j$ (Chun and Griffith, 2013; Ord and Getis, 1995). The threshold parameter *d* defines the distance within which all locations are considered as neighbors (indicated by 1 in the W matrix), and beyond which all locations are not neighbors (indicated by 0 in the *W* matrix or by weights which diminish with distance). $G_i^*$ is only applicable for positive *x*.

The statistical significance in the degree of local autocorrelation between each feature and its neighbors is assessed by the *z*-score test. The *z*-score and *p*-value reported for each feature indicate whether spatial clustering of either high or low values, or a spatial outlier is more pronounced than one would expect in a random distribution, i.e. whether or not it is possible to reject the null hypothesis of no apparent clustering. In order to improve statistical testing, Ord and Getis (1995) developed a *z*-transformed form of $G_i^*$ by taking the statistic $G_i^*(d)$ minus its expectation, divided by the square root of its variance. Using the same symbology, this *z*-transformation, termed the standardized $G_i^*$ statistic is given in Eq. (3). The $G_i^*$ statistic computed by ArcGIS (ESRI, Redlands, CA, USA) uses this version of $G_i^*$ in which the $G_i^*$ index is combined with the *z*-score into one single index. The statistic, still called $G_i^*$, reports a *z*-score and *p*-value for each single feature.

$$G_i^*(d) = \frac{\sum_j w_{ij}(d)\, x_j - \overline{X} \sum_j w_{ij}(d)}{S\sqrt{\frac{n \sum_j w_{ij}^2 \left(\sum_j w_{ij}(d)\right)^2}{n-1}}} \tag{3}$$

with $\overline{X} = \frac{\sum_j x_j}{n}$ and $S = \sqrt{\frac{\sum_j x_j^2}{n} - \left(\overline{X}\right)^2}$

where $G_i^*(d)$ is computed for feature *(i)* at a distance *(d)* standardized as a *z*-score. $x_j$ is the attribute value of each neighbor, $w_{ij}$ is the spatial weight for the target-neighbor *i* and *j* pair and *n* is the total number of samples in the dataset. A Euclidean method is used to calculate the geographical distances from each feature to its neighboring features. The spatial structure of the data (neighbourhood and relationships between features) is represented and quantified as in Eq. (4) by using the spatial weight $(w_{ij})$, calculated based on a spatial weight matrix. The spatial weight matrix is an *n x n* table (n equals to the number of features in the dataset), which surrounds each feature, in which each value in the matrix is a weight representing the relationship between a pair of features in the dataset.

The $G_i^*$ statistic introduced by Getis and Ord in 1995 extended the family of *G* statistics to incorporate non-binary weight matrices and account for a $w_{ij}(d)$ which varies with distance. For example weights can be assigned based on an inverse distance weights matrix (distance decay), or a combination of the inverse distance and the fixed distance band models (similar to a fixed distance with a *fuzzy* boundary). Defining the distance band *(d)* is parametric and depends on the nature of the dataset and on the phenomenon modeled and should be defined according to the distance in which spatial autocorrelation peaks. This can be modeled by applying an iterative and data-driven process which examines how spatial autocorrelation varies at different distances. The output of the $G_i^*$ statistic is a map indicating the location of spatial clusters in the study area. Positive values of $G_i^*$ denote spatial dependence among high values. Negative values of $G_i^*$ indicate spatial dependence for low values. The degree of clustering and its statistical significance is evaluated based on a confidence level and on output *z*-scores. These define whether a data point belongs to a hot-spot (spatial cluster of high data values), cold-spot (spatial cluster of low data values) or an outlier (a high data value surrounded by low data values or vice versa).

## 3.4 Materials and Methods

### *3.4.1 Data collection*

Data was collected in 2011 and 2012 from individual grapefruit trees (*Citrus paradise, cv.* Rio Red) within an irrigated experimental orchard planted in 1993 in an 8 m x 8 m pattern. The orchard was located in the experimental farms of the University of Cukurova, in the vicinity of the city of Adana, Turkey (35°22′55″ E, 37°1′24″ N, mean elevation 53 m) –Fig. 6. Adana has a typical Mediterranean climate with hot-dry summers and mild-wet winters. Orientation of rows was north-east/ south-west with a rather flat topography. Sampling was conducted on 179 individual trees located in 9 adjacent rows. Soil at the site was classified as a Typic Xerofkuvent with clay and clay–loam textures. Data for plant specific properties, collected from individual trees, and environmental data was organized using a geographical information system (GIS) schema in which trees serving as the basic features were tied to a geographical location together with their associated attributes. A projected coordinate system, UTM 36N, was defined for the geodatabase to allow spatial statistical analysis.

The current study utilized yield (total fruit weight per tree) and two possible yield-determining variables, tree trunk circumference [cm] and soil apparent electrical conductivity (ECa [mS/m]) (Kitchen et al., 1999, 2003; Lück et al., 2009), each measured for all 179 trees. Tree trunk circumference has been shown to be an accurate measure of tree size and growth and often related to fruit yield, and soil apparent electrical conductivity has been established as a reliable measure to characterize spatial variability in soil productivity (Corwin and Plant, 2005; Kitchen et al., 1999, 2003). Both these variables are relatively easy to collect.

ECa was measured with 4-point light hp portable galvanic coupled resistivity meter (LGM Lippman, Schaufling, Germany) on the 25$^{th}$ of June 2011. Electrodes were mounted on a wooden frame, linearly arranged with a spacing of 1 m (Wenner array). The measurements were taken adjacent to the trunk of each tree. Depth of investigation at 70% of the signal was 0.78 m (Gebbers et al., 2009). Trunk circumference was measured 10 cm above grafting points on 27$^{th}$ of June, 2011. Fruit per tree fresh weight was determined at harvest, 16–17 of March, 2012. All analysis was performed using the ArcGIS Desktop software package (ESRI, Redlands, CA, USA).

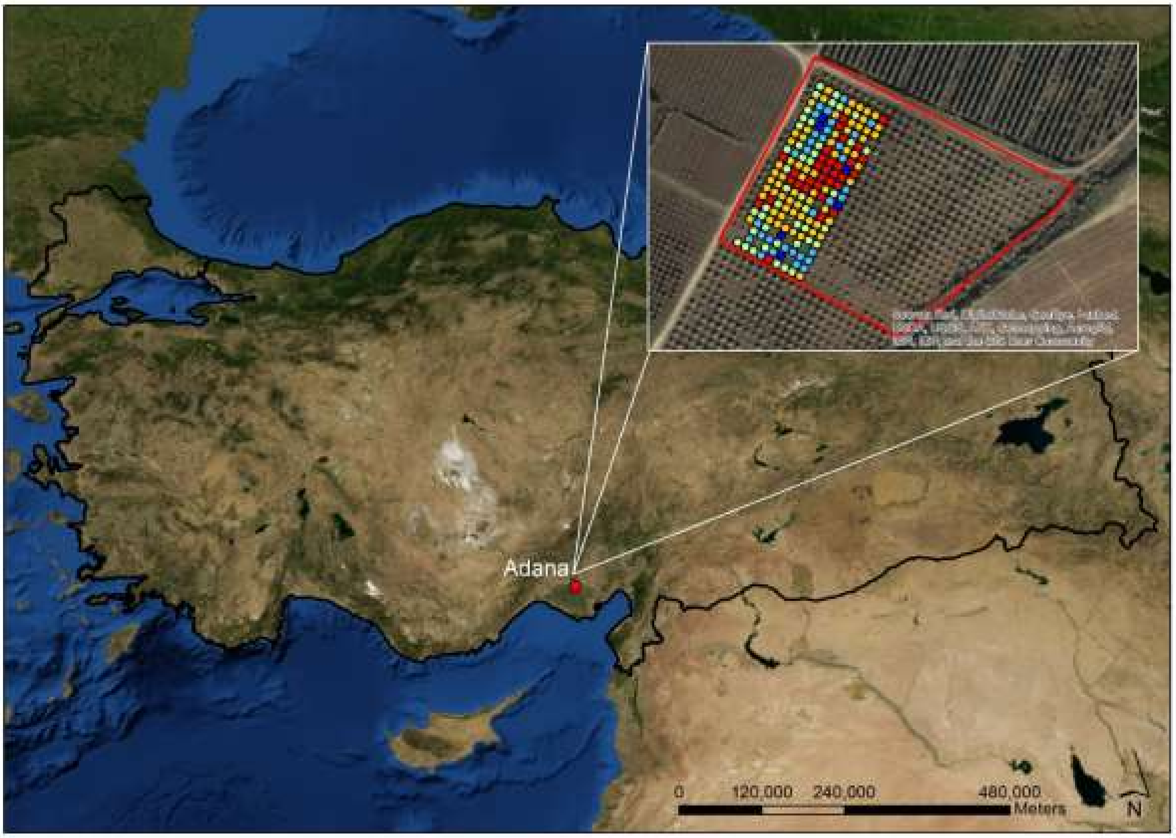


Figure 6. Location of test site in Adana, Turkey. The red polygon shows the orchard's borders highlighting the monitored trees which are color coded according to their trunk circumference size. Base image from ESRI World Map Background, Copyright © 1995–2012 ESRI. (For interpretation of the references to color in this figure legend, the reader is referred to the web version of this article.)

### *3.4.2 Proposed spatial-aspatial approach*

The *k*-means is not, in its basic form, a spatial clustering method as it considers only the differences between the data values. The $G_i^*$ statistic is a spatial clustering method as it accounts for the spatial structure of the data, but as a univariate-based method it considers only one attribute (variable) in the clustering process. However, most problems concerning agricultural practices are of a multidimensional structure requiring multivariate field information (Castrignanò et al., 2012). For practical orchard management considerations, such as class management delineation, and to understand the actual spatial structure of multiple yield-defining variables, it would be valuable to understand not only the spatial structure of each single variable, but the spatial structure of all variables combined. This suggests the use of a multivariate approach to account for multiple variables in partitioning the orchard into spatial clusters.

Spatial clustering approaches in agriculture, as previously explained, often apply spatially constrained clustering, a process in which aspatial multivariate clustering methods are modified by introducing spatial constraints. The proposed spatial–aspatial approach is innovative as it integrates the spatial constraints from the onset, prior to the aspatial clustering, by following a process in which each examined variable is first analyzed for its spatial structure, recognizing spatial hot-spots and cold-spots in the data, followed by the application of *k*-means to introduce a multivariate classification. The developed approach consists of the following steps:

(1) Defining the optimal number of clusters: The $G_i^*$ statistic does not require input definition of a rigid number of clusters. However, the *k*-means, as mentioned earlier, does require the user to pre-define the parameter *k*. Since the spatial recognition of hot- and cold-spots is followed by applying *k*-means clustering, a method is required to determine the number of clusters. Numerous methods exist for assisting in selecting the optimum *k*. These are much debated and a matter of ongoing research. We employ the Calinski–Harabasz pseudo F-statistic (C–H index) (Calinski and Harabasz, 1974; Orpin and Kostylev, 2006), which has been confirmed by previous research as one of the best performing and reliable algorithms for determining the optimum number of clusters in *k*-means clustering with squared Euclidean distances (Cooper and Milligan, 1988; Milligan and Cooper, 1985) and is recommended in recent versions of statistical software (ESRI, 1984; Legendre and Legendre, 2012; Milligan and Cooper, 1985; SAS Institute Inc., 2013; The MathWorks, 2013). In the current research it is applied iteratively to all input variables combined.

(2) Spatial clustering: Applying the $G_i^*$ statistic to partition the different variables into spatially contiguous clusters. $G_i^*$ statistic was calculated with variable spatial weights using an ArcGIS (ESRI, Redlands, CA, USA) model which combines the inverse distance (distance decay) and fixed distance band models, i.e. beyond a *d*-threshold the weighting drops off with distance. The $G_i^*$ statistic outputs a *z*-score and p-value for each data point representing the type of clustering, the degree of clustering and its statistical significance. These *z*-scores can be subsequently classified into *k* number of clusters.

(3) Aspatial clustering: The *z*-score output of the $G_i^*$ statisticis used as the input variable for *k*-means clustering, which is applied to all variables combined to provide multivariate-based clustering. Using the *z*-scores as the input variable for *k*-means instead of following the common *k*-means routine, which considers the raw data

values at each point as input variables, ensures that the spatial structure is taken into account in the multivariate clustering.

### 3.5 Application and results

The following demonstrates the application of the proposed spatial–aspatial approach on the variables collected for the case study orchard in Adana, Turkey: tree trunk circumference, ECa and yield (Table 4). It is important to note that any point-based variable associated with a single-tree, whether plant or environmentally related, can similarly serve in the analysis.

The three variables combined were used in the computation of the C–H index to select the optimal number of clusters. The options $k$ = 1, 2, 3 ... 15 were iteratively assessed for their effectiveness in dividing the trees into groups. The option $k$ = 3 resulted in the highest C–H index statistic indicating that 3 groups would be the optimal number of clusters for partitioning the trees (Fig. 7).

Figs. 8–10 illustrate clustering outputs comparing $k$-means and $G_i^*$ methods for each of the three variables. The methods produce similar patterns of spatial variability and clustering partitioning of the variables with some important notable differences.

Based on the $G_i^*$ results, statistically significant local clustering is indicated for both high values and low values in the study area for all variables. In Figs. 8b–11b red dots denote statistically significant spatial clusters of high values (hot-spots), blue dots indicate statistically significant spatial clusters of low values (cold-spots) and white dots are not considered significant, i.e. random distribution with no spatial clustering of either high or low values. Table 5 indicates the critical $p$-values and $z$-scores associated with Figs. 8b–11b. These indicate the degree of spatial clustering and its statistical significance within a confidence level.

Results of the $G_i^*$ statistic further characterize the type of clustering and its location, whether it is a hot-spot, cold-spot or an outlier. The class partitioning of $k$-means does not indicate the type of cluster in terms of the data values, for example recognize hot-spots and cold-spots, but rather partitions the data into clusters based on similarity measures. In addition, $k$-means does not recognize outliers, while the outputs of the $G_i^*$ statistic clearly indicate the location of outliers. An example of an outlier is illustrated for analysis of trunk circumference within the hot-spot in Fig. 9b.

Table 4. Summary statistics of tree trunk circumference, ECa and yield data.

| | Mean | Min | Max | Std. Dev. | Skewness |
|---|---|---|---|---|---|
| Trunk circumference [cm] | 69.84 | 42.0 | 93.00 | 9.25 | -0.63 |
| Yield [kg/tree] | 316.16 | 16.0 | 640.00 | 133.03 | -0.13 |
| ECa [mS/m] | 79.67 | 27.9 | 260.96 | 36.12 | 1.04 |

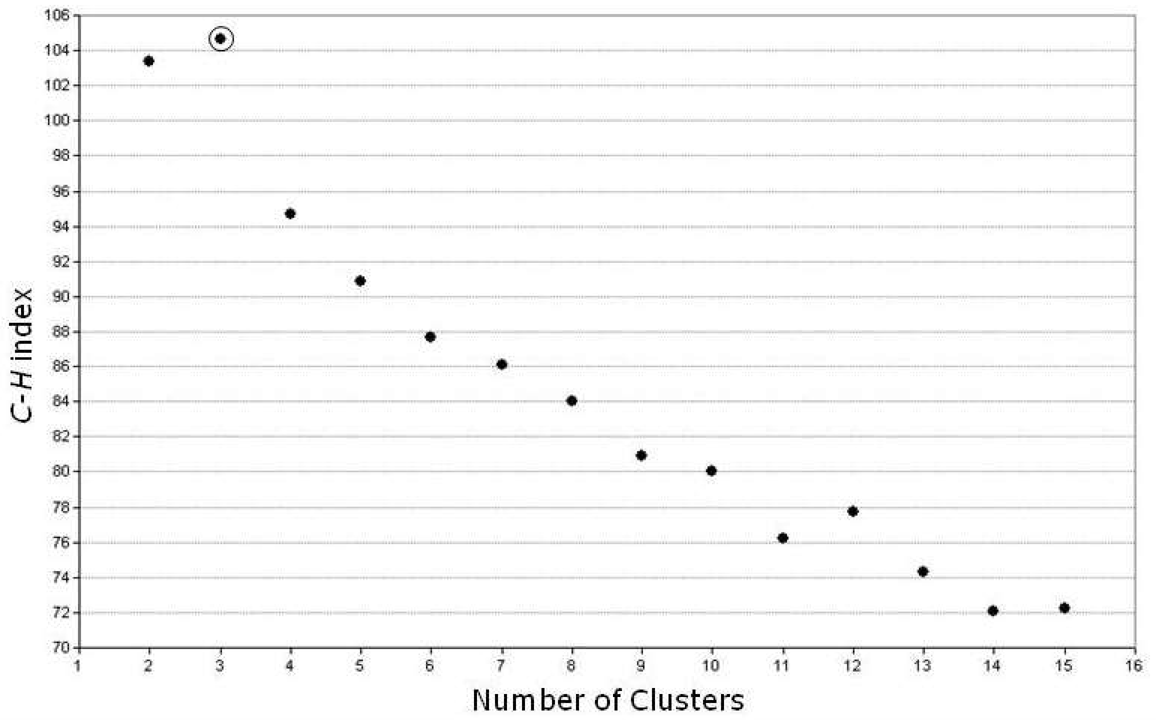


Figure 7. C–H index plot. Large circle represents the maximum C–H index, indicating the optimum number of clusters for the three variables, ECa, trunk circumference and fruit yield, evaluated for 2–15 clusters. Results indicate $k$ = 3 as the optimal number of clusters.

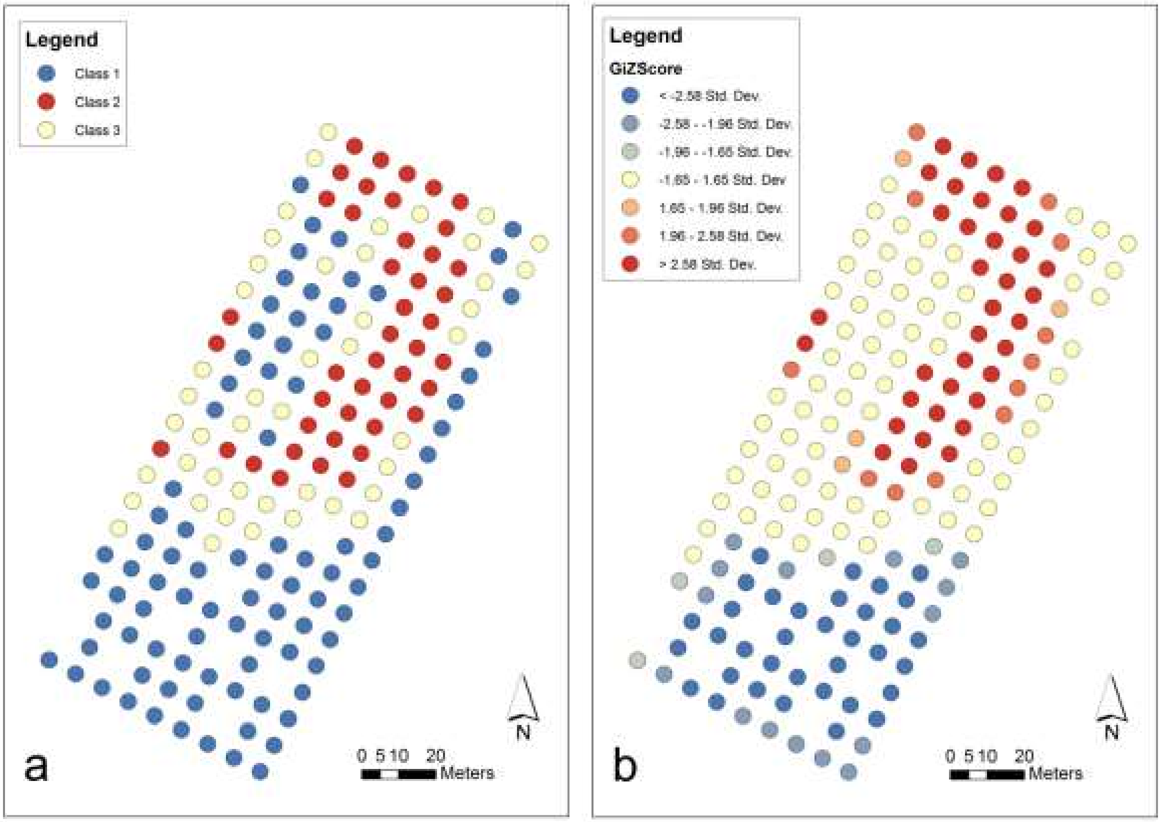


Figure 8. Output of cluster analysis applied to ECa [mS/m]: *k*-means clustering (a) and $G_i^*$ statistic (b). In the spatial method red indicates significant spatial clusters of high values (a hot-spot), blue indicates significant spatial clusters of low values (a cold-spot) and white indicates random distribution with no spatial clustering. In *k*-means the colors represent only the different clusters, and do not refer to the type of clustering. The same symbology refers to Figs. 9–11. (For interpretation of the references to color in this figure legend, the reader is referred to the web version of this article.)

It is clearly noticeable that with all variables *k*-means outputs produce pronounced patchiness and spatial discontinuity, while the $G_i^*$ statistic results in more spatially contiguous clusters.

It is further noticeable from Figs. 8–10 that each variable resulted in a unique spatial structure suggesting that multivariate-based clustering, taking into account all variables combined and resulting in an integrated spatial structure of the orchard, could be considered. The C–H index was applied again to select the optimal number of clusters, only this time the *z*-scores were used as inputs. The highest C–H index was again reported for $k$ = 3, which was therefore selected for partitioning the *z*-scores into clusters. Fig. 11b demonstrates the output of the final step in the model in which the *z*-score outputs of the $G_i^*$ statistic (Figs. 8b–10b) are used as inputs for *k*-means clustering. Results clearly demonstrate three spatially contiguous clusters. However, since *k*-means reports only class numbers without indicating the type of cluster, the question is whether the spatial structure of significant hot-spots and of significant cold-spots, recognized when applying the $G_i^*$ statistic on the single variables, is preserved in the multivariate output clusters.

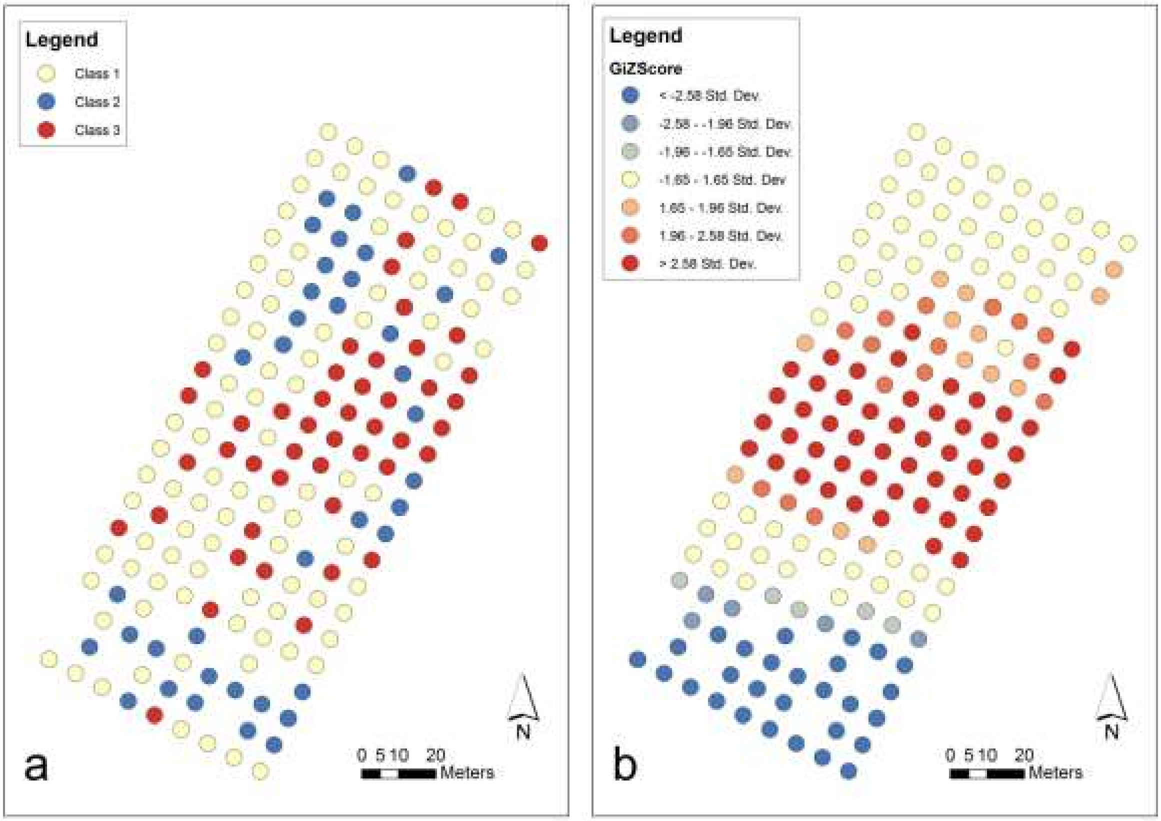


Figure 9. Output of cluster analysis applied to tree trunk circumference [cm]: *k*-means clustering (a), and $G_i^*$ statistic (b).

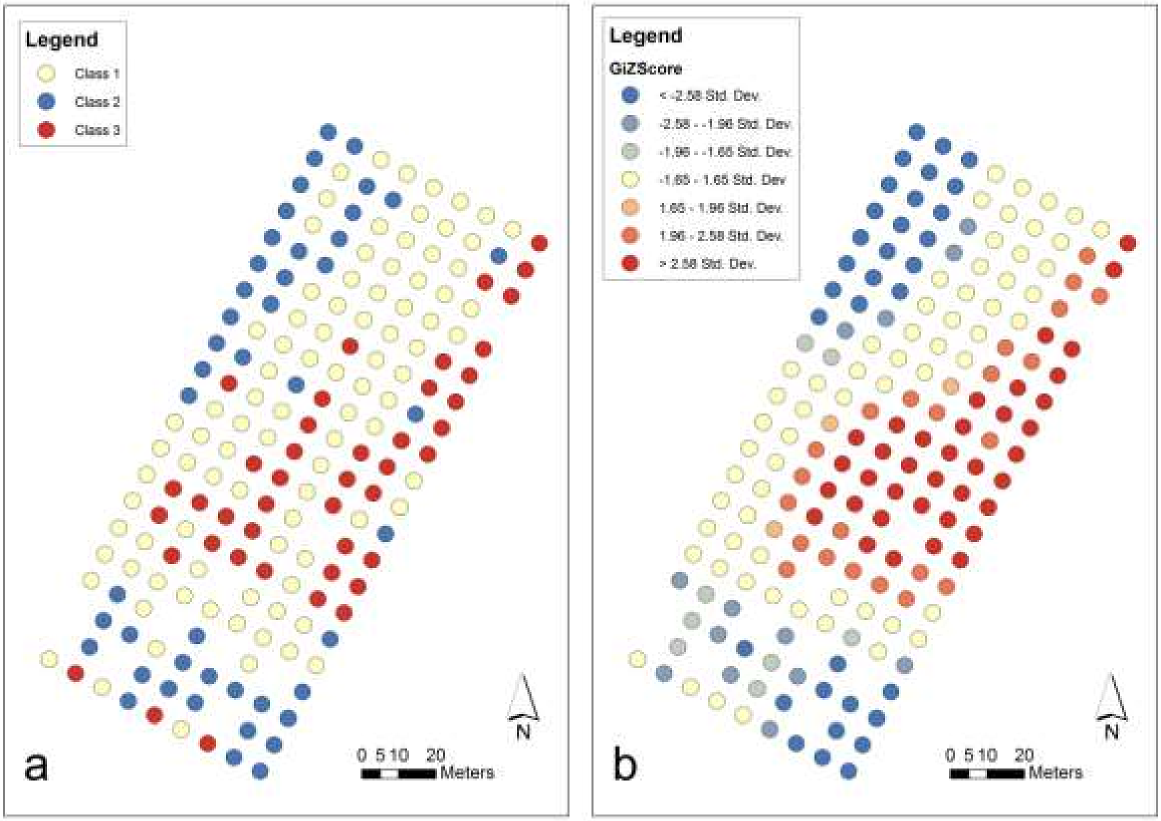


Figure 10. Output of cluster analysis applied to yield (kg fruit per tree): *k*-means clustering (a) and $G_i^*$ statistic.

Table 5. Critical *p*-values and *z*-scores.

| *z*-Score | *p*-Value (probability) | Confidence level |
|---|---|---|
| -1.96 < *z*-score > 1.96 | No statistical significance | |
| *z*-score < -1.65 or *z*-score > 1.65 | <0.10 | 90% |
| *z*-score < -1.96 or *z*-score > 1.96 | <0.05 | 95% |
| *z*-score < -2.58 or *z*-score > 2.58 | <0.01 | 99% |

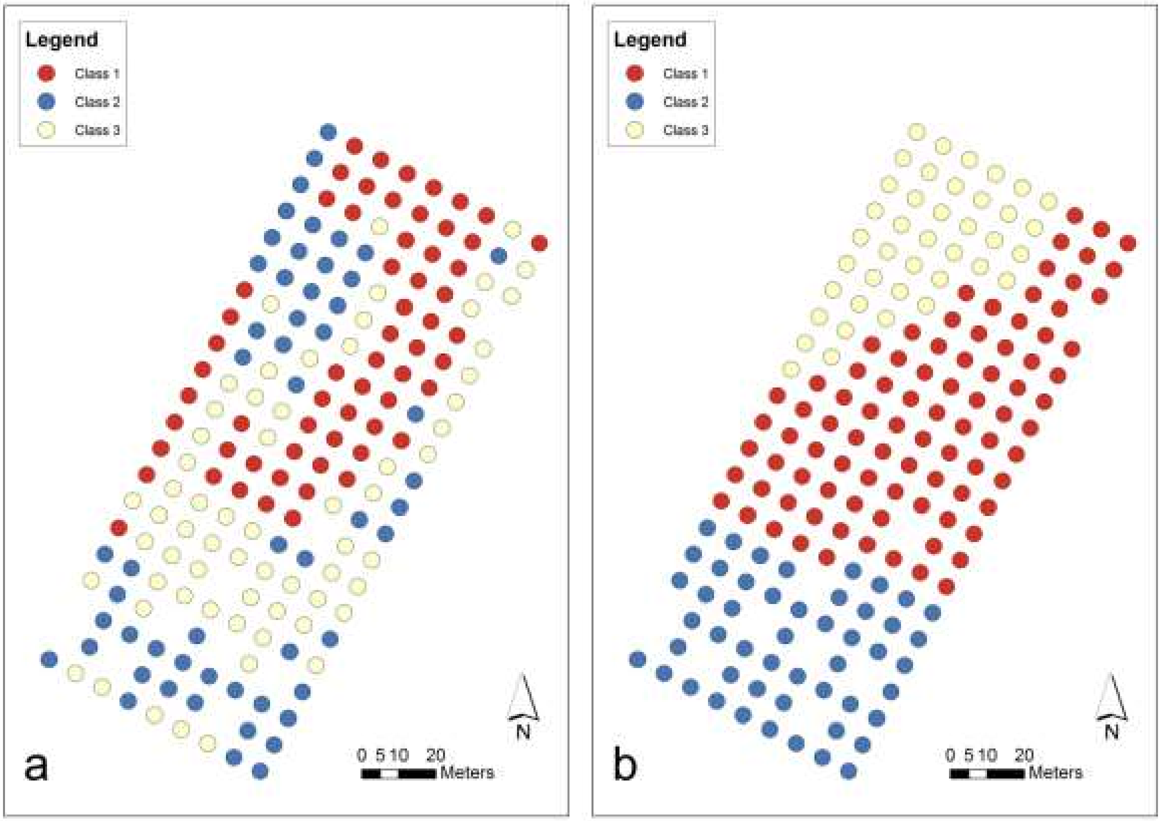


Figure 11. Output of multivariate *k*-means clustering applied to all variables considering the data values of each variable only (a) vs. output of multivariate *k*-means clustering applied to all variables considering the *z*-score outputs (b) of the $G_i^*$ statistic for each variable (Figs. 8b–10b).

### 3.6 Validation of methods

To assess the performance of the proposed approach the output clusters were compared with results of *k*-means using the common routine of considering variable data values only; i.e. no consideration of spatial structure (Fig. 11a).

To compare which method divided the data most effectively i.e. maximizing the degree of within-cluster similarities as well as the degree of between-cluster differences, the goodness of variance fit (GVF) was computed for each variable in each method. The GVF is a well established method for measuring the precision of cluster partitioning (Cauvin et al., 2010) and was computed using Eq. (4):

$$GVF = \frac{SST - SSW}{SST} \tag{4}$$

Table 6. GVF values comparing between the aspatial *k*-means clustering and the proposed spatial–aspatial approach.

| Method | Trunk circumference variable | ECa variable | Yield variable |
|---|---|---|---|
| Multivariate aspatial *k*-means clustering | 0.74 | 0.41 | 0.39 |
| Multivariate spatial–aspatial approach | 0.77 | 0.60 | 0.64 |

where SST reflects between-group differences and SSW reflects within-group similarities. Calculation of SST is based on summing the squared deviations of each value from the global mean of the entire dataset. Calculation of SSW is based on summing the squared differences of every value from the mean value of the class it belongs to. The closer the GVF index is to 1, the more homogenous the clusters are i.e. the better the variable is at partitioning the dataset into clusters. Table 6 compares the GVF values for *k*-means clustering applied to all variables without considering the spatial structure (Fig. 11a) and for the combined spatial–aspatial approach (Fig. 11b). The tree trunk circumference variable has the highest GVF value and is therefore the best of the three variables for discriminating the trees into clusters, i.e. recognizing the underlying structure. The combined spatial–aspatial method better discriminated trees into groups for all variables with a significant improvement recorded for ECa and yield.

To examine how the spatial structure of hot-spots and cold-spots, recognized for the single variables with the $G_i^*$ statistic, is represented in the multivariate output clusters, the distribution of *z*-score values, which served as the input for the multivariate classification, was examined. Table 7 shows the mean *z*-score of each variable within each spatial cluster. The values illustrate that the combined spatial–aspatial method maintains the general spatial structure (hot-spot, cold-spot and no spatial clustering) recognized for the single variables. For each of the variables in the multivariate classification, one class has always a mean *z*-score >1.65 (hot-spot with 90% confidence level), a mean *z*-score <-1.65 (cold-spot with 90% confidence level) and a mean *z*-score between -1.65 and +1.65 (random distribution with no spatial clustering). The spatial structure of the trunk circumference variable is best represented in the multivariate classification, with the mean *z*-score values in the different clusters following a similar pattern to the one recognized with the single variable classification (Fig. 9b): a cold-spot at the southern part of the orchard (Class 2), a hot-spot at the central part (Class 1) and random distribution with no spatial clustering at the northern part (Class 3).

Table 7. Minimum, maximum and mean *z*-score values for each variable in the different spatial clusters of the multivariate clustering.

| **Trunk circumference** | **Min** | **Max** | **Mean** | **Cluster type** |
|---|---|---|---|---|
| Class 1 | -0.1036 | 5.2688 | 2.6865 | Hot-spot |
| Class 2 | -4.6698 | -0.2146 | -2.6111 | Cold-spot |
| Class 3 | -1.4662 | 3.0923 | 0.2654 | No spatial clustering |
| ***Yield*** | | | | |
| Class 1 | -1.2883 | 4.3254 | 1.9938 | Hot-spot |
| Class 2 | -4.6057 | 2.2212 | -1.3614 | No spatial clustering |
| Class 3 | -4.9834 | 0.3433 | -2.6511 | Cold-spot |
| ***ECa*** | | | | |
| Class 1 | -2.5884 | 4.1123 | 0.9425 | No spatial clustering |
| Class 2 | -3.7397 | -1.1026 | -2.8426 | Cold-spot |
| Class 1 | -2.5884 | 4.1123 | 0.9425 | Hot-spot |

## 3.7 Discussion

Although clustering methods have been used in agricultural practices for several decades, only recently has consideration of spatial structure been introduced in the clustering process. Orchards require a spatial clustering approach based on both data collected from individual trees (plant attributes) and on data describing environmental conditions and which considers location and spatial relations between a tree and its neighbors. Combining a spatial method such as the $G_i^*$ statistic with the common aspatial *k*-means clustering method improves clustering results. Outputs of *k*-means clustering or any other aspatial clustering method tend to produce zones which are more irregular and patchy then zones from spatial clustering. In practice, clustering and mapping of clusters should serve as a method for visual and quantitative inspection of complex data sets. If determined appropriate, these clusters could be used for delineating management zones. Spatially contiguous clusters/zones resulting from applying the $G_i^*$ statistic can be beneficial if technology does not allow management of individual trees or if small-scale operational variations are too costly. A particular example for an application which will profit from relatively large contiguous zones would be irrigation.

Consideration of a number of points is advised when combining spatial clustering:

(1) Different input variables result in different output clusters. To create useful management zones, the combination of variables used for partitioning a field into

clusters must have logical management repercussions. For example, if managing for yield, only those variables considered yield defining and representing yield variability need to be considered.

(2) Care should be taken when defining the extent of the spatial neighborhood that surrounds each feature and the type of spatial interactions among features. The $G_i^*$ statistic is affected by the number of neighbors and their spatial interactions, which are used for defining the spatial weight matrix and consequently for quantifying the spatial weights assigned to each of the neighboring features. For example, a variety of spatial weighting schemes could be considered. In addition, the type of variable which is being modeled whether soil, plant or environmental, will influence the size and type of the spatial neighborhood.

(3) Additional spatial-based clustering approaches exist which should be further explored for their robustness in combined spatial–aspatial approaches. One of these is the Local Moran's I statistic (Anselin, 1995), which is the most commonly used method for evaluating local spatial autocorrelation. While the Local Moran's I and $G_i^*$ statistic are similar in terms of the questions that they answer, they have some major differences which will likely generate unique clustering. One of the main differences is that the Local Moran's I does not consider the value of the feature which is being analyzed in the analysis, but only the neighboring values. The $G_i^*$ statistic includes both the values of neighbors as well as the value of the tree in question. Since the value of the feature contributes to the emergence of the cluster, the $G_i^*$ statistic may be more suitable for locating contiguous cold-spots and hot-spots and therefore is expected to better locate potential homogenous areas to be used as management zones.

(4) Point-based spatial clustering methods require sufficient sampling to achieve reliable results in the spatial statistical analysis. The rule-of-thumb considers the number of 30 samples as a lower threshold (ESRI, 1984) in order to mitigate too large an effect by outliers or by points laying on the edge which will inevitably have fewer neighbors. It is also known that *k*-means is sensitive to outliers (Theodoridis et al., 2010).

(5) While we envision the major contribution of the proposed spatial clustering method to be in the determination of zones for optimal precision management of tree crops, it has other potential uses. Since testing of statistical significance of belonging to a certain cluster is based on single trees, decision makers can evaluate both the condition of each tree and its correlation with local influencing variables. The approach can therefore be used, when appropriate, to guide management of individual trees. The tree level spatial statistics provided can also aid in identifying locations for optimal field sampling (of soil or leaves, for example) or of placement of sensors for plant or environmental monitoring (Agam et al., 2014).

## 3.8 Summary and conclusions

A combined spatial–aspatial clustering approach for partitioning tree-based data in orchards has been developed. Essentially, the proposed algorithm spatially scales raw data using the $G_i^*$ statistic and converts it into spatial-variables before submitting it to (aspatial/standard) $k$-means clustering. The approach was applied to a case study to demonstrate its feasibility and assess its performance in relation to the common aspatial $k$-means clustering method. Results demonstrate that point-based spatial-clustering methods and, in particular, the $G_i^*$ statistic, when combined with aspatial clustering, represent a valid method to characterize the spatial structure of point-based data such as single trees in an orchard based on multiple variables. Introducing spatial clustering allows modeling two of the most important concepts in spatial phenomena: spatial autocorrelation and spatial heterogeneity. Another important aspect in the developed approach is that it is based on inferential spatial statistics and thus probabilities are assigned to the conclusions drawn from the analysis. Calculating the probability that an observed spatial cluster is not simply due to random chance is important especially when a high level of confidence is required, as in decision making. This provides tools for promoting reliable, informed decisions and for evaluating management decisions.

The combined spatial–aspatial approach forms a basis for further inquiry regarding application of spatial clustering methods to horticultural data. More research is required to apply and test the validity of the method for cases with other and a larger number of variables.

## 3.9 Acknowledgements

The presented research is part of the *'3D-Mosaic'* project funded by the European Commission's ERA-Net ICT-Agri project contributed to by Israel’s Ministry of Agriculture and Rural Development, Chief Scientist fund, project 304-0450.

## 3.10 References

Agam, N., Segal, E., Peeters, A., Dag, A., Yermiyahu, U., & Ben-Gal, A. (2013). Spatial distribution of water status in irrigated olive orchard by thermal imaging. Precision Agriculture, doi:doi.org/10.1007/s11119-013-9331-8

Aggelopoulou, K. D., Wufsohn, D., Fountas, S., Gemtos, T. A., Nanos, G. D., & Blackmore, S. (2010). Spatial variation in yield and quality in a small apple orchard. Precision Agriculture, 11(538-556)

Aggelopoulou, K., Castrignano, A., Gemtos, T., & Benedetto, D. (2013). Delineation of management zones in an apple orchard in greece using a multivariate approach. Computers and Electronics in Agriculture, 90, 119-130.

Anselin, L. (1995). Local indicators of spatial association - LISA. Geographical Analysis, 27(2), 93-115.

Ball, G., Hall, D., 1965. ISODATA, a novel method of data analysis and pattern classification. Technical report NTIS AD 699616.

Calinski, T., & Harabasz, J. (1974). A dendrite method for cluster analysis. Communications in Statistics, 3, 1-27.

Castrignanò, A., Boccaccio, L., Cohen, Y., Nestel, D., Kounatidis, I., De Papadopoulos, N.T., Benedetto, D., Mavragani-Tsipidou, P., 2012. Spatio-temporal population dynamics and area-wide delineation of Bactrocera olea monitoring zones using multi-variate geostatistics. Precision Agric. 13 (4), 421–441.

Cauvin, C., Escobar, F., Serradj, A., 2010. Thematic Cartography, Cartography and the Impact of the Quantitative Revolution. ISTE Ltd. and John Willey & Sons Inc., NJ, USA.

Chopin, P., Blazy, J.M., 2013. Assessment of regional variability in crop yields with spatial autocorrelation: banana farms and policy implications in Martinique. Agric. Ecosyst. Environ. 181, 12–21.

Chun, Y., & Griffith, D. A. (2013). Spatial statistics & geostatistics. London: SAGE Publications Inc.

Cohen, Y., Sharon, R., Sokolsky, T., & Zahavi, T. (2011). Modefied hot-spot analysis for spatio-temporal analysis: A case study of the leaf-roll virus expansion in vineyards. Spatial2 Conference: Spatial Data Methods for Environmental and Ecological Processes, Foggia, Italy.

Cohen, S., Cohen, Y., Alchanatis, V., Levi, O., 2013. Combining spectral and spatialinformation from aerial hyperspectral images for delineating homogenous management zones. Biosyst. Eng. 114 (4), 435–443.

Cooper, M.C., Milligan, G.W., 1988. The effect of measurement error on determining the number of clusters in cluster analysis. In: Gaul, W., Schader, M. (Eds.), Data, Expert Knowledge and Decisions. An Interdisciplinary Approach with Emphasis on Marketing Applications. Springer-Verlag, Berlin, pp. 319–328.

Córdoba, M., Bruno, C., Costa, J., & Balzarini, M. (2013). Subfield management class delineation using cluster analysis from spatial principal components of soil variables. Computers and Electronics in Agriculture, 97(0), 6-14. doi:http://dx.doi.org/10.1016/j.compag.2013.05.009

Corwin, D. L., & Plant, R. E. (2005). Applications of apparent soil electrical conductivity in precision agriculture. Computers and Electronics in Agriculture, 46(1-3), 1-10.

Cressie, N., & Wikle, C. K. (2011). Statistics for spatio-temporal data [null]. NJ: John Willey & Sons, Inc.

Davatgar, N., Neishabouri, M. R., & Sepaskhah, A. R. (2012). Delineation of site specific nutrient management zones for a paddy cultivated area based on soil fertility using fuzzy clustering. Geoderma, 173–174(0), 111-118. doi: http://dx.doi.org/10.1016/j.geoderma.2011.12.005

ESRI. (1984). ArcGIS® desktop 10.0 copyright © 1999-2010 ESRI inc.

Fleming, K. L., Westfall, D. G., Wiens, D. W., & Brodahl, M. C. (2000). Evaluating farmer defined management zone maps for variable rate fertilizer application. Precision Agriculture, 2, 201-215.

Fraisse, C. W., Sudduth, K. A., & Kitchen, N. R. (2001). Delineation of site-specific management zones by unsupervised classification of topographic attributes and soil electrical conductivity. Transactions of the ASAE, 44(1), 155-166.

Fridgen, J. J., Kitchen, N. R., Sudduth, K. A., Drummond, S. T., Wiebold, W. J., & Fraisse, C. W. (2004). Management zone analyst (MZA): Software for subfield management zone delineation. Agronomy Journal, 96, 100-108.

Fu, Q., Wang, Z., & Jiang, Q. (2010). Delineating soil nutrient management zones based on fuzzy clustering optimized by PSO. Mathematical and Computer Modelling, 51, 1299-1305.

Gebbers, R., Lück, E., Dabas, M., Domsch, H., 2009. Comparison of instruments for geoelectrical soil mapping at the field scale. Near Surf. Geophys. 7, 179–190.

Getis, A., & Ord, J. K. (1992). The analysis of spatial association by use of distance statistics. Geographical Analysis, 24(3), 189-206.

Getis, A., & Ord, J. K. (1996). Local spatial statistics: An overview. In P. Longley, & M. Batty (Eds.), Spatial analysis: Modeling in GIS environment (pp. 261-278). New York, USA: John Wiley & Sons, Inc.

Gordon, A.D., 1996. A survey of constrained classification. Comput. Stat. Data Anal. 21 (1), 17–29.

Guastaferro, F., Castrignanò, A., De Benedetto, D., Sollitto, D., Troccoli, A., & Cafarelli, B. (2010). A comparison of different algorithms for the delineation of management zones. Precision Agriculture, 11(6), 600-620.

Haining, R., 2003. Spatial Data Analysis. In: Theory and Practice. Cambridge University Press, Cambridge, UK.

Jain, A. K. (2010). Data clustering: 50 years beyond K-means. Pattern Recognition Letters, 31(8), 651-666. doi:http://dx.doi.org/10.1016/j.patrec.2009.09.011

Kitchen, N. R., Sudduth, K. A., & Drummond, S. T. (1999). Soil electrical conductivity as a crop productivity measure for claypan soils. Journal of Production Agriculture, 12, 607-617.

Kitchen, N. R., Drummond, S. T., Lund, K. A., Sudduth, K. A., & Buchleiter, G. W. (2003). Soil electrical conductivity and topography related to yield for three contrasting soil-crop systems. Agronomy Journal, 95, 483-495.

Kitchen, N. R., Sudduth, K. A., Myers, D. B., Drummond, S. T., & Hong, S. Y. (2005). Delineating productivity zones on claypan soil fields using apparent soil eleectrical conductivity. Computers and Electronics in Agriculture, 46, 285-308.

Kounatidis, I., Papadopoulos, N.T., Mavragani-Tsipidou, P., Cohen, Y., Tertivanidis, K., Nomikou, M., Nestel, D., 2008. Effect of elevation on spatio-temporal patterns of olive fly (Bactrocera oleae) populations in northern Greece. J. Appl. Entomol. 132 (9–10), 722–733.

Lark, R.M., 1998. Forming spatially coherent regions by classification of multivariate data: an example from the analysis of maps of crop yield. Int. J. Geogr. Inform. Sci. 12 (1), 83–98.

Legendre, P., Legendre, L., 2012. Numer. Ecol., third ed Elsevier, Amsterdam, The Netherlands.

Lloyd, S., 1982. Least squares quantization in PCM. IEEE Trans. Inf. Theory 28, 129–137 (Originally as an unpublished Bell laboratories Technical Note at 1957).

Lloyd, C.D., 2010. Spatial Data Analysis. Oxford University Press Inc., New York.

Lück, E., Gebbers, R., Ruehlmann, J., Spangenberg, U., 2009. Electrical conductivity mapping for precision farming. Near Surf. Geophys. 7, 15–25.

MacQueen, J. B. (1967). Some methods for classification and analysis of multivariate observations. Proceedings of the 5th Berkely Symposium on Mathematical Statistics and Probability. University of California Press. Berkely, California., Vol. 1 281-297.

Mann, K. K., Schumann, A. W., & Obreza, T. A. (2010). Delineating productivity zones in a citrus grove using citrus production, tree growth and temporally stable soil data. [null] Precision Agriculture, 12(4), 457-472.

McQueen, J., 1967. Some methods for classification and analysis of multivariate observations. In: Proceedings of the Fifth Berkeley Symposium on Mathematics, Statistics and Probability, Berkeley, pp. 281–297.

Milligan, G.W., Cooper, M.C., 1985. An examination of procedures for determining the number of clusters in a data set. Psychometrika 50 (2), 159–179.

Mitchell, A. (2005). The ESRI guide to GIS analysis, volume 2: Spatial measurements & statistics. Redlands, CA: ESRI Press.

Mucherino, A., Papajorgji, P., & Pardalos, P. M. (2009). Data mining in agriculture. New York: Springer.

Ord, J. K., & Getis, A. (1995). Local spatial autocorrelation statistics: Distributional issues and an application. Geographical Analysis, 27(4), 286-306.

Orpin, A.R., Kostylev, V.E., 2006. Towards a statistically valid method of textural sea floor characterization of benthic habitats. Mar. Geol. 225 (1–4), 209–222.

Ortega, R. A., & Santibáñez, O. A. (2007). Determination of management zones in corn (zea mays L.) based on soil fertility. Computers and Electronics in Agriculture, 58(1), 49-59. doi:10.1016/j.compag.2006.12.011

Pedroso, M., Taylor, J., Tisseyre, B., Charnomordic, B., Guillaume, S., 2010. A segmentation algorithm for the delineation of agricultural management zones. Comput. Electron. Agric. 70 (1), 199–208.

Perry, E. M., Dezzani, R. J., Seavert, C. F., & Pierce, F. J. (2010). Spatial variation in tree characteristics and yield in a pear orchard. Precision Agriculture, 11, 42-60.

Ping, J.L., Dobermann, A., 2003. Creating spatially contiguous yield classes for sitespecific management. Agron. J. 95 (5), 1121–1131.

Rud, R., Shoshany, M., Alchanatis, V., 2013. Spatial–spectral processing strategies for detection of salinity effects in cauliflower, aubergine and kohlrabi. Biosyst. Eng. 114 (4), 384–396.

SAS Institute Inc., 2013. SAS/STAT 13.1 User's Guide.

Shatar, T.M., McBratney, A.B., 2001. Subdividing a field into contiguous management zones using a k-zone algorithm. In: Proceedings of the 3rd European Conference on Precision Agriculture, Agro Montpellier, Montpellier, France, pp. 115–120.

Steinhaus, H., 1956. Sur la division des corp materials en parties. Bull. Acad´ . Polon. Sci. IV 12, 801–804 (in French).

The MathWorks, 2013. MATLAB Statistical Toolbox R2014a.

Theodoridis, S., Pikrakis, A., Koutroumbas, K., Cavouras, D., 2010. Introduction to Pattern Recognition. Academic Press, Amsterdam, The Netherlands, A MATLAB Approach.

Van Vitharana, U.W.A., Meirvenne, M., Simpson, D., Cockx, L., De Baerdemaeker, J., 2008. Key soil and topographic properties to delineate potential management classes for precision agriculture in the European loess area. Geoderma 143 (1– 2), 206–215.

Yan, L., Zhou, S., Feng, L., & Hong-Yi, L. (2007). Delineation of site-specific management zones using fuzzy clustering analysis in a coastal saline land. Computers and Electronics in Agriculture, 56, 174-186.

Zaman, Q., & Schumann, A. W. (2006). Nutrient management zones for citrus based on variation in soil properties and tree performance. Precision Agriculture, 7(45-63)

Zhang, N., Wang, M., & Wang, N. (2002). Precision agriculture - a worldwide view. Computers and Electronics in Agriculture, 36(3-2), 132-113.

# 4 Evaluating spatially resolved influence of soil and tree water status on quality of European plum grown in semi-humid climate

Jana Käthner, Alon Ben-Gal, Robin Gebbers, Aviva Peeters, Werner B. Herppich, and Manuela Zude-Sasse

(Frontiers in Plant Science, 2017,8, 1-10, DOI: 10.3389/fpls.2017.01053 )

## 4.1 Abstract:

In orchards, the variations of fruit quality and its determinants are crucial for resource effective measures. In the present study, a drip-irrigated plum production (Prunus domestica L. 'Tophit plus'/Wavit) located in a semi-humid climate was studied. Analysis of the apparent electrical conductivity (ECa) of soil showed spatial patterns of sand lenses in the orchard. Water status of sample trees was measured instantaneously by means of leaf water potential, $\Psi_{leaf}$ [MPa], and for all trees by thermal imaging of canopies and calculation of the crop water stress index (CWSI). Methods for determining CWSI were evaluated.

A CWSI approach calculating canopy and reference temperatures from the histogram of pixels from each image itself was found to suit the experimental conditions. Soil ECa showed no correlation with specific leaf area ratio and cumulative water use efficiency (WUEc) derived from the crop load. The fruit quality, however, was influenced by physiological drought stress in trees with high crop load and, resulting (too) high WUEc, when fruit driven water demand was not met. As indicated by analysis of variance, neither ECa nor the instantaneous CWSI could be used as predictors of fruit quality, while the interaction of CWSI and WUEc did succeed in indicating significant differences. Consequently, both WUEc and CWSI should be integrated in irrigation scheduling for positive impact on fruit quality.

Keywords: fruit quality, precision horticulture, plum, spatial variability, tree water status.

## 4.2 Introduction

Following the concept of precision agriculture, correlation of spatial variation of soil and yield data has been analyzed in field crops, vegetable production, vineyards, and orchards. Spatial patterns of fruit yield are typically explained in one of two approaches. The first analyzes the spatial correlation between soil properties influencing the water supply as one main growth factor and yield as the target variable. This is consistent with findings in precision viticulture, where soil maps have provided a basis for delineating management zones (Williams and Araujo, 2002). The second approach is more driven by the endogenous growth factors of the plant. It uses the correlation of plant data such as canopy volume representing the growth capacity, tree water status, and fruit quality at harvest (Zaman and Schumann, 2006). This latter approach may be more appropriate for orchards where fruit quality is crucial for marketing. However, the analysis of spatially-resolved soil and plant data and its influence on fruit quality has rarely been studied.

The most common method for soil mapping is to analyze the apparent electrical conductivity (ECa) of the soil (Bramley and Hamilton, 2004). Soil ECa measurements can be performed at field capacity to gain information regarding texture of the soil, while measurements in dry periods may better indicate soil water distribution. Mapping of electrical properties in orchard soils appears not without its challenges as commercial rolling systems often fail to measure close to the trees. Manually performed readings, most often with equidistant Wenner array, have been used with more success in covering the entire orchard soil (Halvorson and Rhoades, 1976; Gebbers et al., 2009). Experimental-scale ECa mapping, concomitantly performed with fruit yield analyses, confirmed a correlation between soil patterns and yield in various fruit crops including apples (Türker et al., 2011; Aggelopooulou et al., 2013), olives (Fountas et al., 2011; Agam et al 2014), and citrus (Zaman and Schumann, 2006; Peeters et al., 2015). However, while patterns of soil properties are generally stable over time (Mann et al., 2011), spatial patterns of variables measured on trees are more likely to vary (Aggelopoulou et al., 2010). Furthermore in orchards, soil water status is frequently influenced by irrigation causing intentionally reduced impact of a-priori patterns of soil properties on vegetative and generative plant growth. As a result, the effect of soil patterns on the quality of fruit might be reduced.

Using a physiological approach, the spatial variability of yield and quality have been found to be highly correlated with the canopy volume in citrus production (Zaman and Schumann, 2006; Zude et al., 2008). From a physiological point of view, it may be assumed that canopy volume, yield, and fruit quality are influenced by the exogenous water supply and the endogenous crop load (Palmer, 1992; Naor et al., 2001; Naor et al., 2006; Bustan et al., 2016). Strong interaction between water status of soil and trees has been pointed out in arid and semi-arid conditions (Naor et al., 2006; Ben-Gal et al., 2009; Gómez del Campo, 2013; Bustan et al., 2016), but also more ambiguous effects of crop load on tree water status have been reported for crops including peach, apple, and olive (Berman and DeJong, 1996; Bellvert et al., 2016; Bustan et al., 2016). The ultimate objective of orchard management of course would be to optimize not only the fruit quality, but also the cumulative water use efficiency (WUEc) in terms of yield per liter of totally applied irrigation and precipitation water (Viets, 1962).

The measurement of both, soil water status and plant water status, is challenged by the fact that any individual proximal sensor represents only a small volume of interest; a tree or part of a tree or a small volume of soil. Consequently, measuring the spatial distribution of water status in fruit trees has been approached by means of remote sensing, often via thermal imaging. Thermal images of canopies provide a measure of instantaneous tree water status interpreted by means of the crop water stress index (CWSI) (Jones, 1992). The CWSI is a surface-temperature based index between 1 and 0, with 1 representing the temperature of non-transpiring dry leaves and 0 equivalent to that of fully transpiring wet leaves (Jackson et al., 1981; Sammis et al., 1988; Maes and Steppe, 2012). While application of thermal imaging is easily applied in the laboratory, the technique has also been developed for field studies, particularly in the semi-arid and arid sub-tropics (Jones, 1992; Cohen et al., 2005; Hellebrand et al., 2006). Thermal imaging of canopies has been applied by means of unmanned aerial systems (Berni et al., 2009; Gonzáles-Dugo et al., 2013) and frequently tractor-mounted cameras providing either top or side views. The method has further been refined to measure CWSI and guide irrigation protocols in olives in Israel (Ben-Gal et al., 2009). In peach orchards located in a semi-arid environment, the CWSI was found to successfully differentiate between irrigation treatments (Bellvert et al., 2016). In differently irrigated apple trees under a hail net, CWSI values ranged between 0.08 and 0.55. Values > 0.3 were considered as stressed trees under the given conditions (Nagy, 2015). The development and use of CWSI has focused on sub-tropical, arid and semi-arid climates and has not yet been sufficiently studied under semi-humid conditions, where improving fruit quality, instead of providing for canopy transpiration, may be the most significant driver of irrigation water management. It is questionable if instantaneous methods for measuring water status, such as the thermal based CWSI, can support optimization of fruit quality on one hand and WUEc on the other side.

Consequently, this study aimed (i) to select a feasible method for utilization of thermal imaging in a semi-humid climate, (ii) to spatially characterize the soil ECa and instantaneous water status of fruit trees in an orchard, and (iii) to analyze the interaction of tree water status and quality of fruit.

## 4.3 Material and Methods

### *4.3.1 Site Description and Plant Material*

The experiment was carried out in a 0.37 ha commercial Prunus domestica L. (plum) orchard located in the ‘Werder fruit production’ area in Brandenburg, Germany (52° 28′ 1.56″ N, 12° 57′ 28.8″ E). The soil is typical for fruit production in temperate climate of Europe and Asia formed by glacial and post-glacial deposits after the last ice age about 10,000 years ago with typically small scale variability. The cultivar was 'Tophit plus' with 'Jojo' serving as a pollinator. 104 seven year old 'Tophit plus' trees, located every 4 m in 4 rows spaced 5 m apart, were considered. On average, trees were 2.10 m tall and insertion height of the first branch varied between 0.46 m and 0.96 m above the soil. Mean soil texture was 45 % sand, 29 % silt, and 26 % clay with a mean pH of 7.72. Plum trees were irrigated using a drip system with one line per row and two emitters every 0.5 m. The irrigation laterals and drippers were mounted 50 cm above the ground to facilitate mechanical weed control. Independent of precipitation, trees were irrigated twice a week for 1.5 h with flow rate of 0.96 L $h^{-1}$.

### *4.3.2 Meteorological readings*

Global radiation, wind speed, air temperature, air pressure, precipitation, and relative humidity were measured at 24 minutes intervals by a weather station (UNIKLIMA vario, Toss, Germany) positioned 100 m from the experimental orchard. Canopy temperature and relative humidity (Modul DLTi, UP GmbH, Germany) were recorded in 18 trees every 5 minutes. Water vapor pressure deficit (VPD) of the air was calculated according to the Goff-Gratch-equation (Jones, 1992; von Willert et al., 1995) from hourly averages of air temperature, relative humidity and air pressure.

### *4.3.3 Soil readings*

A resistivity meter (4-point light hp, LGM, Germany) was used to map the ECa of the soil at the experimental site on 16th August 2012 and 2nd August 2013. The four electrodes were arranged in a Wenner array with the tree trunk in the center to obtain ECa values representing 25 cm depth (Telford et al., 1990). Full details are given in Käthner and Zude-Sasse (2015). Soil water matric potential (pf-meter 80, ecoTech Umwelt-Messsysteme GmbH, Germany) was measured at 15 cm, 35 cm, and 45 cm depths. In addition, the gravimetrical soil water content (GWC) was ascertained by drying soil samples at 105 °C for 48 hours with n = 26 in 2012 and n = 6 in 2013.

### *4.3.4 Leaf water status*

Three mature leaves were randomly detached from the north-eastern side of each tree and rapidly transported to the laboratory. Here, projected surface area [cm²] was measured for each leaf with a portable area meter (CI-203, CID Bio-Science, Inc., USA). Leaf dry mass [g] was consequently obtained after oven drying at 65 °C for 24 h and specific leaf area (SLA) was calculated as the ratio of leaf area and dry mass.

In the orchard, leaf water potential ($\Psi_{leaf}$) was measured with a Scholander bomb (Plant Water Status Console 3000, Soilmoisture Equipment Corp., USA) on three shaded leaves from the lower part of the canopy on the east side of the tree. In 2012, 44 trees were analyzed predawn and midday over 4 days (19th June - 27th June). In 2013, 67 trees were sampled over 5 days (19th July – 2nd August). Following determination of $\Psi_{leaf}$, the leaves were rapidly packed in plastic bags, transported to the laboratory, frozen at -30°C. After thawing, centrifuged tissue sap was analyzed for osmotic content ($c_{osmol}$) with a water vapor osmometer (Vapro 5520, Wescor Inc., USA). The osmotic potential ($\Psi_{\pi}$) of tissue sap was calculated according to the van't Hoff's equation (von Willert et al., 1995).

### *4.3.5 Crop water stress index*

Thermal images of the canopies were taken with an uncooled infrared thermal camera (ThermaCAM model SC 500, FLIR Systems, Inc., USA) with resolution of 320 pixel x 240 pixel and spectral sensitivity range from 7.5 µm to 13.0 µm in the temperature range of -50 to 60 °C on 15th August 2012 and 25th July 2013. The camera was mounted on a tractor with z = 3.3 m above ground and pointed to the top of the canopies. Images were acquired with an opening angle (β) of 45° resulting in the length (l) of the imaged area (Equ. 5).

$$l = 2 \cdot z \cdot \tan(\frac{\beta}{2}) \qquad (5)$$

For extraction of temperature values, the raw thermal images were obtained in the FLIR systems' proprietary format and converted to text file format for the processing with MATLAB® (R2010B, MathWorks, USA). Crop water stress index ($CWSI_J$) was calculated (Equ. 6) according to Jones (1992) ranging from 0 - 1:

$$CWSI_J = \frac{Tc - Twref}{Tdref - Twref} \qquad (6)$$

where Tc is actual canopy temperature, Tw is temperature of a fully transpiring leaf with open stomata obtained from a wet paper leaf analog, and Td is temperature of a non-transpiring leaf. When using references Tdref was obtained from a dry and Twref from paper leaf analog (Jones, 2004). For this purpose, green paper leaves were cut to the formerly measured mean leaf area of 6 cm², mounted on a 2 m stick, and manually placed in the center of the canopy in each tree.

In addition, CWSI was also calculated according to three alternative methods. Irmak et al. (2000) calculated the $CWSI_I$ (Equ. 7) setting non-transpiring leaf temperature at 5°C higher than air temperature (Td+5) and Tw as the minimum temperature found in the canopy.

$$\mathrm{CWSI_I} = \frac{\mathrm{Tc-Twmin}}{\mathrm{Td+5-Twmin}} \quad (7)$$

As described by work groups of Jones (1999) and Ben-Gal (2009), Tw and Td was obtained analytically (Appendix) to calculate $CWSI_{JB}$ (Equ. 8).

$$\mathrm{CWSI_{JB}} = \frac{\mathrm{Tc-Twana}}{\mathrm{Tdana-Twana}} \quad (8)$$

$CWSI_R$ was determined according to the work of Rud et al. (2015). Likely the most suitable for automated readings, this method calculates (Equ. 9) the canopy temperature ($Tc_{histo}$) and reference temperatures of dry ($Td_{histo}$) and wet ($Tw_{histo}$) leaves from the histogram of pixels from each image itself.

$$\mathrm{CWSI_R} = \frac{\mathrm{Tchisto-Twhisto}}{\mathrm{Tdhisto-Twhisto}} \quad (9)$$

In the $CWSI_R$ approach, before processing histograms, extreme values above air temperature representing Fresnel reflection from the sun were removed from the further analysis. In the histogram of pixels, thresholds were determined for separating temperatures of soil, grass, and canopy. Dry reference, $Td_{histo}$, was defined as the minimum temperature of soil visible as a peak with high values in the histogram. Wet reference, $Tw_{histo}$, was taken as the minimum temperature of canopy. Since the canopy and grass partly coincided, pixels were spatially compared considering equal values as grass and varying values as canopy. This threshold was found with Wiener filter to enhance the contrast (Honig and Goldstein, 2002; Chen et al., 2006). After removing the soil and grass data, the Tdhisto and mean canopy temperature ($Tc_{histo}$) were extracted and averaged for each tree.

### *4.3.6 Water Use Efficiency*

On the day of CWSI measurement, a portable porometer (CIRAS-1, PP Systems, Hitchin, UK) was used to monitor the diurnal course (n = 3) of $CO_2$ exchange and transpiration. The instantaneous water use efficiency (WUEi) was calculated as ratio of these parameters (von Willert et al., 1995) in µMol $CO_2$ $m^{-2}$ $s^{-1}$ / mMol $H_2O$ $m^{-2}$ $s^{-1}$.

The cumulative water use efficiency (Eq. 10) of the production system represents the ratio of yield (y) and water volume supplied to the plants [g $L^{-1}$],

$$WUEc = y/((i+pp)) \qquad (10)$$

with i = irrigation water, pp = precipitation from the start of vegetation period until harvest time.

In 2012, the accounted period lasted from 17th April – 30th August during which 182 mm of irrigation and 273 mm rain with a total of 455 mm water were supplied. In 2013, irrigation water was given from 22nd April – 9th September accounting for 168 mm of irrigation water and 248 mm of rain was recorded summing up to 416 mm water supply.

### *4.3.7 Fruit quality*

Soluble solids content [%] of fruit was analyzed using a digital refractometer (DR 301-95, A. Krüss Optronic, Germany). Dry matter content of fruit [%] was calculated as the ratio of fruit dry mass and fruit fresh mass. Fruit flesh firmness [N $cm^{-2}$] was analyzed as maximum force measured with a convex plunger at a velocity of 200 cm $min^{-1}$ (TA-XT Plus Texture Analyzer, Stable Micro Systems, UK). Fruit size measured as height [mm], fresh mass [g], and yield as number of fruits per tree and fresh mass per tree, was measured at harvest. In 2012, the analysis of fruit quality was carried out on all fruit of every tree, while in 2013, 3 fruits per tree were analyzed.

### *4.3.8 Data analysis*

Statistical analyses were carried out using the statistical package for MATLAB® (R2014b, MathWorks, U.S.). Multi-way analysis of variance (ANOVA) was used for testing the effects of multiple factors on the plant variables. Therefore, the ECa data were grouped in 8 classes (Käthner and Zude, 2015), while CWSI and WUEc were grouped according to the results of hotspot analysis.

Descriptive statistics of spatially resolved data was carried out using hotspot analysis according to Peeters and co-authors (Peeters et al., 2015), who used ArcGIS (ESRI, Redlands, CA, USA). In the present study, the algorithm was adapted for using the free spatial Matlab toolbox (Spatial Filtering, Max Planck Institute for Biochemistry, Germany). The method is based on the general (G) statistic for testing the effect of spatial autocorrelation (Getis and Ord, 1992) of the variables. Thereby a locally weighted mean around each observation is separately compared with the mean of the whole data (Anttila and Kairesalo, 2010). The outputs of the statistic are the z-score and the p-value, which indicate whether an observed pattern of clusters is statistically significant. Spatial clusters with statistically significant positive z-score are called hot spots, whereas the clusters with statistically significant negative z-score are called cold spots (Getis and Ord, 1992; Ferstl et al., 2007).

## 4.4 Results

### *4.4.1 Soil, meteorological conditions, and thermal imaging*

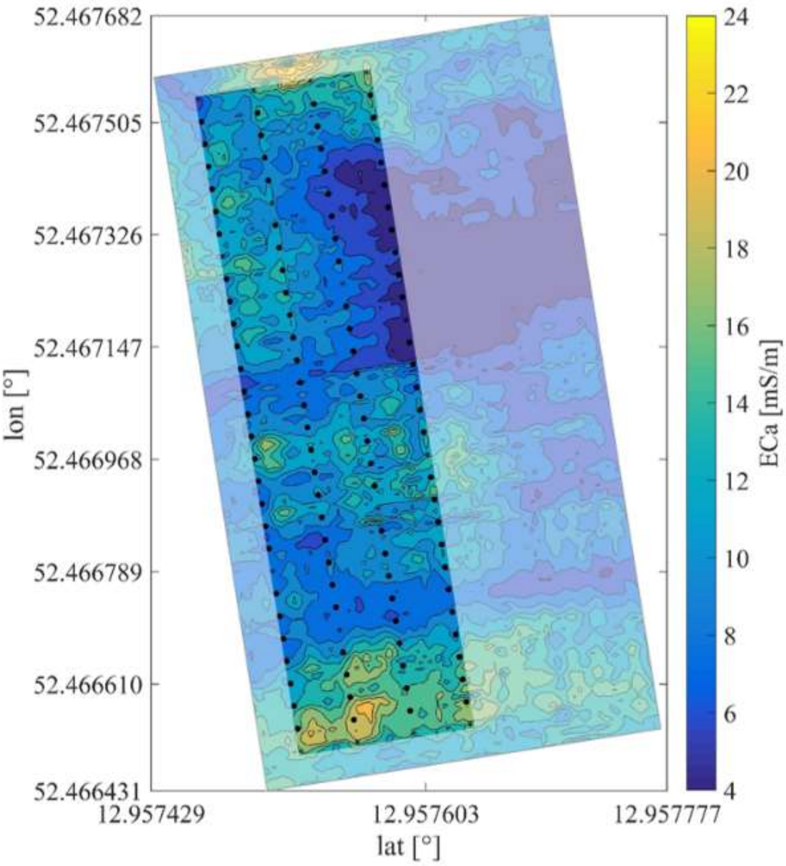


Figure 12. Plum orchard in north orientation with trees marked, showing apparent electrical conductivity of soil in false color.

The ECa of soil at 25 cm depth indicated small-scale variability (Figure 12). The values of soil ECa reached a maximum of 24 mS $m^{-1}$ with a pattern of reduced values pointing to a sand lens visible in the center-eastern part of the experimental field (Figure 12) and neighboring area. Another sandy area was located in the south-west of the orchard. Values of soil ECa measured in 2013, increased compared to those obtained in 2012. This may be due to wetter soils, which was caused by the relatively high precipitation occurring in July and August 2013. This assumption is further supported by the close correlations found between the gravimetrical soil water content and ECa with R = 0.45 and R = 0.68 in 2012 and 2013, respectively (Table 8). In contrast, correlation coefficients of soil matric potential (pF) and soil ECa were only R = 0.15 and R = 0.44 in 2012 and 2013, respectively (Table 8). Repeated analyses showed similar pattern in different years with R = 0.88 considering 2011 and 2012 and R = 0.71 for years 2012 and 2013.

Table 8. Summary of soil properties measured in plum orchard.

| Variable | n | Mean | Minimum | Maximum | SD | Skewness |
|---|---|---|---|---|---|---|
| **2012** | | | | | | |
| ECa [mS/m] | 104 | 7.09 | 1.67 | 15.38 | 2.77 | 0.90 |
| pf-meter [0;7] | 19 | 1.63 | 0.04 | 2.10 | 0.44 | -2.58 |
| Water content [%] | 26 | 7.61 | 4.43 | 9.63 | 1.37 | -0.57 |
| **2013** | | | | | | |
| ECa [mS/m] | 180 | 32.43 | 8.89 | 83.89 | 13.69 | 0.75 |
| pf-meter [0;7] | 19 | 1.70 | 0.01 | 3.30 | 0.98 | -0.51 |
| Water content [%] | 6 | 18.58 | 9.14 | 31.13 | 4.07 | 0.25 |

In 2012, during the acquisition of thermal images on 15th August from 13:40 until 16:19 (Figure 13), the mean global radiation was 641.1 W $m^{-2}$. August was the warmest month of the year with a mean maximum temperature of 25.6 °C. The maximum air temperature on the day of measurement was 25.4 °C. The diurnal increase of air temperature coincided with increasing VPD. The mean wind speed was 0.9 m $s^{-1}$. In 2013, mean global radiation of 306.8 W $m^{-2}$, maximum air temperature of 25.4 °C, and wind speed of 1.2 m $s^{-1}$ were measured.

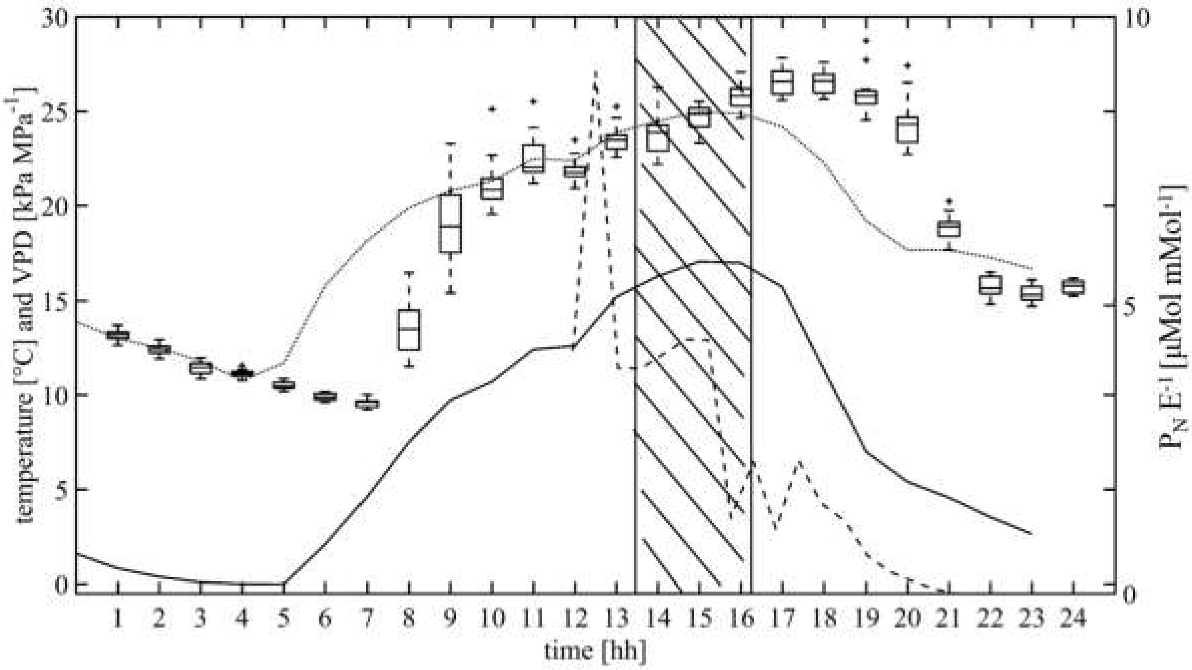


Figure 13. Air temperature (dotted line), water vapor pressure deficit (VPD; solid line) and instantaneous water use efficiency (WUEi as PN $E^{-1}$, dashed line) measured in the orchard on 15th August 2012. In addition, the variation (n = 18) and diurnal course of tree canopy temperature is shown as boxplot. The dashed area indicates the period used for analyzing the CWSI.

Compared to the free air temperature recorded by the automatic weather station, maximum temperature measured within the tree canopy occurred with a 3 h-delay. Maximum instantaneous water use efficiency was calculated just before noon and then declined during the rest of the day. In general, it ranged from 4.42 to 1.28 µMol $CO_2$ $m^{-2}$ $s^{-1}$/ mMol $H_2O$ $m^{-2}$ $s^{-1}$ (Figure 13). Inside the canopy, the VPD increased midday reaching a maximum in the afternoon at 17:00.

The instantaneous $\Psi_{leaf}$ at midday varied between -0.40 and -2.14 MPa and $\Psi_{\pi}$ between -1.93 and -2.56 MPa. At predawn, $\Psi_{leaf}$ varied between -0.12 and -1.48 MPa and $\Psi_{\pi}$ between -1.50 and -2.46 MPa.

Thermal images were acquired on partially cloudy days and wet and dry leaf-references were moved with the camera for each tree record within the orchard. With our camera set-up, I = 2.734 m and thus one pixel corresponded to 8.543 mm in width. This resolution was, thus, high enough to differentiate leaves, and to select the pixels that represent the wet and dry leaf-references (Table 9). In 2012, Vaseline® covered leaves were additionally used as dry leaf-references; however, the fingerprints of the application procedure remained visible on thermal images thus producing artefacts (data not shown).

The reference temperatures calculated with the analytical method (Ben-Gal et al., 2009) were always lower ($Tw_{ana}$ 12 – 15 and $Td_{ana}$ 17) compared to those measured on paper references or obtained from the histogram of images ($Tw_{histo}$ 16 – 21°C and $Td_{histo}$ 21 – 25°C). Furthermore, the correlations between leaf water potential ($\psi_{leaf}$) or osmotic potential ($\psi_{\pi}$) and the different crop water stress indexes were analyzed using data that were all obtained on the same day. Of all tested approaches, correlation coefficients for both $\psi_{leaf}$ and $\psi_{\pi}$ were highest for $CWSI_{JB}$, i.e. when the dry and wet temperatures were calculated analytically. In contrast, correlation between $CWSI_J$ and $\psi_{leaf}$ was low, showing enhanced variability caused by the appearance of clouds (Table 9). The use of air temperature plus 5° as Td and minimum temperature in the image as Tw for calculating $CWSI_I$ (Irmak et al., 2000) resulted in a bias with overestimated values and also tremendously high variability due to clouds and, therefore, data were not used further. The $CWSI_R$ ranged from 0.15 to 0.88, while the $CWSI_J$ and $CWSI_{JB}$ ranged from 0.03 to 0.78 and from 0.47 to 0.51, respectively. For $CWSI_{JB}$ correlation with $\psi_{leaf}$ was high, while the automated analysis of $CWSI_R$ resulted in slightly reduced, but significant ($p < 0.001$) correlation coefficient of R = 0.52 (Table 9). However, the latter approach provided the advantage of feasible analysis of Td and Tw based on the individual images taken in the varying environment. Consequently, all further analyses were based on $CWSI_R$.

Table 9. Ranges of wet (Tw) and dry (Td) reference temperatures obtained according to work groups of Jones and Ben-Gal (Ben-Gal et al., 2009) using weather data ($CWSI_{JB}$), Jones (Jones, 1992) using dry and wet paper leaves ($CWSI_J$), and Rud (Rud et al., 20015) using both references from the histogram of image ($CWSI_R$). Correlation coefficients (R) and F-values, asterisks (***) denoting significance at p<0.001 considering leaf water potential ($\psi_{leaf}$), osmotic potential ($\psi_{\pi}$), and crop water stress indexes are given of the same measuring day.

| Variable | n | $CWSI_{JB}$ | $CWSI_J$ | $CWSI_R$ |
|---|---|---|---|---|
| Tw | | 12.07-15.03 | 19.98 | 16.10-20.80 |

| | | | | | |
|---|---|---|---|---|---|
| Td | | | 16.95-17.06 | 24.93 | 21.00-24.00 |
| $\psi_{leaf}$ | 11 | R | - 0.65 | - 0.12 | - 0.52 |
| | | F | 4800*** | 3671*** | 3671*** |
| $\psi_T$ | 11 | R | - 0.57 | 0.33 | - 0.11 |
| | | F | 872*** | 911*** | 911*** |

*4.4.2 Hotspot anayses*

Hotspot analysis of ECa revealed one cold spot representing extreme low conductivity and 5 hot spots showing soil of high conductivity. Around the cold spot with critical z value of < -1.65 (90% confidence level) a sand lens with an extension of approx. 20 m x 25 m was found (Figure 12), while at the hot spots with critical value > 1.65 (90% confidence level) water logging was observed after heavy rain fall indicating soil with lower particle size (Figure 14). The soil ECa was correlated with the number of leaves per tree. Consistently, spatial variability of canopy VPD within the orchard was found in the x-direction, which pointed to an influence of geographical position in the orchard (Rx = 0.31, Ry = 0.03, Rz = 0.20). This is the same direction as found for extreme values of soil ECa.

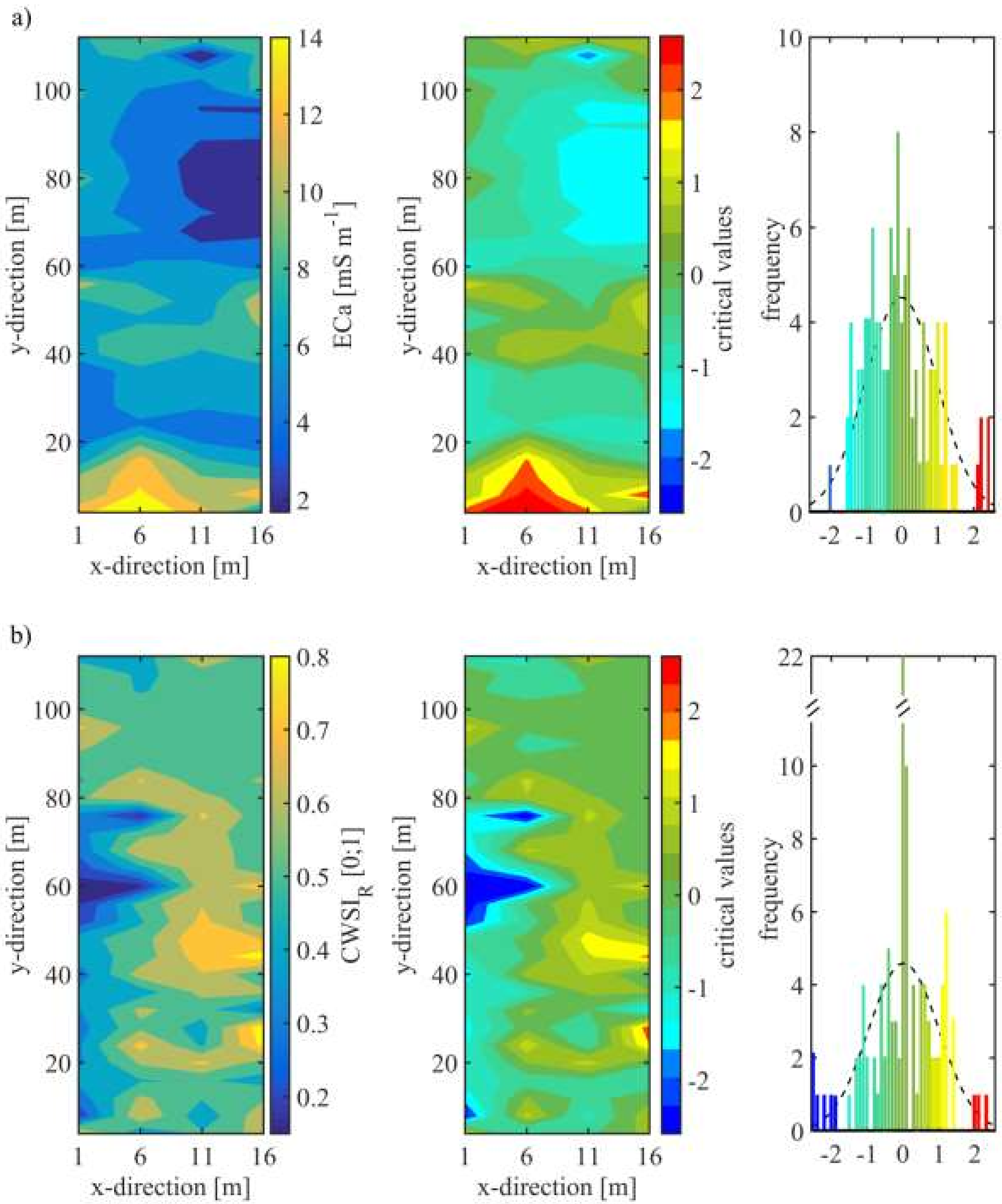


Figure 14. False colour maps providing the spatial distribution of (a) soil apparent electrical conductivity (ECa) and (b) instantaneous tree water status measured as crop water stress index (CWSI$_R$) in the experimental plum orchard. Given are raw data (left), critical values by hotspot analysis (middle), and histograms of critical values (right).

The CWSI$_R$ ranged from 0.15 to 0.88. The hotspot analysis of CWSI$_R$ revealed 5 cold spots occurring at z values < -1.65 representing trees with no water shortage. The 3 hot spots appeared at critical value >1.65 referring to high $CWSI_R$. Here, the hot spots refer to unfavorable conditions with enhanced water deficit. The hot spots appeared on the east side of the orchard, within and adjacent to the position of the central sand lens (Figure 14). The cold spots were found in the western positions of the orchard.

The comparison of spots considering soil ECa and $CWSI_R$ pointed to no correlation. Also, no correlation was found between canopy size dimension and $CWSI_R$ considering the canopy length parallel to the row (R = 0.010), canopy width perpendicular to the row (R = 0.015), and volume calculated from length, width, and distance between first branch and last shoot (R = 0.001).

### *4.4.3 Tree Water Status and Fruit Quality*

In 2012, the average leaf number per tree was 2362. The SLA ranged from 32.00 cm² $g^{-1}$ to 59.76 cm² $g^{-1}$ and showed no correlation with soil ECa. The fruit size was correlated with soil ECa at R = 0.223 considering the hot and cold spots. However, other fruit quality variables did not correlate with soil properties.

No correlation between leaf water potential and fruit quality was found in the few trees measured. $CWSI_R$ was correlated with SLA, but no significant difference was found for the number of leaves or fruit quality (Table 10). Cumulative water use efficiency obviously depends primarily on the degree of crop load, because the water supply was kept uniform in the orchard. Mean WUEc was 2.362 g $L^{-1}$ in 2012 and 2.521 g $L^{-1}$ in 2013. In 2012, WUEc seemed only slightly, if at all, affected by soil ECa (R = 0.133), while in 2013, the correlation increased (R = 0.274).

The WUEc showed a correlation of R = -0.367, R = 0.183, and R = -0.270 with the fruit size, dry matter, and fruit flesh firmness, respectively, in 2012 (Table 10). Particularly, larger fruit size was correlated with low WUEc, and consequently with decreased crop load (Figure 15). Correlation between the above parameters seemed to be stronger in 2013. However, the reduce sample size in 2013 hampered the statistical comparison of the influence of slight drought stress on fruit quality in the different years.

Table 10. Mean values and p-level of plant variables grouped according to low (cold spot), random, and high (hot spot) crop water stress index ($CWSI_R$) and cumulative water use efficiency (WUEc) considering mean values of all fruits and leaves of each tree.

| Variable | $CWSI_R$ | $CWSI_R$ | $CWSI_R$ | p | WUE | WUE | WUE | p |
|---|---|---|---|---|---|---|---|---|

| | cold-spot | random | hot-spot | | cold-spot | random | hot-spot | |
|---|---|---|---|---|---|---|---|---|
| # leaves per tree | 1973 | 2341 | 2734 | 0.589 | 2180.58 | 2399.26 | 2266.36 | 0.5681 |
| Specific leaf area [$cm^2$ $g^{-1}$] | na | 47.07 | 49.27 | 0.0229 | 29.05 | 29.29 | 28.48 | 0.7300 |
| Fruit size [mm] | 58.22 | 55.04 | 54.67 | 0.6704 | 59.82 | 54.79 | 52.34 | < 0.0001 |
| Firmness [N/cm²] | 3.59 | 2.70 | 2.80 | 0.6346 | 3.29 | 2.75 | 2.23 | 0.1093 |
| Dry matter [%] | 33.97 | 32.37 | 32.08 | 0.3931 | 32.30 | 32.27 | 32.96 | 0.0312 |

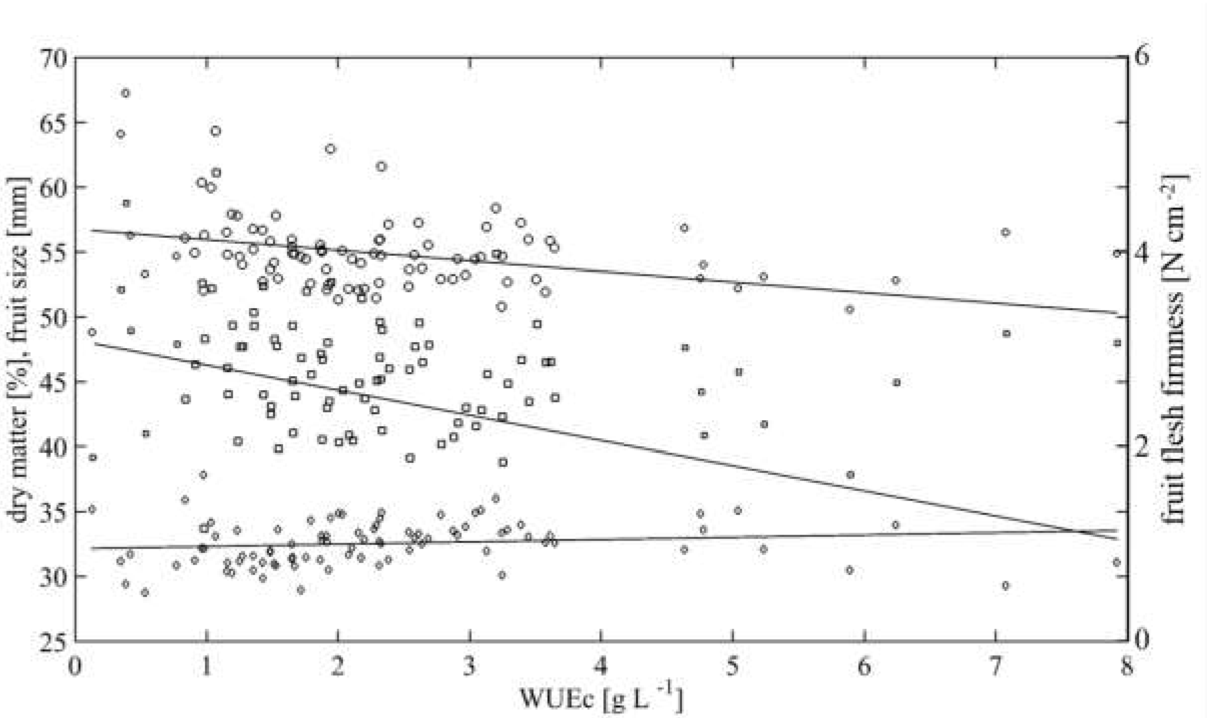


Figure 15 Regression analyses of data (means per tree; n = 88) of fruit dry matter (diamonds, y = $5.903x^1 + 34.67$), fruit size (circles, y = $-80.17x^2 + 24.29$), fruit flesh firmness (squares, y = $-0.129x^3 + 3.017$), and cumulative water use efficiency (WUEc). Increased symbol size represents cold and hot spots.

WUEc showed no correlation with $CWSI_R$ with R = 0.071 and R = 0.093 in 2012 and 2013, respectively. However, fruit quality was strongly affected considering the interaction of both variables (Table 11). Grouping according to WUEc and the instantaneous values of $CWSI_R$ resulted in highly significant differences for fruit size and dry matter.

Table 11. Interaction of cumulative water use efficiency (WUEc) x crop water stress index ($CWSI_R$) and its effect on fruit quality analyzed by 2 factorial ANOVA considering all data and data excluding hot and cold spots.

| | WUE x $CWSI_R$ | | WUE_Spot x $CWSI_R$_Spot | |
|---|---|---|---|---|
| | F | p | F | p |
| Fruit height [mm] | 1.94 | < 0.0001 | 1.89 | < 0.0001 |
| Dry matter [%] | 1.91 | < 0.0001 | 1.82 | < 0.0003 |
| Fruit flesh firmness [N/cm²] | 1.16 | 0.2178 | 0.5 | 0.9977 |

## 4.5 Discussion

### *4.5.1 Spatial Patterns in the Orchard*

Shortly before harvest, the spatial patterns of soil ECa appeared closely related to soil water content with decreased ECa values at the positions of a sand lens found in the experimental orchard. This finding is consistent with earlier investigations carried out in areas with arid conditions (McCutcheon et al., 2006). The low correlation between soil matric potential and soil apparent electrical conductivity could be expected because previous chemical analyses of soils (Käthner and Zude-Sasse, 2015) at 10 spots of the same experimental site indicated only marginal < 5 % variations of phosphorus and potassium content, salinity, and pH. Increased, but still < 10 % variation was found for magnesium, calcium, sodium, and chloride contents. Nevertheless, the analyses of the variations of soil ECa during fruit development may provide data and information for the evaluation of spatial distribution pattern of water, which could potentially affect the quality of the mature fruit.

The $\Psi_{leaf}$ measured predawn showed high variability and minimum value of -1.48 MPa indicating at least slight drought stress in some trees. Based on the measurements of weather and tree canopy microclimate, stable environmental conditions (Bellvert et al., 2014) during thermal imaging between 13:40 and 16:19 can be assumed for both years. Only the variation of radiation due to changing cloud cover could have slightly impaired thermal imaging due to the different dynamics of surface and air (ambient) temperatures (Agam et al. 2013). On the other hand, the analysis of the instantaneous WUEi, performed at the same time, revealed diurnal changes in a value range reported in other investigations on plum trees under similar conditions (Flores et al., 1985). Consequently, consistent sets of thermal readings may have been obtained on each measurement day.

The influence of clouds indeed appeared as a perturbing factor in the present study, especially when using dry and wet paper as references for obtaining Tw and Td. The use of air temperature plus 5 K for setting Td with low difference of Td and Tw resulted in high bias of $CWSI_I$. The analytical analysis of Td and Tw, as well as the automated approach resulted in significant correlation of CWSI and $\Psi_{leaf}$. Calculating Td and Tw analytically (Jones, 1999; Ben-Gal et al., 2009) had the disadvantage that weather data were needed. However, this method provided some insurance against artefacts. In the approach of intrinsic analysis of thermal images to calculate $CWSI_R$ (Rud et al., 2015), references are directly obtained from the images, which is presumably the most feasible approach for an application of thermal imaging in a real world orchard avoiding the need for additional measurements. The approach appeared to be appropriate for the semi-humid summer rain region with cloudy conditions of the current study. The correlation coefficient of R = -0.52 considering $\Psi_{leaf}$ and $CWSI_R$ was at least encouraging to estimate the water stress of the plum trees.

Hotspot analysis (Getis and Ord, 1992) was applied to identify geographically located trees that differ from the mean. The spots found in the ECa data set point to significantly different clusters of trees appearing in the orchard. This small scale variability of soil ECa is typical for postglacial deposits which are common sources of soils in fruit production regions in temperate areas of Europe and Asia.

The $CWSI_R$ varied between 0.15 and 0.88 presumably indicating a range of unstressed to stressed trees in the orchard. As for the ECa patterns, the appearance of significant clusters considering instantaneous $CWSI_R$ points to a possible impact of tree water status on plant growth. However, we can certainly make no a-priori assumption on stable CWSI patterns, since crop load, stage of fruit development, and vegetative growth are all expected to influence water demand. This said, neither ECa nor crop load in the current study showed a correlation with $CWSI_R$.

#### *4.5.2 Potential of Irrigation Adjustment for Improving Fruit Quality*

Bellvert and co-authors identified an influence of the fruit development stage on the correlation coefficient of leaf water potential and CWSI in peach and nectarine (Bellvert et al. 2016) with increased correlation shortly before harvest, which is developmental stage 3. In olive fruits, less severe but equally directed correlation was found (Martin-Vertedor et al., 2011). In the current study, $CWSI_R$ was similarly measured in stage 3 of plum fruit development corresponding to the second peak of fruit growth rate with high water demands.

In plum production, fruit size is of highest economic importance. In the present study, no effect of instantaneous tree water status as indicated by $CWSI_R$ on fruit size was found. However, at high crop load, fruit size was reduced and water required to produce high quality (large enough) fruits may have been deficient. While the instantaneous canopy transpiration based $CWSI_R$ alone did not indicate this level of potential water deficit, cumulative data of WUEc was correlated with fruit quality.

The reducing effect of crop load on $\Psi_{leaf}$ or stem water potential has been pointed out previously (Naor et al., 2001; Marsal et al., 2010), particularly under very high crop load (Sadras and Trentacoste, 2011). An impact on the fruit size is consequent. WUEc, by definition, was dependent of crop load, since, as said, the water supply was uniform in the orchard. However, the variability of soil ECa might point to differences in effective water supply, which would be worthwhile to consider in future studies for calculating the effective WUEc.

Considering the spatial variability measured in the present study, the factor combination of the cumulative WUEc and instantaneous $CWSI_R$ resulted in highly significant interaction with fruit quality. The effects of WUEc and CWSI outweighed the effect of soil ECa on the fruit quality. However, these findings certainly need additional experimentation and confirmation before development as a practical management tool.

## 4.6 Conclusions

Spatially resolved soil analysis is commonly applied in precision horticultural applications. In the present study, analysis of histograms of thermal images in a plum orchard located in a temperate climate characterized by cloud cover and semi-humid conditions was additionally confirmed as a feasible method for spatial quantification of water status.

Different spatial clusters of apparent electrical conductivity of soil and instantaneous crop water stress index were found, but none was correlated with fruit quality in the evenly irrigated orchard. While the cumulative water use efficiency showed an effect on fruit size, only combined analysis of instantaneous water status and cumulative water use efficiency yielded a close correlation with various fruit quality parameters. In practice, i.e. in model-based regulated deficit irrigation of orchards with frequently present small scale variability of soil and varying crop load, the coupled CWSI and WUEc, together with the stage of fruit development, is expected to be an effective driver.

## 4.7 Conflict of Interest

The authors declare that the research was conducted in the absence of any commercial or financial relationships that could be construed as a potential conflict of interest.

## 4.8 Acknowledgments

Research has been carried out in the framework of the 3D-*Mosaic* project (FP7, ICT-AGRI, 2810ERA095), targeting the Advanced Monitoring of Tree Crops for Optimized Management and the USER-PA project (FP7, ICT-AGRI, 2812ERA038) USability of Enviromentally sound and Reliable techniques in Precision Agriculture.

## 4.9 Literature

Agam, N., Segal, E., Peeters, A., Levi, A., Dag, A., Yermiyahu, U., and Ben-Gal, A. (2014). Spatial distribution of water status in irrigated olive orchards by thermal imaging. Precision Agriculture 15, 346-359.

Agam, N., Cohen, Y., Alchanatis, V., and Ben-Gal, A. (2013). How sensitive is the CWSI to changes in solar radiation? International Journal of Remote Sensing 34, 6109-6120.

Aggelopooulou, K., Castrignanò, A., Gemtos, T., and De Benedetto, D. (2013). Delineation of management zones in an apple orchard in Greece using a multivariate approach. Computers and Electronics in Agriculture 90, 119-130.

Anttila, S. and Kairesalo, T. (2010). Mean and variance estimations with different pixel sizes: case study in a small water quality monitoring area in southern Finland. Boreal environment research 15, 335–346.

Ben-Gal, A., Agam, N., Alchanatis, V., Cohen, Y., Zipori, I., Presnov, E., Yermiyahu, U., Sprintsin, M., and Dag, A. (2009). Evaluating water stress in irrigated olives: correlation of soil water status, tree water status, and thermal imagery. Irrigation Science 27, 367-376.

Bellvert, J., Zarco-Tejada, P. J., Girona, J., and Fereres, E. (2014). Mapping crop water stress index in a Pinot-noir vineyard: comparing ground measurements with thermal remote sensing imagery from an unmanned aerial vehicle. Precision Agriculture 15, 361–376.

Bellvert, J., Marsal, J., Girona, J., Gonzalez-Dugo, V., Fereres, E., Ustin, S. L., and Zarco-Tejada, P.J. (2016). Airborne thermal imagery to detect the seasonal evolution of crop water status in peach, nectarine and saturn peach orchards. Remote Sensing 8, 1-17.

Berman, M.E. and DeJong, T. M. (1996). Water stress and crop load effects on fruit fresh and dry weights in peach (Prunus persica). Tree Physiology 16, 859-864.

Berni, J. A. J., Zarco-Tejada, P.J., Sepulcre-Cantó, G., Fereres, E., and Villalobos, F. (2009). Mapping canopy conductance and CWSI in olive orchards using high resolution thermal remote sensing imagery. Remote Sensing of Environment 113, 2380–2388.

Bramley, R. G. V. and Hamilton, R.P. (2004). Understanding variability in winegrape production systems. Australian Journal of Grape and Wine Research 10, 32-45.

Bustan, A., Dag, A., Yermiyahu, U., Erel, R., Presnov, E., Agam, N., Kool, D., Iwema, J., Zipori, I., and Ben-Gal, A. (2016). Fruit load governs transpiration of olive trees. Tree Physiology 36, 380-391.

Chen, J., Benesty, J., Huang, Y., and Doclo, S. (2006). New insights into the noise reduction Wiener filter. IEEE Transactions on audio, speech, and language processing 14, 1218-1234.

Cohen, Y., Alchanatis, V., Meron, M., Saranga, Y., and Tsipris, J. (2005). Estimation of leaf water potential by thermal imagery and spatial analysis. Journal of Experimental Botany 56, 1843-1852.

Ferstl R. (2007). Spatial Filtering with EViews and MATLAB. Australian Journal of Statistics 36, 17-26.

Flores, J. A., Lakso, A. N., and Moon, J. W. (1985). The effect of water stress and vapor pressure gradient on stomatal conductance, water use efficiency, and photosynthesis of fruit crops. Acta Horticulturae 171, 207-218.

Fountas, S., Aggelopoulou, K., Bouloulis, C., Nanos, G. D., Wulfsohn, D., Gemtos, T. A., Paraskevopoulos, A., and Galanis, M. (2011). Site-specific management in an olive tree plantation. Precision Agriculture 12, 179–195.

Gates, D.M. (1980). Biophysical Ecology. Dover Publications, INC, Dover.

Grant, O. M., Tronina, L., Jones, H. G., and Chaves, M. M. (2007). Exploring thermal imaging variables for the detection of stress responses in grapevine under different irrigation regimes. Journal of Experimental Botany 4, 815-825.

Gebbers, R., Lück, E., Dabas, M., and Domsch, H. (2009). Comparison of instruments for geoelectrical soil mapping at the field scale. Near Surface Geophysics 88, 179-190.

Getis, A. and Ord, J. K. (1992). The analysis of spatial association by use of distance statistics. Geographical Analysis 24, 189-206.

Goff, J. A. and Gratch, S. (1946). Low pressure properties of water from 160 to 212 °F. Trans. Amer, Soc. Heat and Vent. Engl. 52, 95-121.

Gómez-del-Campo, M. (2013). Summer deficit irrigation in a hedgerow olive orchard cv. Arbequina: relationship between soil and tree water status, and growth and yield components. Spanish Journal of Agricultural Research 11, 547-557.

Gómez Gallindo, F., Herppich, W. B., Gekas, V., and Sjöholm, I. (2004). Factors affecting quality and postharvest properties of vegetables: integration of water relations and metabolism, Critical reviews in food science and nutrition 44, 1-16.

González-Dugo, V., Zarco-Tejada, P., Nicolás, E., Nortes, P. A., Alarcón, J. J., Intrigliolo, D. S., and Fereres, E. (2013). Using high resolution UAV thermal imagery to assess the variability in the water status of five fruit tree species within a commercial orchard. Precision Agriculture 14, 660-678.

Halvorson, A. D. and Rhoades, J.D. (1976). Field mapping soil conductivity to delineate dryland saline seeps with four-electrode technique. Soil science society of America journal 40, 571-575.

Hellebrand, H.J., Beuche, H., Linke, M. (2006). Thermal imaging a promising high-tec method in agriculture and horticulture, In: Blahovek, J. and Kutlick, M. (eds.), Physical Methods in Agriculture, Springer.

Honig, M. L. and Goldstein J. S. (2002). Adaptive reduced-rank interference suppression based on the multistage wiener filter. IEEE Transactions on Communications 50, 986-994.

Irmak, S., Haman, D., and Bastug, R. (2000). Determination of crop water stress index for irrigation timing and yield estimation of corn. Agronomy Journal 92. 1221-1227.

Jackson, R.D., Idso, R.J., Reginato, P., and Printer, J. (1981). Canopy temperature as a crop water stress indicator. Water resources research 1133-1138.

Jones, H. (1992). Plants and Microclimate, a Quantitative Approach to Enviromental Plant Physiology. 2nd Edition and 3rd Edition (2004), Cambridge University Press.

Jones, H. G. (1999). Use of thermography for quantitative studies of spatial and temporal of stomatal conductance over leaf surfaces. Plant, Cell and Environment 22, 1043-1055.

Jones, H. G., Stoll, M., Santos, T., de Sousa, C., and Chaves, M.M. (2002). Use of infrared thermography for monitoring stomatal closure in the field: application to grapevine. Journal of Experimental Botany 378, 2249-2260.

Jones, H.G. (2004). Irrigation scheduling: advantages and pitfalls of plant-based methods. Journal of Experimental Botany 55, 2427-2436.

Käthner, J., and Zude-Sasse, M. (2015). Interaction of 3D soil electrical conductivity and generative growth in Prunus domestica L. European Journal of Horticultural Science 80, 231–239.

Lück, E., Gebbers, R., Ruehlmann, J., and Spangenberg, U. (2009). Electrical conductivity mapping for precision farming. Near Surface Geophysics 7, 15–25.

Maes, W. H., and Steppe, K. (2012). Estimating evapotranspiration and drought stress with ground-based thermal remote sensing in agriculture: a review. Journal of Experimental Botany 13, 4671-4712.

Mann, K. K., Schumann, A.W., and Obreza, T.A. (2011). Delineating productivity zones in a citrus grove using citrus production, tree growth and temporally stable soil data. Precision Agriculture 12, 457-472.

Marsal, J., Behboudian, M.H., Mata, M., Basile, B., Del Campo, J., Girona, J., Lopez, G. (2010). Fruit thinning in 'Conference' pear grown under deficit irrigation to optimise yield and to improve tree water status. Journal of Horticultural Science and Biotechnology 85, 125-130.

Martin-Vertedor A I, Pérez-Rodrigue J M Prieto-Losada H Fereres-Castiel E (2011). Interactive responses to water deficits and crop load in olive (Olea europea L., cv. Morisca). Agriculture Water Management 98, 941-949.

Meron, M., Grimes, D. W., Phene, C. J., and Davis, K.R. (1987). Pressure chamber procedures for lead water potential measurements of cotton. Irrigation Science 8, 215-222.

McCutcheon, M. C., Farahani, H.J., Stednick, J. D., Buchleiter, G.W., and Green, T.R. (2006). Effect of soil water on apparent soil electrical conductivity and texture relationships in a dryland field. Biosystems Engineering. 94, 19-32.

Nagy, A. (2015). Thermographic evaluation of water stress in an apple orchard. Journal of Multidisciplinary Engineering Science and Technology (JMEST) 2210-2215.

Naor, A., Gal, Y., and Peres, M. (2006). The inherent variability of water stress indicators in apple, nectarine and pear orchards, and the validity of a leaf-selection procedure for water potential measurements. Irrigation science 24, 129-135.

Naor, A., Hupert, H., Greenblat, Y., Peres, M., Kaufman, A., and Klein, I. (2001). The response of nectarine fruit size and midday stem water potential to irrigation level in stage III and crop load. Journal of the American Society for Horticultural Science 126, 140-143.

Palmer, JW. 1992. Effects of varying crop-load on photosynthesis, dry matter production and partitioning of Crispin/M.27 apple trees. Tree Physiology 11: 19–33

Peeters, A., Zude, M., Käthner, J., Ünlü, M., Kanber, R., Hetzroni, A., Gebbers, R., and Ben-Gal, A. (2015). Getis–Ord's hot-and cold-spot statistics as a basis for multivariate spatial clustering of orchard tree data. Computers and Electronics in Agriculture 111, 140-150.

Rud, R., Cohen, Y., Alchanatis, V., Beiersdorf, I., Klose, R., Presnov, E., Levi, A., Brikman, R., Agam, N., Dag, A., and Ben-Gal, A. (2015). Characterization of salinity-induced effects in olive trees based on thermal imagery. 1-8. Abstract retrieved from Abstracts in Precision agriculture'15.

Sadras V O Trentacoste E R (2011). Phenotypic plasticity of stem water potential correlates with crop load in horticultural trees. Tree Physiology 31, 494-499.

Sammis, T.W., Riley, W.R., and Lugg, D.G. (1988). Crop water stress index of pecans. Applied Engineering in Agriculture 1, 39-45.

Sun, X.P., Yan, H.L., Kang, X.Y., and Ma, F.W. (2013). Growth, gas exchange, and water-use efficiency response of two young apple cultivars to drought stress in two scion-one rootstock grafting system. Photosynthetica 51, 404-410.

Telford, W. M., Geldart, L. P., and Sheriff, R. E. (1990). Applied Geophysics. s.l.: Cambridge University Press, 522-562.

Türker, U., Talebpour, B., and Yegül, U. (2011). Determination of the relationship between apparent soil electrical conductivitiy with pomological properties and yield in different apple varieties. Žemdirbystė=Agriculture 98, 307-314.

Viets, F.G., Jr. (1962). Fertilizers and the efficient use of water. Advances in Agronomy 14, 223-264.

von Willert, D., Herppich, W.B., Matyssek, R. (1995). Experimentelle Pflanzenökologie: Grundlagen und Anwendungen, Thieme, Stuttgart

Williams, L. E. and Araujo, F. J. (2002). Correlations among predawn leaf, midday leaf, and midday stem water potential and their correlations with other measures of soil and plant water status in Vitis vinifera. Journal of the American Society for Horticultural Science. 127, 448-454.

Zaman, Q. and Schumann, A.W. (2006). Nutrient management zones for citrus based on variation in soil properties and tree performance. Precision Agriculture. 7, 45-63.

Zude, M., Pflanz, M., Kaprielian, C., and Aivazian, B. L. (2008). NIRS as a tool for precision horticulture in the citrus industry. Journal Biosystems Engineering 99, 455–4

## 4.10 Appendix

Calculation of analytical analysis of wet and dry reference temperature

$$\mathrm{Twana} = \mathrm{T_{air}} + \frac{\mathrm{R_{n_i} r_{HR}}}{\rho \mathrm{C_p}} \tag{11}$$

$$\mathrm{Tdana} = \mathrm{T_{air}} + \frac{\mathrm{r_{HR} r_v}\,\gamma}{\rho \mathrm{C_p}(\mathrm{s r_{HR}} + \mathrm{r_v}\,\gamma)} \mathrm{R_{n_i}} - \frac{\mathrm{r_{HR}}}{\mathrm{s r_{HR}} + \mathrm{r_v}\,\gamma} \mathrm{VPD} \tag{12}$$

Where ρ is the density of dry air [kg $m^{-3}$], Cp the specific heat of dry air at constant pressure [J $kg^{-1}$ $K^{-1}$], γ the thermodynamic psychrometer constant (≈0.066 kPa $K^{-1}$), rv the aerodynamic resistance [s $m^{-1}$] calculated by latent heat transport ($r_H$/1.08), Tair the air temperature [K], the VPD [kPa], and s representing the slope of the curve relating saturation vapor pressure to temperature. The aerodynamic resistance to sensible heat transport $r_H$ [m $s^{-1}$] and the resistance for radiative heat loss $r_R$ [s $m^{-1}$] are compiled into the resistance to sensible heat transport $r_{HR}$ [s $m^{-1}$].

$$\mathrm{r_H} = 100\sqrt{\frac{\mathrm{d}}{\mathrm{u}}} \tag{13}$$

$$\mathrm{r_R} = \frac{\rho \mathrm{C_p}}{4\varepsilon\sigma \mathrm{T_{air}^3}} \tag{14}$$

Where d is the characteristic length [m] of the leaf in the direction of the prevailing wind, u represents the wind speed [m $s^{-1}$], ε the emittance of the canopy with 0.99 (Jones, 2014) and σ refers to the Stefan-Boltzmann constant (5.67 * $10^{-8}$ W $m^{-2}$ $K^{-4}$).

$$\mathrm{r_{HR}} = \frac{1}{\frac{1}{\mathrm{r_H}} + \frac{1}{\mathrm{r_R}}} \tag{15}$$

The net energy at the canopy Rn [W $m^{-2}$] is the sum of the incoming short-wave radiation $R_{SW}$ [W $m^{-2}$] and the incoming and outgoing long-wave radiations (Ben-Gal et al., 2009):

$$\mathrm{R_n} = \mathrm{R_{sw}}(1-\alpha) + 1.24\left(\frac{10\mathrm{e_{air}}}{\mathrm{T_{air}}}\right)^{\frac{1}{7}} \sigma \mathrm{T_{air}^4} - \varepsilon_c \sigma \mathrm{T_c^4} \tag{16}$$

Where $R_{SW}$ is the incoming short-wave radiation [W $m^{-2}$], α is the albedo of the canopy, set to 0.16 (Jones, 2014). The eair is the ambient water vapor pressure [kPa] and Tc the temperature of the canopy [K]. The VPD [kPa] was determined by calculating the difference of the saturation vapor pressure eabs [kPa] and the actual vapor pressure eair [kPa] following Goff (1981) modified by (Gomez Galindo et al., 2004). The actual vapor pressure was calculated using the measured relative humidity ϕ [%] and air pressure $p_{air}$ [MPa].

$$\mathrm{VPD} = \frac{\frac{e_{air}}{e_{abs}}}{p_{air}} \tag{17}$$

with

$$e_{air} = e^{\left(\frac{52.57633-6790.4985}{T_{air}}-5.02808\ln T_{air}\right)} \tag{18}$$

$$e_{abs} = e_{air}\frac{\varphi}{100} \tag{19}$$

## 5 Discussion

For the first time, the connection between spatial variability of soil and plant water status related to generative growth of fruit trees was shown.

For an evaluation of the potential and for the investigation of applicability, comprehensive insights into site-specific soil and plant information from the plantation are essential. As basic data, blanket information about the variability of soil data with the help of ECa were used along with CWSI and topographical data, which are already commonly used in soil mapping for precision agriculture.

In the following illustration (Figure 16), aspects of the concept of precision fruticulture are presented. With the aid of ECa and CWSI, the plantation was characterized comprehensively. By using the hot-spots, the spatial data was divided into three areas. These were further used to determine the interaction between plant variables. From this, conclusions may be drawn about the WUE and quality.

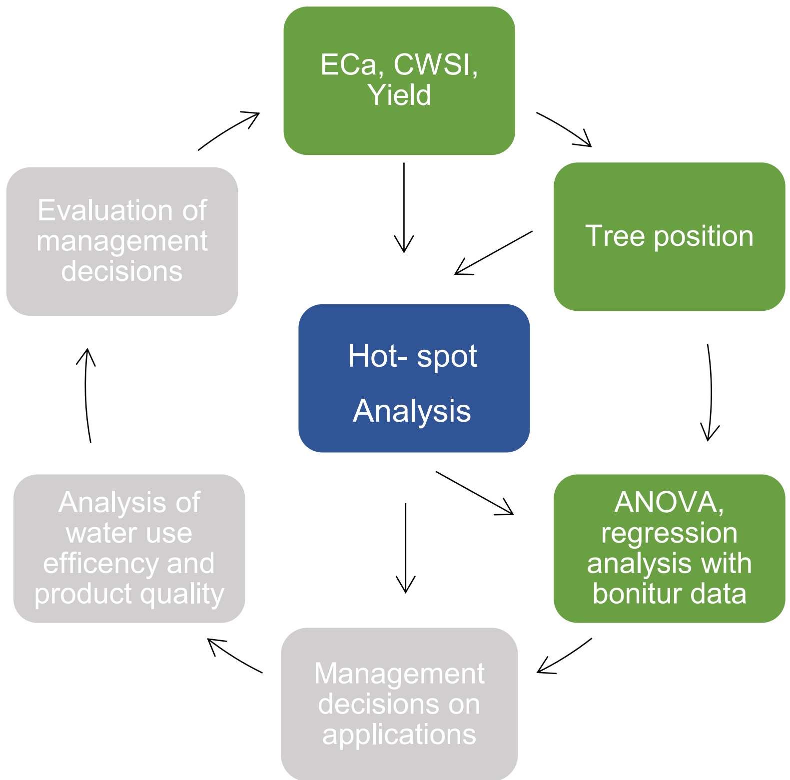


Figure 15. Modified circle system of the concept of precision fruticulture with the concrete realisation approached in this thesis. The transparent (grey) steps were not included.

The highlights of the thesis considering the three chapters on specific objectives are:

- Yield and fruit quality correlate with soil ECa and instantaneous water status of fruit trees
- Yield and fruit quality correlate with soil ECa and topography, with soil $ECa_{topsoil}$ is the most dominant factor
- Isolines of critical values (extremes) enlighten effect of soil ECa on instantaneous CWSI. Isolines of critical values effectively removed extreme trees
- Spatial pattern of plant data were revealed considering fruit quality (height, SSC, firmness, dry matter)
- Water use efficiency
    - Intrinsic WUE points to midday CWSI acquisition and potentially automated analysis in semi-humid climate of Brandenburg
    - Enhanced cumulative WUE resulted in high fruit quality and potentially ressource-efficient fruit production

## 5.1 Spatial variability of soil ECa, topography and plant water status

### *5.1.1 Spatial variability of soil ECa*

The ECa values indicated that the local variability of soil and plant information in the tested plantation in Brandenburg was high (see Manuscript 1, Manuscript 3), so that a randomly performed spot check measurement was not enough to characterize the plantation. It should be kept in mind that the ECa value is only an integrative value and this method is not evaluable without reference analysis such as texture or chemical analysis. Furthermore, this type of measurement is currently not able to be automated, since only measurements right on the fruit tree get the desired information (Manuscript 1).

The spot check reference analyses of the soil were usable in the study's own work when targeted with the ECa-mapped pattern. Through the local analysis of selected areas, effective work is possible and sampling can be optimized. Further, the costs can be optimized as well. With these cost savings, a soil test becomes possible to determine the content of various substances like nitrogen (ion balance and osmosis regulation), phosphorous (energy budget for the plant), potassium (co-factor by enzyme reactions), sulfur (ion balance), and minerals like iron, zinc, copper, manganese, and magnesium (co-factor by enzyme reactions), which affect plant health and the harvest yield (Konopatzki et al., 2008, Kumar et al., 2011).

In addition it was indicated that the patterns that were investigated are stable over the years, which leads to savings on measurements (Manuscript 1; Manuscript 3). The same could be demonstrated by the workgroup of Mann et al. (2011) in a grapefruit orchard in Florida.
This leads to a new potential in precision fruticulture by using the spatial patterns for irrigation in accordance to the soil properties.
Furthermore, the spatial soil ECa patterns may be used to customize and localize fertilizer distribution. Currently in fruticulture, a blanket fertilization is applied to the entire plantation, but spatial variations in ECa values show that this is not an effective use of fertilizer.

### *5.1.2 Spatial variability of the topography*

By using a real-time kinematic global positioning system (RTK-GPS), highly precise positioning of each tree was performed and a precise characterization of the orchard with respect to topography was completed (Manuscript 1).

Exact positioning is a necessity prerequisite for precise and individualized evaluation of the data. For the highest possible precision in positioning the trees, the rover was manually repositioned using RTK-GPS. This is tied to a very high time investment and is therefore impractical for commercial farmers. Only thus can this necessary precise and tree-specific evaluation take place. In an alternative measurement setup that is less time- and cost-intensive, the rover is installed on a platform and driven at a constant walking speed through the orchard (Fukatsu et al., 2014). This was tested in the plum orchard. As it turned out, that tiniest changes in speed, vibrations because of uneven ground, or disturbances in reception to the reference base station lead to a great loss of precision or position data and to deviations from position. However, for finding the blanket elevation information for the whole orchard, it is a viable method.

In the plum orchard, the topography plays only a marginal role (Manuscript 1). It was shown that the topography does not have any significant influence on the yield in the general too gross parameters in the tested orchard with a slope of 3° (Manuscript 1). This was confirmed by the results from Faniadia et al (2010) in sweet cherries. For sweet cherries with an elevation difference of 507 m, it was shown that the elevation difference had no influence on the fruits' physical character (Faniadia et al., 2010).

### *5.1.3 Spatial variability of CWSI*

#### *5.1.3.1 Instantaneous plant water status*

The CWSI is an established method for the blanket collection of plant water status in a semi-arid climate and thus makes efficient irrigation possible. The measurements that form the basis of this study made it possible to modify the analytic equation that enabled the use of this method in a semi-humid area (Manuscript 3). Further factors formed the basis for this modification (Manuscript 3). Thus information was required for this analytical approach such as wind speed, air temperature, and environmental radiation (Manuscript 3). The prerequisite for this data is a weather station located nearby and additional reference sensors located in the plantation itself. These reference sensors are useful for determining temperature variations, so that the data may be corrected if necessary. To minimize the resultant costs, a mobile weather station would make sense. However, installation of such a station on the platform would not be possible because of the driving speed and the resulting air currents, because these would influence the additional information being collected. Furthermore, the values collected by Jones in 2014 for emissions and albedo for the canopy of a leafy tree served as a basis for the analytical computations (Jones, 2014). For an exact computation of the CWSI, these parameters must however be determined specific to the species, since every species has specific characteristics (López et al., 2012). Aside from that, the median leaf area per tree was used for the computation, and because of the measurement apparatus design, only a part of the canopy was measured. For the optimization of the method, the median leaf area of the leaves visible in the thermal images should be used. The weighting of the visible leaves could imply a change in the median leaf area. Further aspect that could be optimized is taking into account the distorted optics that result from the imaging geometry. The geometric calibration of the system can reduce such errors.

Alternatively, with the aid of image editing software, the required reference temperatures were taken directly from the thermal images (Manuscript 3). This form of evaluation does, on the one hand, enable automated measurements, but no surrounding factors whatsoever are taken into account. This could lead to an over- or underestimation of the CWSI. It should also be noted that any cloud cover might negatively influence the capture of thermal images in open fields. This aspect was taken into account in this study by taking measurements on a particularly clear ($R_G$ [W/m²] = 288.00) and calm (u = 0.9 m/s) day. The comparison of the analytical equation with the alternative approach showed only minimal differences (Manuscript 3).

With all that it can be said that for experimental orchards, and automated measurement and evaluation was possible. However, this cannot be copied one to one to a commercial orchard. The crowded planting typical in commercial orchards in the “Schlanke Spindel” form, or fruit bushes or trees planted in walls, prohibit a tree-specific determination of CWSI through image processing. Even an individual tree-by-tree identification by hand was barely possible. To make this concept transferable, a modification of the measurement method is necessary.

For the blanket characterization of plant water status for an entire orchard, the developed method seems to be very effective. It is cost-effective and quickly performed. With it, an efficient and customized water use in semi-humid regions can be implemented and possible negative influences on quality can be reduced. This characterization represents only a snapshot of the plant water status because of the climactic conditions. This aspect must be taken into account as a result of the varying water requirements of the fruit bushes and trees depending on the fruit development phase (Bellvert et al., 2016). One possible implementation would be to monitor fruit development and CWSI long term in order to effectively determine CWSI. This aspect in the study is based on the determined influence of low water stress on the commercially relevant fruit quality.

#### *5.1.3.2 Cumulative plant water status*

How optimally the fruit tree was supplied can be illustrated long-term using laser scanner data. With the help of the automatically collected laser data, the orchard was quickly and comprehensively characterized (Käthner et al., 2014). We can further show that we only need a few destructive tests of leaf area to determine total leaf area, which we in turn use in measurement point graphs to calculate the leaf area per tree (Käthner et al., 2014). The leaf area proportion can additionally be used to adjust the leaf-to-fruit proportion. The disadvantage of this method is that the result is only visible in the following year. The result is also a relative value, which could be improved with 3D images of the tree and a precise evaluation. As with to the thermal images, the transfer of this process to commercial orchards is made difficult by the very tight spacing of the plants.

## 5.2 Hot-spot analysis — characterizing the extreme values

Hot-spot analysis was introduced as a new alternative static distribution method for $ECa_{soil}$ and CWSI data for location-specific management. Spatial soil as well as plant data are useful for analysis (Manuscript 2, Manuscript 3). Consequently, blanket measurements must take place to serve as a basis for decision-making using the location-specific data (Manuscript 2; Manuscript 3).

In this study, a comparison of hot-spot analysis with the established *k*-mean analysis showed that hot-spot analysis is useful as an alternative method (Manuscript 2). In particular the threefold division into cold-spot, random, and hot-spot makes the evaluation method very user-friendly and it is easily turned into a color scale for maps. In the process, individual trees are investigated, which can be quite different even from neighboring trees. It should be taken into account that the spots found with this message are extreme values. These extreme values can simultaneously be used as pointers for the orchard. Thus sensors can be targeted for the exact spots to define boundary values for the orchard. These boundary values can also be used for controlling irrigation. By using these spots to position sensors, the sensors' use becomes more effective and thus saves costs. In addition, hot-spot analysis allows an evaluation of measurement data to be performed and as a result the data can be more precisely evaluated.

This provides a possible model for DSS and can lead to an improved precision management in fruticulture. The further advantage of this method lies in its portability to various comprehensive data — an aspect that is far more difficult with other common methods.

Because of the requirement for comprehensive information, remote sensing is necessary (Fountas et al., 2011). This means and increased time investment in the measurement and in editing, in particular because large gaps in data lead to unreal spots. Furthermore it should be noted that the spots do not confirm the null hypothesis and are not randomly distributed. For precise management, an analysis that produces these spots leaves its mark.

### 5.2.1 Extreme values of soil ECa

The discovered spots that result from the soil and $ECa_{soil}$ data can have many causes. For example, concretion could be an explanation for the spots. A concretion leads to a reduction in pore volume and therefore to poor aeration of the soil. This in turn prevents the water from soaking into the soil and the ground stays wetter longer. As a result, the ground becomes slimy over time and the water cannot be stored in the soil. Furthermore, a concretion can limit root density at greater depths (Bengough and Mullins, 1991).

In the reference plum orchard, a concretion could partly be confirmed as a reason for the spots (Manuscript 1). A further explanation for the spots could be pre-existing plant material, like old roots.

Furthermore, the spots could be an indication of short-term flooding or possibly extreme dryness. Flooding prevents the release of $CO_2$ from cell respiration and hinders the oxygen supply leading to an oxygen deficit, which as a result limits cell respiration.

The ground moisture was measured with pF meter data (Manuscript 1; Manuscript 3). This only explains the cold-spots. The measured values do not exceed a value of 3.3 (Manuscript 3) and thus there are no dry areas that could explain the hot-spots. Besides that, it could be shown that the spots were not explained by a deficit or surplus in chemical components. A spot check of randomized samples showed no extreme properties and therefore no explanation for the spots (Manuscript 1).

### 5.2.2 Extreme values of CWSI

The study showed that the spots could be correlated to the texture shown by the ECa values. Thus the spots in the plum orchard can be assigned to loamy and loam-sandy areas. Additionally, the ECa values can be influenced by chemical substances.

Due to the topography differences in global radiation could occur. The spots found in the CWSI data can be caused by maxima and minima in wind, irradiation, moisture, and air temperature. The study's analytical computation of CWSI did not show any anomalies in the weather data. Due to the topography differences in global radiation could occur. The spots in the topography were located by the pollenating trees and were therefore not relevant for the investigation.

Furthermore, the calibration of the camera could lead to anomalies. However, this was taken into account in data collection and checked afterwards. Above and beyond that, reflections could lead to extreme values. An evaluation routine was programmed for this calculation to remove these values from the computation of the index and replaced with *NaN*.

In addition, the spots could be caused by the general situation. For one thing, the study could indicate that the stage of development like the tree's age should be taken into account in the evaluation (Manuscript 1). The same was shown by Khalid et al. (2012) for 3, 6, 18, and 35 year old mandarin trees in Pakistan.

Another aspect was that the study showed that in spite of constant irrigation, there was a high variability in canopy temperature in the orchard (Manuscript 3). This was a sign of stress, which influenced photosynthesis. The lack of water limited enzyme and physiological processes as well as membrane transport (Jones und Tardieu, 1998). Furthermore, the transpiration was also limited. Consequently, the leaf surface temperature rose.

Water consumption varies by plant type and therefore must be determined for each culture. The established LWP measurement confirmed this, and was additionally shown with a CWSI of 0.69 in the plum orchard. This confirmed what González-Dugo et al. (2013) found in their study of five different fruit types.

The spots could be used for more precise irrigation control. Since CWSI is a snapshot of the plant water status, hot-spot analysis could help locate the distressed areas and allow for timely intervention to prevent possible reductions in fruit quality. Precise data in the form of 3D images could improve hot-spot analysis.

## 5.3 Interaction of soil ECa and CWSI with plant growth (and fruit quality)

With the help of descriptive, inductive, and spatial statistics, the interaction was indicated between soil ECa and CWSI with growth variables and fruit quality (Manuscript 1; Manuscript 3). Thanks to the additional recognition of its impact, possibly new knowledge about the potential for precise management of fruit cultures has been generated. Additionally, it was shown with the ANOVA which depth of the soil ECa had the greatest influence on growth variables and fruit quality (Manuscript 1). By charting the soil ECa at various depths, whole new approaches may have been opened. In the process, the root growth may be charted indirectly. Limited deep root growth can lead to fruit trees having limited health and are susceptible to tree diseases. The causes can be physiological constraints such as water-saturated soil and/or mechanical compression.

Underlying causes can lead to physiological limitations like waterlogged soils and mechanical limitations like concretion. Additionally, the substrate's properties can lead to reduced deep root growth. This assumption is reinforced by the results from various plum cultivars from Grzyb et al. (1998). In the plum orchard, however, this could not be shown. The cultivar as well as the pollenator are on the same substrate and show no significant difference. Hence the influence of the substrate may be discounted.

At the same time, ground sensors may be placed at the depth needed to investigate irrigation and fertilizer requirements. A subsurface irrigation system offers the potential for remote ECa measurements. A further advantage would be the use as a mechanical weed control. For phytosanitary reasons, this must be performed periodically. In so doing, the pressure damage is reduced in the plantation.

Contrary to expectations, the evaluation showed that the topsoil has a significant influence on the plum orchard (Manuscript 1). This was clearer in the grapefruit plantation (Manuscript 2). Thus sandy soils lead to rather less vegetative growth in the grapefruit orchard (Manuscript 2). The same could be confirmed in the study of an apple orchard from Blumenstein (1986). Additionally, the ground level had an influence on yield and fruit quality. The result is surprising, since previous studies showed this only with great variation in elevation, for example *Prunus avium L.* at 507 m (Faniadia et al., 2010) and *Malus domestica L. Borkh* at 250 m difference in elevation (Cin et al., 2007). In a combined look at ECa values in topsoil and the ground level, a significant connection with vegetative growth variables was recognizable (Manuscript 1). Furthermore, there was a positive connection between yield and soil ECa (Mann et al. 2011). In particular the fruit height showed a significant relationship to the $ECa_{topsoil}$ (Manuscript 1). Thus could be used to improve the marketability (Theron, 2011) in that one can produce using selective management in the orchard.

Thus it could be shown in a semi-humid area that trees in sandy areas in the plum orchard were more stressed than trees in loamy-sandy areas (Manuscript 3). Unlike in the study from Milošević und Milošević (2011), they show that plum trees from loamy-sandy areas have a decrease in the median fresh weight.

This study was able to show that water stress also influences quality (Manuscript 3). This was already shown in many other studies. Among others, Chalmers et al. (1981) demonstrated that irrigation can positively influence fruit quality in the form of increases in sugar content in peaces. Irrigation can not only influence the quality, but also the vitality, growth, fruit bud formation, lifespan, and frost and heat resistance (Levitt, 1951; Hoad, 1983). Sensationaly is the fact that one must rely on irrigation even in semi-humid areas (Manuscript 3). This is supported by our demonstration that even a small amount of water stress has an effect on fruit quality (Manuscript 3). The same was found by Intrigliolo and Castel (2006b) with Japanese plums. With apples, it was shown that a high crop load leads to high transpiration (Naor et al., 2008). Furthermore, a clear connection between SWP and yield in apples (Naor, 2004) and plums (Naor and Cohen, 2003) has been shown. By increasing evapotranspiration, surface temperature falls (Maes and Steppe, 2012). It is thus possible through targeted irrigation including precipitation to keep evapotranspiration stable. Using the CWSI, a possible method was shown to characterize this for an entire area. The same was shown by Bellvert et al. (2014a) for peaches and Nagy (2015) for apples. Given that fruit trees require differing amounts of water at different growth stages (Bellvert et al. 2016), a long-term monitoring of fruit development and CWSI should be performed to deduce the actual CWSI.

All these insights could be used for fruit trees in semi-humid areas to intervene with irrigation in a targeted manner, and thus reach the highest possible quality with less water usage. This will be supported by the work from Ruiz-Sánchez et al (2000) on apricot and González-Altozano and Castel (2000) on citrus.They show that full irrigation influence the fruit growth postively.Futhermore, Fereres et al. (2007) could show how important irrigation is in the semi-arid area in fruit treesand through targeted irrigation management can be save water.

# 6 Conclusion

The results of this study indicated that in domestic orchards, there is a variability in soil and plant water status. In addition, the results implied that soil ECa and CWSI affect the fruit quality. The cumulative WUE of trees and the fruit quality were improved on soils with higher soil ECa and lower CWSI values. Particularly, the recognition that irrigation is necessary for fruit quality indicates that a precise management is necessary for an optimized irrigation of orchards.

Furthermore, the results demonstrated that the spatial pattern remains stable in the soil ECa. Besides, the study pointed to another possibility for improving the precision management using the 3D mapping of the soil's ECa. It is worth noting that in the examined plum tree, the topsoil had a significant impact on the variables of growth and fruit size. The evaluation could further lead to the conclusion that the tree's age should be taken into account.

By modifying the equation for the CWSI, it seemed possible to characterize the plant water status of the facility in semi-humid climate. By calculating the CWSI directly from thermal imaging, an alternative possibility was introduced to automatically measure and evaluate the plant water status. Both approaches were verified with established LWP methods.

Despite standard irrigation, the CWSI indicated a high variability in both approaches in the plum orchard in semi-humid climate. Furthermore, the two approaches for calculating the CWSI lead to assume that the fruit quality is affected by the plant water status. The water use efficiency might by a more complex, but feasible variable to assess the optimum water status within the orchard.

The study also presented a method for the classification of management zones. The comparison of the hot-spot analysis to the traditional *k*-mean classification came to comparable results when determining spatial patterns. Spatial grouping allows for precise causal research and opens up new possibilities for evaluations. Thus, better conclusions for the increase in quality could be drawn. Based on the detected spatial patterns in the orchard, a potential for site-specific management may have been revealed. With the triple subdivision, the data is likely more user-friendly and could be evaluated more simply. At the same time, the hot-spot analysis highlighted the extreme values in the spatial soil's ECa and CWSI. In addition, the study argued that the variability of the data could be minimized by the removal of the extreme values in the data. Hence management could be performed in a better way. Thus, significant correlations appeared in the remaining trees' fruit quality and growth variables. With the results of WUE, a potential opportunity for resource-efficient irrigation was presented. The rapid analysis of thermal images of spindle-like plum trees could create an opportunity to carry out automatic monitoring of the current water status in a semi-humid climate.

In summary, it could be said that adequate data is a necessary precondition for the characterization of the orchard. The analysis of the interaction between spatial soil ECa and CWSI to the vegetative and generative growth variables indicated a significant correlation. This information could be used to optimize the management of orchards.

## 7 References

Ač, A., Malenovský, Z., Olejníčková, J., Gallé, A., Rascher, U., Mohammed, G. (2015). Meta-analysis assessing potential of steadystate chlorophyll fluorescence for remote sensing detection of plant water, temperature and nitrogen stress plant. Remote Sensing of Environment 168, 420–436. http://dx.doi.org/10.1016/j. rse.2015.07.022.

Acevedo-Opazo, C., Ortega-Farias, S., Fuentes, S. (2010). Effects of grapevine (Vitis vinifera L.) water status on water consumption, vegetative growth and grape quality: An irrigation scheduling application to achieve regulated deficit irrigation. Agricultural Water Management, 97, 956-964.

Acevedo-Opazo, C., Tisseyre, B., Guillaume, S., Ojeda, H. (2008). The potential of high spatial resolution information to define within-vineyard zones related to vine water status. Precision Agriculture, 9, 285-302.

Agam, N., Segal, E., Peeters, A., Levi, A., Dag, A., Yermiyahu, U., Ben-Gal, A. (2014). Spatial distribution of water status in irrigated olive orchards by thermal imaging. Precision Agriculture 15, 346– 359. http://dx.doi.org/10.1007/s11119-013-9331-8.

Aggelopoulou, K., Castriganò, A., Gemtos, T., De Benedetto, D. (2013). Delineation of management zones in an apple orchard in Greece using a multivariate approach. Computers and Electronics in Agriculture, 119-130.

Aggelopoulou, K., Pateras, D., Fountas, S., Gemtos, T., Nanos, G. (2011). Soil spatial variability and site-specific fertilization maps in an apple orchard. Precision Agric., 118-129.

Allred, B.J., Ehsani, M.R., and Daniels, J.J. (2008). Chapter 1 – General considerations for geophysical methods applied to agriculture. In: Handbook of Agricultural Geophysics, edited by Allred, B.J., Daniels, J.J., and M.R. Ehsani. CRC Press LLC. Boca Raton, Florida. 3-16.

Auernhammer, H. (2001). Precision farming—the environmental challenge. Computers and electronics in agriculture, 30, 31-43.

Beddington, J., Cooper, C.L., Field, J. et al. (2008). The mental wealth of nations. Nature, 455, 1057–1060.

Bellvert, J., Marsal, J., Girona, J., Gonzalez-Dugo, V., Fereres, E., Ustin, S., Zarco-Tejada, P. (2016). Airbone thermal imagery to detect the seasonal evalution of crop water status in peach, nectarine and saturn peach orchards. Remote Sensing, 1-17.

Bellvert, J., Mata, M., Girona, J., Zarco-Tejada, P., González-Dugo, V., Fereres, E. (2014a). Detection of fruit tree water status in orchards from remote sensing thermal imagery. Irrigation Science, 33, 81-93.

Bellvert, J., Zarco-Tejada, P., Girona, J., Fereres, E. (2014b). Mapping crop water stress index in a 'Pinot-noir' vineyard: comparing ground measurements with thermal remote sesing imagery from an unmanned aerial vehicle. Precision Agric., 361-376.

Bendig, J.V. (2015). Unmanned aerial vehicles (UAVs) for multitemporal crop surface modelling. A new method for plant height and biomass estimation based on RGB-imaging. Doctoral dissertation, University of Köln, Germany.

Ben-Gal, A., Agam, N., Alchanatis, V., Cohen, Y., Yermiyahu, U., Zipori, I., ..., Dag, A. (2009). Evaluating water stress in irrigated olives: correlation of soil water status, tree water status, and thermal imagery. Irrigation Science, 27(5), 367-376.

Ben-Gal, A., Ityel, E., Dudley, L., Cohen, S., Yermiyahu, U., Presnov, E., ..., Shani, U. (2008). Effect of irrigation water salinity on transpiration and on leaching requirements: A case study for bell peppers. agricultural water management, 95, 587-597.

Bengough, A.G., Mullins, C.E. (1991). Penetrometer resistance, root penetration resistance and root elongation rate in two sandy loam soils. Plant and Soil 131, 59±66.

Berman, M., DeJong, T. (1996). Water stress and crop load effects on fruit fresh and dry weights in peach (Prunus persica). Tree Physiology, 859-864.

Berni, J.A.J., Zarco-Tejada, P.J., Sepulcre-Cantó, G., Fereres, E., Villalobos, F. (2009). Mapping canopy conductance and CWSI in olive orchards using high resolution thermal remote sensing imagery. Remote Sensing of Environment 113, 2380–2388. http://dx.doi. org/10.1016/j.rse.2009.06.018.

Blackmore, S., Godwin, R., Fountas, S. (2003). The analysis of spatial and temporal trends in yield map data over six years. Biosystems Engineering 84, 455–466. http://dx.doi.org/10.1016/ S1537-5110(03)00038-2.

Blume, H. P., Brümmer, G. W., Horn, R., Kandeler, E., Kögel-Knabner, I., Kretzschmar, R., ... Welp, G. (2010). Böden als Pflanzenstandorte. Lehrbuch der Bodenkunde, 379-448.

Blumenstein, O. (1986). Die Kennzeichnung des Zustandes von Apfelkulturen mit Methoden der Geofernerkundung. Hochschulschrift: Potsdam, Pädagog. Hochschule, Math.-nat. Fak., Diss. (A).

BMEL. (2016). Pro-Kopf-Konsum von Obst in Deutschland in den Wirtschaftsjahren 2004/2005 bis 2014/2015 (in Kilogramm). In Statista - Das Statistik-Portal. Zugriff am 21. September 2016, von https://de.statista.com/statistik/daten/studie/6300/umfrage/pro-kopf-verbrauch-von-obst-in-deutschland/.

Bongiovanni, R., Lowenber-Deboer, J. (2004). Precision Agriculture and Sustainability. Precision Agriculture, 359-387.

Bouma, J., Fox, C. A., Miedema, R. (1990). Micromorphology of hydromorphic soils: applications for soil genesis and land evaluation. Developments in Soil Science, 19, 257-278.

Bramley, R. G. V., Hamilton, R. P. (2004). Understanding variability in winegrape production systems. Australian Journal of Grape and Wine Research, 10, 32-45.

Chalmers, D.J., Mitchell, P.D., van Heek, L., (1981). Control of peach tree growth and productivity by regulated water supply, tree density, and summer pruning. J. Am. Soc. Hortic. Sci. 106, 307–312.

Choné X., van Leeuwen C., Dubourdieu D., Gaudillère J.-P., (2001). Stem water potential is a sensitive indicator for grapevine water status. Annals Botany 87, 477-483.

Cin, V. D., Danesin, M., Botton, A., Boschetti, A., Dorigoni, A., Ramina, A. (2007). Fruit load and elevation affect ethylene biosynthesis and action in apple fruit (Malus domestica L. Borkh) during development, maturation and ripening. Plant, cell & environment, 30(11), 1480-1485.

Cohen, Y., Alchanatis, V., Sela, E., Saranga, Y., Cohen, S., Meron, M., . . . Brikman, R. (2015). Crop water status estimation using thermography: multi-year model development using ground-based thermal images. Precision Agric, 311-329.

Cohen, Y., Alchanatis, V., Prigojin, A., Levi, A., Soroker, V. (2012). Use of aerial thermal imaging to estimate water status of palm trees. Precision Agriculture 13, 123–140. http://dx.doi.org/10.1007/ s11119-011-9232-7.

Cohen, Y., Alchanatis, V., Meron, M., Saranga, Y., Tsipris, J. (2005). Estimation of leaf water potential by thermal imagery and spatial analysis. Journal of Experimental Botany, 56, 1843-1852.

Corwin, D.L., Lesch, S.M. (2003). Application of soil electrical conductivity to precision agriculture: Theory, Principles and Guidelines. Agronomy Journal. 95, 455-471.

Eccher Zerbini, P. (2002). The quality of pear fruit. Acta Horticulturae 596, 805-810

Elsayed-Farag S., Melgar, J.C. (2015). Efficiency of Tree-Based Water Status Indicators at the Onset of Water Deficit in Citrus. Hort. Environ. Biotechnol. 56(3):305-309. DOI 10.1007/s13580-015-0136-8.

Ehsani, R., Karim, D. (2010). Yield monitors for specialty crops. In Advanced engineering systems for specialty crops: A review of precision agriculture for water, chemical, and nutrient, VTI Agriculture and Forestry Research 59, No. 309.2009, S. Upadhyaya, K. Giles, S. Haneklaus, E. Schnug, eds. (Braunschweig, Germany: Johann Heinrich von Thünen-Institut), 31–43.

Faniadis, D., Drogoudi, P. D., Vasilakakis, M. (2010). Effects of cultivar, orchard elevation, and storage on fruit quality characters of sweet cherry (Prunus avium L.). Scientia Horticulturae, 125, 301-304.

Faostat (2016). FAO Statistics Division, 05. August 2016. Available at http://faostat3.fao.org/faostat-gateway/go/to/download/Q/QC/E.

Fereres, E., Soriano, M. A. (2007). Deficit irrigation for reducing agricultural water use. Journal of experimental botany, 58, 147-159.

Fereres, E., Goldhamer, D. A., Parsons, L. R. (2003). Irrigation water management of horticultural crops. HortScience, 38, 1036-1042.

Fountas, S., Aggelopoulou, K., Bouloulis, C., Nanos, G.D., Wulfsohn, D., Gemtos, T.A., Paraskevopoulos, A., Galanis, M. (2011). Site-specific management in an olive tree plantation. Precision Agriculture 12, 179–195. http://dx.doi.org/10.1007/s11119-010- 9167-4.

Fountas, S., Wulfsohn, D., Blackmore, S., Jacobsen, H.L., Pedersen, S.M. (2006). A model of decision making and information flows for information-intensive agriculture. Agricultural Systems 87, 192– 210. http://dx.doi.org/10.1016/j.agsy.2004.12.003.

Fuchs, M. (1990). Infrares Measurement of Canopy Temperature and Detection of Plant Water Stress. Theoretical and Applied Climatology, 53-261.

Fukatsu, T., Endo, G., Ito, Y., Kobayashi, K., Saito, Y. (2014). Mobile robotic field server for field-scale and fruit-scale crop monitoring. Agricultural Information Research 23, 140–153. http://dx.doi. org/10.3173/air.23.140.

Gates, S. J., Hull, C. M., Rocek, M. (1984). Twisted multiplets and new supersymmetric non-linear σ-models. Nuclear Physics B, 248(1), 157-186.

Garcia, A., Albisu, L.M. (2001). Food consumption in the European Union: main determinants and country differences. Agribusiness 17, 469–488.

Gebbers, R., Adamchuk, V. (2010). Precision agriculture and food security. Science 12, 828–831. http://dx.doi.org/10.1126/ science.1183899.

Gebbers, R., Lück, E., Dabas, M., Domsch, H. (2009). Comparison of instruments for geoelectrical soil mapping at the field scale. Near Surface Geophysics. 88, 179-190.

Gebbers, R., Lück, E. (2008). 22 Comparison of Geoelectrical Instruments in Different Soilscapes. Handbook of Agricultural Geophysics, 295.

Gebbers, R., Zude, M. (2008). Spatial distribution of drought stress and quality-related apple fruit monitoring on tree. In Central theme, technology for all: sharing the knowledge for development. Proceedings of the International Conference of Agricultural Engineering, XXXVII Brazilian Congress of Agricultural Engineering, International Livestock Environment Symposium-ILES VIII, Iguassu Falls City, Brazil, 31st August to 4th September, 2008. International Commission of Agricultural Engineering (CIGR), Institut fur Landtechnik.

Gómez-del-Campo, M. (2013). Summer deficit irrigation in a hedgerow olive orchard cv. Arbequina: relationship between soil and tree water status, and growth and yield components. Spanish Journal of Agricultural Research, 11, 547-557.

González-Altozano, P., Castel J.R. (2000). Effects of regulated deficit irrigation on 'Clementina de Nules' citrus trees growth, yield and fruit quality. Acta Hortic 537, 749-758.

González-Dugo, V., Goldhamer, D., Zarco-Tejada, P. J., Fereres, E. (2015). Improving the precision of irrigation in a pistachio farm using an unmanned airborne thermal system. Irrigation Science, 33, 43-52.

González-Dugo, V., Zarco-Tejada, P., Nicolás, E., Nortes, P. A., Alarcón, J. J., Intrigliolo, D. S., Fereres, E. (2013). Using high resolution UAV thermal imagery to assess the variability in the water status of five fruit tree species within a commercial orchard. Precision Agriculture, 14, 660-678.

González-Dugo, M. P., Moran, M. S., Mateos, L., Bryant, R. (2006). Canopy temperature variability as an indicator of crop water stress severity. Irrigation Science, 4, 233-240.

Goodwin, I., O'Connell, M., Whitfield, D. (2008). Optimising irrigation management units in a nectarine orchard. Australian Fruitgrower 2, 28–30.

Govender, M., Chetty, K., Bulcock, H. (2007). A review of hyperspectral remote sensing and its application in vegetation and water resource studies. Water Sa, 33.

Girona, J., Mata, M., Del Campo, J., Arbonés, A., Bartra, E., Marsal, J. (2006). The use of midday leaf water potential for scheduling deficit irrigation in vineyards. Irrigation Science, 24(2), 115-127.

Grzyb, Z. S., Sitarek, M., Kozinski, B. (1998). Effect of different rootstocks on growth, yield and fruit quality of four plum cultivars (in central of Poland). In VI International Symposium on Plum and Prune Genetics, Breeding, Pomology 478, 239-242.

Hall, A., Lamb, D. W., Holzapfel, B., Louis, J. (2002). Optical remote sensing applications in viticulture-a review. Australian Journal of Grape and Wine Research, 8(1), 36-47.

Halvorson, A. D., Rhoades, J. D. (1976). Field mapping soil conductivity to delineate dryland saline seeps with four-electrode technique. Soil science society of America journal, 40, 571-575.

Hartsock, N.J., Mueller, T.G., Thomas, G.W., Barnhisel, R.I., Wells, K.L., and Shearer, S.A. (2000). Soil electrical conductivity variability. In. P.C. Robert et al. (ed.) Proc. 5th international conference on precision Agriculture. ASA Misc. Publ., ASA, CSSA, and SSSA, Madison, WI.

Herrero-Langreo, A., Tisseyre, B., Goutouly, J. P., Scholasch, T., & van Leeuwen, C. (2013). Mapping grapevine (Vitis vinifera L.) water status during the season using carbon isotope ratio (δ13C) as ancillary data. American Journal of Enology and Viticulture, 64(3), 307-315.

Hedley, C. (2015). The role of precision agriculture for improved nutrient management on farms. Journal of the Science of Food and Agriculture 95, 12–19. http://dx.doi.org/10.1002/jsfa.6734.

Hoad, G. V. (1983). Hormonal regulation of fruit-bud formation in fruit trees. Flowering and Fruit Set in Fruit Trees 149, 13-24.

Idso, S. B. 1982. Non-water-stressed baselines: a key to measuring and interpreting plant waterstress. Agricultural Meteorology 27, 59-70.

Intrigliolo, D. S., Castel, J. R. (2006a). Usefulness of diurnal trunk shrinkage as a water stress indicator in plum trees. Tree Physiology, 303-311.

Intrigliolo, D. S., Castel, J. R. (2006b). Performance of various water stress indicators for prediction of fruit size response to deficit irrigation in plum. Agricultural Water Management, 83, 173-180.

Irmak S, Haman D, Bastug R. (2000). Determination of crop water stress index for irrigation timing and yield estimation of corn. Agron J. 92, 1221-1227.

Jackson, J.E. (2005). Biology of horticultural crops. Biology of apples and pears. Cambridge University Press, 4-9, 22-23, 74-75.

Jackson, R. D., Idso, R. J., Reginato, P., Printer, J. (1981). Canopy temperature as a crop water stress indicator. Water Res., 1133-1138.

Jones, H. G. (2014): Plants and Microclimate - A Quantitative Approach to Environmental Plant Physiology. 3. ed. New York: Cambridge University Press.

Jones, H. G. (2007). Monitoring plant and soil water status: established and novel methods revisted and ther relevance to studies of drought tolerance. Journal of Experimental Botany, Special issue paper (2), 119-130.

Jones, H. G. (2004). Irrigation scheduling: advantages and pitfalls of plant-based methods. Journal of experimental botany, 55, 2427-2436.

Jones, H. G., Stoll, M., Santos, T., de Sousa, C., Chaves, M. M. (2002). Use of infrared thermography for monitoring stomatal closure in the field: application to grapevine. Journal of Experimental Botany, 378, 2249-2260.

Jones, H. G. (1999). Use of thermography for quantitative studies of spatial and temporal of stomatal conductance over leaf surfaces. Plant, Cell and Environment, 22, 1043-1055.

Jones, H.G., Tardieu, F. (1998). Modelling water relations of horticultural crops: a review. Sci. Hort. 74, 21–46.

Jones, H. (1992). Plants and mircoclimate, a quantitative approach to enviromental plant physiology. 2nd Edn. ed. s.l.:Cambridge University Press.

Jafari, A., Arzani, K., Fallahi, E., Barzegar, M. (2014). Optimizing Fruit Yield, Size, and Quality Attributes in'Malase Torshe Saveh'Pomegranate through Hand Thinning. Journal of the american pomological society, 68(2), 89-96.

Kadereit, J. W., Körner, C., Kost, B., & Sonnewald, U. (2014). Strasburger− Lehrbuch der Pflanzenwissenschaften. Springer-Verlag.

Kang, S., Hu, X., Goodwin, I., Jerie, P. (2002). Soil water distribution, water use, and yield response to partial root zone drying under a shallow groundwater table condition in a pear orchard. Scientia Horticuturae, 277-291.

Käthner, J., Alchanatis, V., Selbeck, J., Peeters, A., Ben-Gal, A., Blumenstein, O., Zude, M. (2014). Influence of small scale variability of soil ECa on the crop water stress index, leaf area ratio, and yield in *Prunus domestica* orchard. In: Proceedings. International Conference of Agricultural Engineering AgEng 2014. Eur. Soc. Ag. Eng. (EurAgEng), Zürich, p. 1. Online: http://ISBN: 978-0-9930236-0-6.

Khalid, S., Malik, A. U., Saleem, B. A., Khan, A. S., Khalid, M. S., Amin, M. (2012). Tree age and canopy position affect rind quality, fruit quality and rind nutrient content of ‘Kinnow’mandarin (Citrus nobilis Lour× Citrus deliciosa Tenora). Scientia Horticulturae, 135, 137-144.

Kleber, A. (1992). Periglacial slope deposits and their pedogenic implications in Germany. Palaeogeography, palaeoclimatology, palaeoecology, 99, 361-371.

Konopatzki, M.R., Souza, E.G., Nóbrega, L.H., Bazzi, C.L., and Rocha, D.M. (2015). Spatial variability of chemical attributes of the soil, plant and yield in a pear orchard. Journal of Plant Nutrition 39 (3), 323–336. http://dx.doi.org/10.1080/01904167.2015.1014562.

Konopatzki, M.R.S., De Souza, E.G., Nóbrega, L.H.P., Uribe-Opazo, M.A., Suuszek, G., Rodrigues, S. (2008). Spatial variability of the soil properties in a pear tree. Proceedings CIGR International Conference of Agricultural Engineering, XXXVII Congress Brasileiro de Engenharia Agricola.

Kumar, S., Kamboj, J., Sharma, S. (2011). Overview for various aspects of the health benefits of Piper longum linn. fruit. Journal of acupuncture and meridian studies, 4, 134-140.

Kutílek, M., Nielsen, D. R. (1994). Soil hydrology: texbook for students of soil science, agriculture, forestry, geoecology, hydrology, geomorphology and other related disciplines. Catena Verlag.

Leib, B. G., Caspari, H. W., Redulla, C. A., Andrews, P. K., Jabro, J. J. (2006). Partial rootzone drying and deficit irrigation of ‘Fuji’apples in a semi-arid climate. Irrigation science, 24(2), 85-99.

Leinweber, P., Blumenstein, O., Schulten, H. R. (1996). Organic matter composition in sewage farm soils: Investigations by 13C-NMR and pyrolysis-field ionization mass spectrometry. European Journal of Soil Science, 1, 71-80.

Levitt, J. (1951). Frost, drought, and heat resistance. Annual Review of Plant Physiology, 2(1), 245-268.

Liakos, V., Tagarakis, A., Aggelopoulou, K., Kleftaki, X., Mparas, G.,Fountas, S., Gemtos, T. (2011). Yield prediction in a commercial apple orchard by analyzing RGB and multi-spectral images of trees during flowering period. In Precision Agriculture, Proceedings of the 8th European Conference on Precision Agriculture, J. Stafford, ed. (Prague: Czech Centre for Science and Society). 617–627.

Link, H. (2000). Significance of flower and fruit thinning on fruit quality. Plant growth regulation, 31, 17-26.

Ling, P. (2004). A review of soil moisture sensors. Assn. Flor. Prof. Bull, 886, 22-23.

López A., Molina-Aiz, F.D., Valera D.L., Peña A. (2012). Determining the emissivity of the leaves of nine horticultural crops by means of infrared thermography. Scientia Horticulturae, 137, 49–58

Lück, E., Ruehlmann, J. (2013). Resistivity mapping with GEOPHILUS ELECTRICUS—Information about lateral and vertical soil heterogeneity. Geoderma, 199, 2-11.

Lück, E., Gebbers, R., Ruehlmann, J., Spangenberg, U., 2009. Electrical conductivity mapping for precision farming. Near Surf. Geophys. 7, 15–25.

Maes, W. H., Steppe, K. (2012). Estimating evapotranspiration and drought stress with ground-based thermal remote sensing in agriculture: a review. Journal of Experimental Botany, 13, 4671-4712.

Mahhou, A., DeJong, T. M., Shackel, K. S., Cao, T. (2006). Water stress and crop load effects on yield and fruit quality of Elegant Lady Peach [ Prunus persica (L.) Batch]. Fruits, 407-418.

Mann, K. K., Schumann, A. W., Obreza, T. A. (2011). Delineating productivity zones in a citrus grove using citrus production, tree growth and temporally stable soil data. Precision Agriculture, 12, 457-472

Meron, M., Tsipris, J., Orlov, V., Alchanatis, V., Cohen, Y. (2010). Crop water stress mapping for site-specific irrigation by thermal imagery and artificial reference surfaces. Precision Agric, 48-162.

Milošević, T., Milošević, N. (2011). Growth, fruit size, yield performance and micronutrient status of plum trees (Prunus domestica L.). Plant, Soil and Environment, 57, 559-564.

Möller, M., Alchanatis, V., Cohen, Y., et al. (2007). Use of thermal and visible imagery for estimating crop water status of irrigated grapevine. Journal of Experimental Botany 58, 827–838. http:// dx.doi.org/10.1093/jxb/erl115.

Moriana, A., Orgaz, F., Pastor, M., Fereres, E. (2003). Yield responses of a mature olive orchard to water deficits. Journal of the American Society for Horticultural Science, 128, 425-431.

Moriana, A., Fereres, E. (2003). Establishing reference values of trunk diameter fluctuations and stem water potential for irrigation scheduling of olive trees. In IV International Symposium on Irrigation of Horticultural Crops 664. 407-412.

Nadler, A. (2004). Relations between soil and tree stem water content and bulk electrical conductivity under salinizing irrigation. Soil Sci. Soc. Am. J., 779-783.

Nagy, A. (2015). Thermographic evaluation of water stress in an apple orchard. Journal of Multidisciplinary Engineering Science and Technology (JMEST), 2210-2215.

Naor, A., Naschitz, S., Peres, M., Gal, Y. (2008) Responses of apple fruit size to tree water status and crop load. Tree Physiology 2008; 28: 1255-1261.

Naor, A., Gal, Y., Peres, M. (2006). The inherent variability of water stress indicators in apple, nectarine and pear orchards, and the validity of a leaf-selection procedure for water potential measurements. Irrigation science, 24, 129-135.

Naor, A. (2004). The interactions of soil-and stem-water potentials with crop level, fruit size and stomatal conductance of field-grown 'Black Amber'Japanese plum. The Journal of Horticultural Science and Biotechnology, 79, 273-280.

Naor, A., Cohen, S. (2003). Sensitivity and variability of maximum trunk shrinkage, midday stem water potential, and transpiration rate in response to withholding irrigation from field-grown apple trees. HortScience, 38, 547-551.

Naor, A., Hupert, H., Greenblat, Y., Peres, M., Kaufman, A., Klein, I. (2001). The response of nectarine fruit size and midday stem water potential to irrigation level in stage III and crop load. Journal of the American Society for Horticultural Science, 126, 140-143.

Naor, A. (2000). Midday stem water potential as a planet water stress indicator for irrigation scheduling in fruit trees. Acta Hort, 447-454.

Nink, S., Hill, J., Buddenbaum, H., Stoffels, J., Sachtleber, T., Langshausen, J. (2015). Assessing the suitability of future multi- and hyperspectral satellite systems for mapping the spatial distribution of Norway spruce timber volume. Remote Sensing, 7, 12009–12040. http://dx.doi.org/10.3390/rs70912009.

Panda, S.S., Hoogenboom, G., Paz, J.O. (2010). Remote sensing and geospatial technological applications for site-specific management of fruit and nut crops: A review. Remote Sensing, 2, 1973–1997. http://dx.doi.org/10.3390/rs2081973

Peeters, A., Zude, M., Käthner, J., Ünlü, M., Kanber, R., Hetzroni, A., . . . Ben-Gal, A. (2015). Getis–Ord's hot-and cold-spot statistics as a basis for multivariate spatial clustering of orchard tree data. Computers and Electronics in Agriculture, 140-150.

Richard, G., Cousin, I., Sillon, J. F., Bruand, A., Guérif, J. (2001). Effect of compaction on the porosity of a silty soil: influence on unsaturated hydraulic properties. European Journal of Soil Science, 52, 49-58.

Ritthaler H. (2012) Pfälzer Obstkultur : Geschichte und Verhältnisse des Obstbaues in der Pfalz ; 25 Sortenportraits und Liste pfälzischer Baumobst-Sorten / Arbeitskreis Historische Obstsorten Pfalz, Elsaß, Kurpfalz, Pomologen-Verein e.V.

Robinson, D. A., Campbell, C. S., Hopmans, J. W., Hornbuckle, B. K., Jones, S. B., Knight, R., ... & Wendroth, O. (2008). Soil moisture measurement for ecological and hydrological watershed-scale observatories: A review. Vadose Zone Journal, 7(1), 358-389.

Rosell Polo, J. R., Sanz, R., Llorens, J., Arnó, J., Escolà, A., Ribes-Dasi, M., . . . Palacín, J. (2009). A tractor mounted scanning LIDAR for the non-destructive measurement of 2 vegetative volume and surface area of tree-row plantations: A comparison with 3 conventional destructive measurements. Biosystems Engineering, 2, 128-134.

Rud, R., Cohen, Y., Alchanatis, V., Beiersdorf, I., Klose, R., Presnov, E., . . . Ben-Gal, A. (2015). Characterization of salinity-induces effects in olive trees based on thermal imagery. Precision Agriculture, 11-517.

Ruiz-Sánchez, M.C., Torrecillas, A., Pérezpastor, A., Domingo R. (2000). Regulated deficit irrigation in apricot trees. Acta Hortic 537, 759-766.

Sadeghi, A., Scott, H., Ferguson, J. (1984). Estimating evaporation: A comparsion between Penman, Idso-Jackson, and zero-flux methods. Agricultural and Forest Meteorology, 225-238.

Sadler, E. J., Busscher, W. J., Bauer, P. J., Karlen, D. L. (1998). Spatial scale requirements for precision farming: A case study in the southeastern USA. Agronomy Journal, 90, 191-197.

Schneider, G. W., Childers, N. F. (1941). Influence of soil moisture on photosynthesis, respiration, and transpiration of apple leaves. Plant physiology, 16, 565.

Scharf, P.C. (2015). Determining the optimal nitrogen rate: N credits, soil tests, and crop-based diagnosis. Crops and Soils 48, 34–42.

Schirrmann, M., Gebbers, R., Kramer, E., Seidel, J. (2011). Soil pH mapping with an on-the-go sensor. Sensors, 11, 573-598.

Schirrmann, M., Domsch, H. (2011). Sampling procedure simulating on-the-go sensing for soil nutrients. Journal of Plant Nutrition and Soil Science, 174, 333-343.

Schuricht W. (2009). Zur Geschichte des Obstbaus Mitteldeutschlands / Teil 1. Der Obstbau Mitteldeutschlands vom Mittelalter bis zum Jahre 1945. 1. Aufl. Förderverein Deutsches Gartenbaumuseum Erfurt. 1-115.

Scholander, P. F., Hammel, H. T., Bradstreet, E. D., Hemmingsen, E. A. (1965). Sap pressure in vascular plants. Science 148:339-46.

Seifert, B., Zude, M., Spinelli, L., Torricelli, A. (2015). Optical properties of developing pip and stone fruit reveal underlying structural changes. Physiologia Plantarum, 327-336.

Sepaskhah, A., Kashefipour, S. (1994). Relationships between leaf water potential, CWSI, yield and fruit quality of sweet lime under drip irrigation. Agricultural Water Management, 13-22.

Shewfelt, R.L. (1999). What is quality? Postharvest Biology and Technology, 15, 197-200

Simon, S., Lauri, P. E., Brun, L., Defrance, H., Sauphanor, B. (2006). Does manipulation of fruit-tree architecture affect the development of pests and pathogens? A case study in an organic apple orchard. The Journal of Horticultural Science and Biotechnology, 81, 765-773.

Srinivasan, A. (2006). Precision agriculture: an overview. Handbook of precision agriculture: Principles and applications, 3-18.

Stafford, J.V. (2000). Implementing precision agriculture in the 21st century. Journal of Agricultural Engineering Research 76, 267–275. http://dx.doi.org/10.1006/jaer.2000.0577.

Telford, W. M., Geldart, L. P., Sheriff, R. E. (1990). Applied geophysics. s.l.: Cambridge university press, 522-562.

Theron, K. (2011). Size Matters: Factors Influencing Fruit Size in Pear. Acta horticulturae, 545-555.

Thorp, K. R., & Tian, L. F. (2004). A review on remote sensing of weeds in agriculture. Precision Agriculture, 5, 477-508.

Tromp, J. (1984) Diurnal fruit shrinkage in apple as affected by leaf water potential and vapour pressure deficit of the air. Scientia Horticulturae 22: 81-87

Tucker, C. J. (1980). Remote sensing of leaf water content in the near infrared. Remote Sensing of Environment, 10, 23 – 32.

Usha, K., Singh, B. (2013). Potential applications of remote sensing in horticulture – A review. Scientia Horticulturae 153, 71–83. http://dx.doi.org/10.1016/j.scienta.2013.01.008.

UNECE (2014). UNECE NORM FFV-29 für die Vermarktung und Qulitätskontrolle von Pflaumen, Vereinte Nationen, New York und Genf

UNECE (2012). UNECE Standard FFV-14 für die Vermarktung und Qulitätskontrolle von Zitrusfrüchten, Vereinte Nationen, New York und Genf

Ünlü, M., Kanber, R., Koç, D., Özekıcı, B., Kekeç, U., Yeşıloğlu, T., . . . Ben-Gal, A. (2014). Irrigation scheduling of grapefruit trees in a Mediterranean environment throughout evaluation of plant water status and evapotranspiration. Turkish Journal of Agriculture and Forestry, 908-915.

Winter F.; Link H. (2002): Lucas' Anleitung zum Obstbau, 32. Aufl. Ulmer, Stuttgart-Hohenheim.

Williams, L. E., & Araujo, F. J. (2002). Correlations among predawn leaf, midday leaf, and midday stem water potential and their correlations with other measures of soil and plant water status in Vitis vinifera. Journal of the American Society for Horticultural Science, 127, 448-454.

Xujun, Y., Sakai, K., Manago, M., Asada, S., Sasao, A. (2007). Prediction of citrus yield from airborne hyperspectral imagery. Precision Agriculture 8, 111–125. http://dx.doi.org/10.1007/s11119-007-9032-2.

Zaman, Q.U., Salyani, M. (2004). Effects of foliage density and ground speed on ultrasonic measurement of citrus tree volume. Applied Engineering in Agriculture 20, 173–178. http://dx.doi. org/10.13031/2013.15887.

Zaman, Q.-u., Schumann, A. W. (2006). Nutrient management zones for citrus based on variation in soil properties and tree performance. Precision Agric, 7, 45-63.

Zhang, N., Wang, M., Wang, N. (2002). Precision agriculture*/a worldwide overview. Computer and Electronics in Agriculture, 113-132.

Zude-Sasse, M., Fountas, S., Gemtos, T.A., Abu-Khalaf, N. (2016) Applications of precision agriculture in horticultural crops. European Journal of Horticultural Science, 81, 78-90

Zude, M., Pflanz, M., Kaprielian, C., Aivazian, B.L. (2008). NIRS as a tool for precision horticulture in the citrus industry. Journal Biosystems Engineering 99, 455–459. http://dx.doi.org/10.1016/j. biosystemseng.2007.10.016.

Zude, M. (2003). Comparison of indices and multivariate models to non-destructively predict the fruit chlorophyll by means of visible spectrometry in apple fruit. Analytica Chimica Acta. 481, 119-126. http://dx.doi.org/10.1016/S0003-2670(03)00070-9.

**Declaration of Academic Honesty**

*Declaration of Academic Honesty*

I herewith declare, that I have prepared this thesis with the title “Interaction of spatial variability characterized by soil electrical conductivity and plant water status related to generative growth of fruit trees“ on my own, using only the materials (devices) mentioned. This work has not been submitted to another examination office.

*Eidesstattliche Erklärung*

Hiermit erkläre ich, dass ich die von mir vorgelegte Dissertation mit dem Titel “Interaction of spatial variability characterized by soil electrical conductivity and plant water status related to generative growth of fruit trees“ selbstständig und nur unter Verwendung der angegebenen Quellen und Hilfsmittel angefertigt habe. Ich erkläre außerdem, dass diese Dissertation noch keiner anderen Fakultät oder Hochschule zur Prüfung vorgelegt wurde.

Potsdam, den 05. October 2016

**Acknowledgements**

It would not have been possible to write this thesis without the support of many people; it is only possible to give particular mention here to some of them. First of all, I want to express my deep gratitude to my supervisors, Prof. Dr. habil. Oswald Blumenstein and Prof. Dr. habil. Manuela Zude-Sasse, for supporting my PhD project.

Prof. Dr. Oswald Blumenstein supported me on behalf of the University of Potsdam. Many thanks for his willingness to engage a lot of discussions with me. He was always able to motivate and guide me in some difficult situations. It was a very cooperative and constructive collaboration. His careful reviewing of my manuscripts was essential to finish the work at all.

Special thanks to Prof. Dr. Manuela Zude-Sasse, who stood beside me during my work at the ATB as a teacher and mentor. She introduced me to the field of scientific fruit production and made it possible to write this work. Especially during the difficult time after restarting the promotion, she always tended to me helpfully. I thank her for providing an excellent working environment. Particular thanks for introducing me to the world of horticulture and for giving me the opportunity to work together in a great international team. Her vast knowledge in the field of horticulture, her careful review of my manuscripts, and the numerous discussions whenever necessary were fundamental for the success of this work. Prof. Dr. Zude-Sasse gave me valuable advice, and at the same time she gave me the freedom to pursue my own ideas. In the last five years we worked together as a team. I owe Prof. Dr. Zude-Sasse for my participation in numerous national and international conferences. This gave me the opportunity to make a name in science nationally and internationally and build a business network. Additionally, she gave me the opportunity to work in a transnational interdisciplinary team.

I especially want to thank Dr. Martin Geyer, who received me as a graduate student in the research group of his department Horticultural Engineering at the Leibniz Institute for Agricultural Engineering and Bioeconomy (ATB).

The result of a close collaboration with this excellent scientists and colleagues are a few scientific papers. A warm thank you goes to all participants from the 3D Mosaic and USER–PA project for inspiring discussions during our project meeting. This helped me gain a more differentiated point of view and to receive a variety of viewpoints. I would particularly like to thank Dr. Aviva Peeters., Dr. Alon Ben-gal, Dr. Amots Hertzroni, Dr. Ronit Rud, Prof. Dr. Simon Blackmore, Dr. Dominique Fleury, Dr. Spyros Fountas, Dr. Victor Alchanati, Prof. Dr. Stavros G. Vougioukas, Prof. Dr. Alessandro Torricelli, Dr. Lorenzo Spinelli, Cleas Dühring-Hansen, Prof. Dr. Mustafa Ünlü, Dr. Florian Pforte, Dr. Sören Pedersen, and Dr. Martin Maiwald for the good cooperation during field experiments.

Results of a close collaboration with excellent scientists and colleagues are a few scientific papers. A warm thank you goes to all participants from the 3D-Mosaic and USER –PA project for inspiring discussions during our project meetings. I had the opportunity to get differentiated perspectives and representations of different perceptions. I particularly would like to thank Dr. Aviva Peeters, Dr. Alon Ben-gal, Dr. Amots Hertzroni, Dr. Ronit Rud, Prof. Dr. Simon Blackmore, Dr. Dominique Fleury, Dr. Spyros Fountas, Dr. Victor Alchanati, Prof. Dr. Stavros G. Vougioukas, Prof. Dr. Alessandro Torricelli, Dr. Lorenzo Spinelli, Cleas Dühring-Hansen, Prof. Dr. Mustafa Ünlü, Dr. Florian Pforte, Dr. Sören Pedersen, and Dr. Martin Maiwald for the good cooperation during the field experiments.

I also thank Prof. Dr. Kerri Walsh who has provided himself as third assessor.

I would like to thank Dr. Werner B. Herppich and Dr. Robin Gebbers for reviewing several manuscripts and advising me in many ways. Thank you for keeping your door always open for questions and discussions!

Numerous colleagues have made life in the orchard or behind the PC more fun: Thank you Birgit, Micha, Antje, and Nicole providing critical and valuable feedbacks during the last years. A special thank goes to Jörn, Gabi, David, Corinna, Antje G., Hans-Jürgen, Marc, Yousef, Volker, and Rolf for their support in many ways and the wonderful time we have together within and beyond the walls of the ATB. I particularly wish to thank Andrea for her continuous help and guiding me through the administration of the ATB.

Thanks also to Christian for his magic touch to keep my computer running. Thanks to Ingo, Uwe, and Wilfried for spontaneous repairs of my measuring equipment. I also thank numerous students and volunteers from department 4 and 6 who have worked with me in the orchard and counted all possible bonitur data from all trees. Additionally, I thank all hands who helped me to measure the plant water status. Unfortunately I cannot name all of you here.

I would also like to thank my English teacher John Grantham, who among other things helped me lose the fear of reading aloud. Furthermore I would like to thank the working group of applied geophysics from the University of Potsdam, particularly Dr. Erika Lück and Marko Dubnitzki, who always stood by me with advice and practical help in our several coffee sessions.

I would also like to thank my friends for their interest in my work, their support, and the fun we have together. I am very grateful to my friend Kathrin for her patience during the last months while I was finishing my thesis. She has accompanied this work, always critical and helpful.

Finally, I am particularly grateful to my family, especially my parents, in-laws, siblings and grandparents for their continued support and patience. My last and most intense thanks to my husband Steffen and my daughter Anika, for their great patience, their love and support. Thank you for sharing life with me and that you have supported me in the recent years.

Yours Jana Käthner